A study towards the use of semiconductors as mediators in organic oxidation transformations.

Thesis submitted to:

The University of
KwaZulu-Natal
Pietermaritzburg
South Africa

For the Title of

**Master of Science
(Chemistry)**

By

Timothy Michael Underwood

March 2015

UNIVERSITY OF
KWAZULU-NATAL

Thesis Declaration

The project described herein (experimental research and compilation of this thesis) was conducted and completed at the School of Chemistry and Physics, University of KwaZulu-Natal (Pietermaritzburg campus) under the supervision of Professor Ross S. Robinson.

All research findings presented in this thesis by Timothy Michael Underwood are of original findings that have not been presented elsewhere for the application of an academic degree.

Signed:………………………………………………………….........T. M. Underwood (Candidate)

Signed:………………………………………………………….....Professor R. S. Robinson (Supervisor)

The University of KwaZulu-Natal

(Pietermaritzburg Campus)

School of Chemistry and Physics

South Africa

January 2015

Acknowledgements

Firstly, a special thank you to Professor Ross Robinson for his supervisory role throughout the course of this project for the countless hours spent discussing methods to photo-activate synthetic CVD diamonds. As a result, not only have my interests in synthetic diamond studies been elevated to new heights but the experience has provided me with the skills to think laterally, problem solve and delve into new areas of highly thought provoking science.

Special thanks must also go to Craig Grimmer and Caryl Janse Van Rensburg who provided an overabundance of technical expertise using nuclear magnetic resonance and gas chromatography-mass spectrometry analytical techniques respectively. Without their guidance and support, this project would not have achieved the level of success that has been obtained.

In addition, I would like to thank the technical staff of the University of KwaZulu-Natal: Mr. Shall Ball, Mr. Faysil Shaik, Mr. Bheki Dlamini, Ms. Prudence Lubanyana, Mr. Paul Forder, Mr. Clarence Mortlock and Mr. Cornel Van Derwatt for their continued support.

A special mention must also go to my fellow Warren Lab students., whose cheerful laughs made the learning process exciting every day in the lab.

Finally, an exceptional thank you to my family, without whose continued support and telling me to endure mixing my chemicals, the success of this synthetic CVD diamond study would not have been achieved.

To be given the opportunity to study is the greatest gift in life, to which I am eternally grateful…

Mike and Jenni.

My parents.

TABLE OF CONTENTS

Abstract

The semiconductor-mediated oxidation of alcohols to pharmaceutical and biologically relevant intermediary reactants has long been a fascinating research field for organic chemists. Alcohols have been conventionally oxidised while using harsh organic acids and oxidising agents that are toxic, noxious and costly. However, recent developments in the field of photocatalysis have produced excellent results that have led to the discovery of environmentally friendly semiconductor-mediated oxidation reactions which have effectively oxidised activated, heterocyclic and highly unreactive alcohols.[1],[2],[3]

In the present study, novel synthetic chemical vapour deposition (CVD) diamond semiconductors were introduced to attempt alcohol oxidations and dye degradations, while only being activated using radiant energy (ultraviolet emissions). Preliminary investigations produced non-selective and irreproducible benzyl alcohol conversions until 1,1,2-trichloroethane and saturated oxygen solutions were applied to the synthetic CVD diamond photo-oxidation study. While using 1,1,2-trichlorethane and oxygen, the gas chromatographic yields of benzoic acid rose drastically with multiple reactions having excellent conversions (70-99%).

However, as later discovered, oxygen gas was identified to be the true benzyl alcohol oxidant after radicalising during UVA-UVB (280-400 nm) exposure. In addition, the UVA-UVB radiation was identified as emitting photonic energies below the band gap of synthetic CVD diamond (5.5 eV) that were incapable of photo-activating the synthetic CVD diamond's band gap. Further investigations identified that the synthetic CVD diamond powders were unsuitable for alcohol oxidations since the boron dopant levels were too low (boron promoted electrical conductivity throughout the synthetic CVD diamond). Therefore, the project required a heavily boron doped synthetic CVD diamond square that was generously provided by the University of Bristol from the United Kingdom.

The heavily boron doped synthetic CVD diamond square was tested in various benzyl alcohol oxidation studies while using a stronger UVC (100-280 nm) radiation source. However, the synthetic CVD diamond was unable to mediate the conversion of benzyl

alcohol into neither benzaldehyde nor benzoic acid. Even after a brief visit to the University of Bristol in the United Kingdom, the research revealed that synthetic CVD diamonds were incapable of performing oxidations reactions due to the relative bang gap positioning of the valence and conduction bands respectively. Despite the synthetic CVD diamonds being unsuitable for alcohol oxidations, an interesting discovery identified that the band gap of synthetic CVD diamond possessed conduction band electrons with strong reduction potentials.

In addition to investigating the synthetic CVD diamond study, a brief interlude focused on alcohol oxidations while using a silver/alizarin red/zinc oxide photocatalytic system that had been previously developed within this research group. The technique was optimised to yield higher alcohol conversions while using less silver equivalents as a sacrificial electron donor. The addition of coupling the valuable aldehyde intermediates to nucleophilic trapping agents (benzyl ammine and methyl [triphenylphosphoranylidene]acetate) produced a range of *N*-benzylidenebenzylamines and methyl acrylates.

CHAPTER 1: Introduction

1.1.1) Oxidation reactions

Oxidation reactions are a ubiquitous assortment of chemical transformations that exist together with a plethora of reduction, alkylation, methasis, sulfonation and amination reactions amongst others. Each type of reaction that has been mentioned above retains a unique feature that enables it to be implemented by chemists to assist in the synthesis of a target molecule. In oxidation chemistry, highly specialised functions are performed by organic and inorganic oxidation reactions, which are expressed in this thesis due to their noteworthy capabilities.

1.1.2) Organic oxidations

Organic oxidation reactions advance through the abstraction of hydrogen and/or the addition of oxygen atoms from a parent molecule. Typical organic oxidations proceed as illustrated in figure 1 below. 2-(4-chlorophenyl)-2-phenylethanolbenzyl alcohol is oxidised *via* 2-(4-chlorophenyl)-2-phenylactaldehyde and finally onto 2-(4-chlorophenyl)-2-phenylacetic acid from the action of an oxidising agent ([O]). The oxidation will reach completion with the use of an oxidising agent such as potassium permanganate ($KMnO_4$) or Dess-Martin Periodane (DMP) or semiconductors including titanium dioxide (TiO_2) and zinc oxide (ZnO).
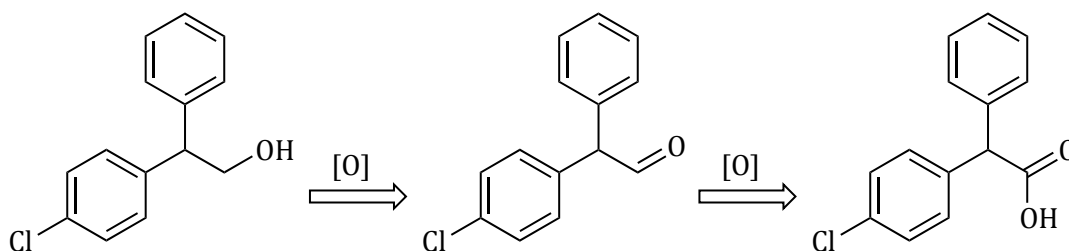
Figure 1: 2-(4-chlorophenyl)-2-phenylethanolbenzyl alcohol oxidation via proton removal and oxygen addition.

However, more highly advanced reaction systems are regularly investigated in the organic laboratory when unique biologically active compounds are desired. Therefore in order to synthesise such molecules that have projected biological properties, an assortment of synthetic techniques are implemented to reach the final synthesised product. During the course of study, various oxidation, de-methylation, reduction and cyclisation reactions (to mention a few) may be required. As reported by Groot,[4] labdane diterpenoids which originate in nature from a family of diterpenes (found in the gut of *Physeter macrocephalus L.* sperm whales) have been shown to be highly valuable as fragrance materials. Various derivatives exist with a decalin chain system being substitutionally present at the C_9 position. For example, the active sweet smelling perfumed component, 6α-hydroxy-Ambrox® has indispensible value in the fragrance industry and new synthetic methods requiring multiple oxidative routes are continuously being investigated (figure 2).
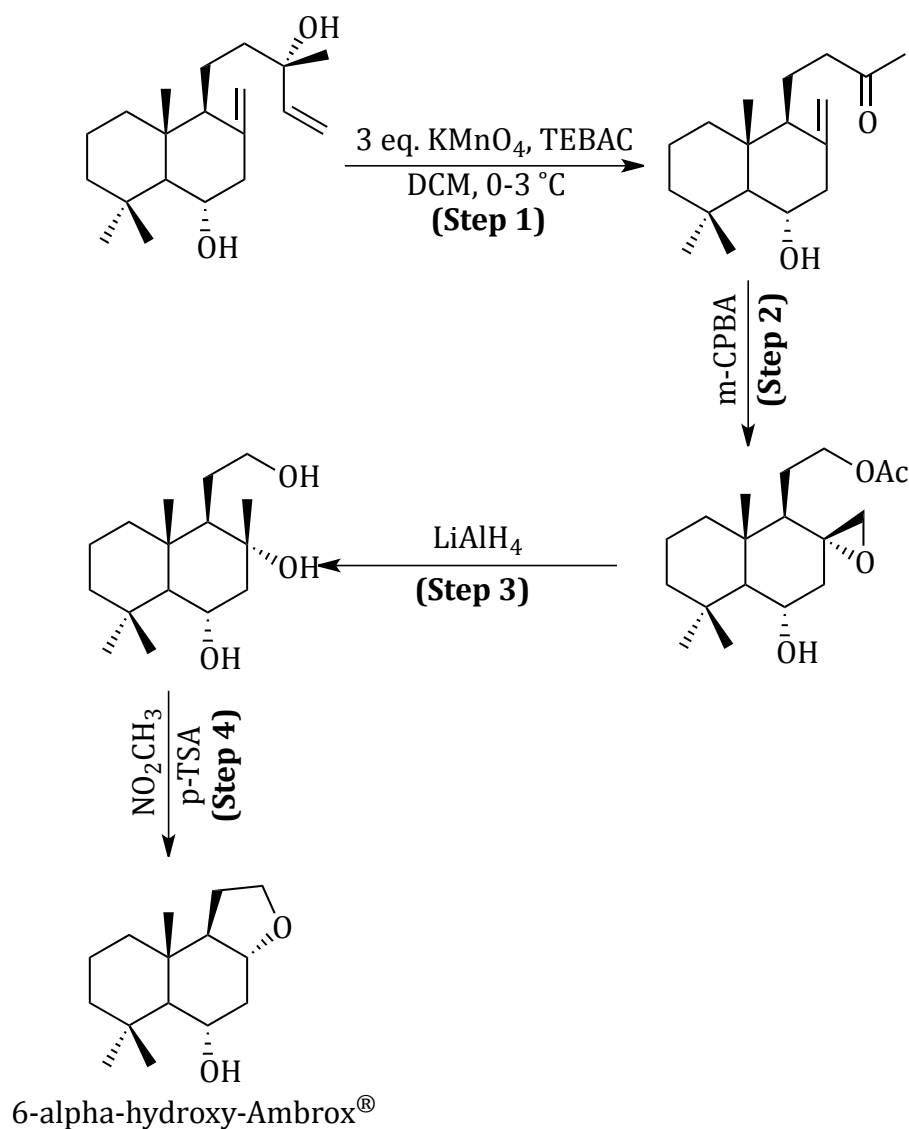
Figure 2: Groot's synthetic methodological approach towards the synthesis of (–)-Ambrox.

The research in figure 2 has clearly illustrated how oxidation reactions form a vital component of complex multi-step reactions. Without potassium permanganate ($KMnO_4$ [step 1]), the production of the methyl ketone would not be possible nor would the introduction of the acetate group while using a Baeyer Villiger oxidation with *meta*-chloroperoxybenzoic acid (*m*-CPBA [step 2]).

1.1.3) Inorganic oxidations

The alternative approach of an oxidation reaction is *via* electron transfer. An inorganic oxidation reaction involves the oxidation state of an inorganic specie by increasing its positive charge through the loss of electrons to the oxidant that is simultaneously reduced. An example of such an inorganic reaction occurs between the oxidation of iron and the reduction of oxygen as seen below (Equation 1).

$$4\ Fe^{2+} + O_2 \longrightarrow 4\ Fe^{3+} + 2\ O^{2-} \tag{1}$$
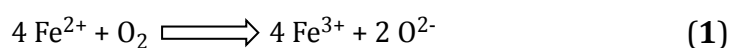
Iron is oxidised from Fe^{2+} to Fe^{3+}, while oxygen is reduced to singlet oxygen (O^{2-}). Numerous ferrous oxidation procedures have been discovered and reported in literature for a wide range of alcohol oxidations.[5] A recognised example of iron oxidation is the rusting of the *ss* Great Britain in Bristol, United Kingdom (figure 3).
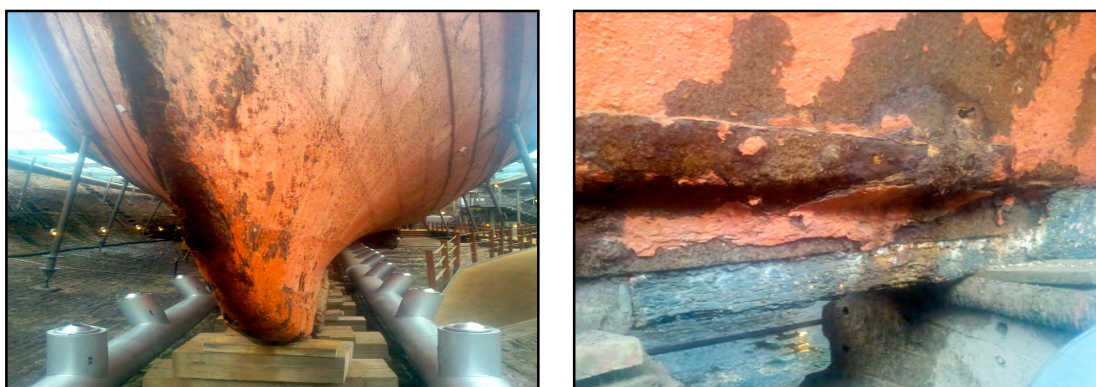
Figure 3: Rusting of the *ss* Great Britain's hull.

While the deck and inside of the *ss* Great Britain have been fully restored (figure 4), the hull has been severely damaged.

Figure 4: Restoration images of the *ss* Great Britain.

The rusting process on the hull is a form of oxidation, which occurs when ferrous metals are exposed to oxygen, forming ferric oxides (Fe_2O_3), 'rust'. Rust is a brittle form of iron oxide that is flake-like in appearance and can be easily displaced when agitated. Apart from moisture, seawater contains sodium chloride that rapidly reacts with ferrous metals and significantly enhances the oxidation process, forming ferric chlorides that can further degrade any ship's hull at an alarming rate. Therefore, in order to reduce further oxidation of the *ss* Great Britain's hull, dehumidifiers have been used to remove all traces of moisture (figure 5).
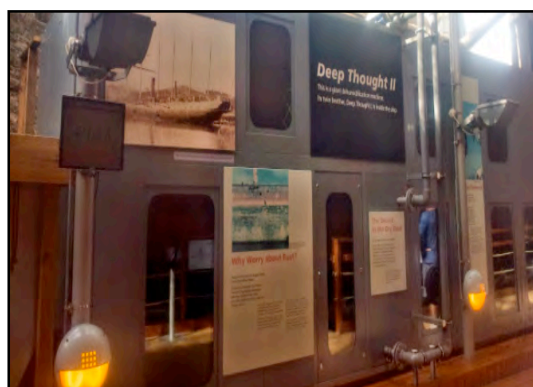
Figure 5: Air dehumidifier near the *ss* Great Britain's hull, Bristol, United Kingdom.

After having briefly introduced the two categories of oxidation reactions, this introduction will focus on accessing various organic and inorganic oxidation systems

(their advantages, disadvantages, selective oxidation control and scope), which will then be followed by identifying safer methods of oxidative catalysis using semiconductor oxidants. Lastly a review of synthetic chemical vapour deposition diamonds will be explored to establish an understanding of electrochemical grade synthetic chemical vapour deposition (CVD) diamonds and their role in semiconductor mediated oxidation reactions. The knowledge gathered from the synthetic CVD diamond research will be applied to semiconductor facilitated alcohol oxidation studies during the course of the report that follows.

1.2) Typical oxidation reagents

There is an overabundance of oxidation techniques for the conversion of alcohols, carbonyls, amines, amides, phenols, sulfides and a myriad of other compounds available. However, for the course of this study, emphasis on alcohol oxidations will be discussed with a brief review of the literature by reporting the highlights of these oxidation studies. Furthermore, each of the oxidation topics mentioned in the following chapter has a large number of variations available, with only the most appropriate examples being used for discussion in this study.

1.2.1) Natural product synthesis

Natural product chemistry is an important field in organic synthesis. As the name suggests, natural product molecules originate from nature and have typically been harvested from plants and animals for various studies. Although, as governmental laws and environmental protection agencies (World Wildlife Fund) are raising flora and fauna protection, the collection of various natural products is rapidly declining. A good example is from the previously mentioned Ambrox® report. The active pleasant aroma (Ambrox®) has been conventionally harvested from whales. Due to moratoriums on whaling, governmental laws have prohibited the collection of such compounds from oceanic fauna. There is still an ever-growing need for natural products in synthetic chemical procedures, which has driven chemists to manufacture natural products using synthetic methodologies to meet the requirements of industry.

One further organic oxidation example has been addressed below to illustrate the importance of oxidative chemistry to natural product synthesis that will be followed by the application of various inorganic oxidations in chemical procedures.

Ascorbic acid is a component of liquid refreshments and functions as a widely acknowledged palliative to prevent flu. As reported by Fleming,[6] ascorbic acid was extracted and crystallised from orange juice in 1928. Furthermore, Haworth clarified its chemical structure by reporting two synthetic procedures in 1933 (figure 6).
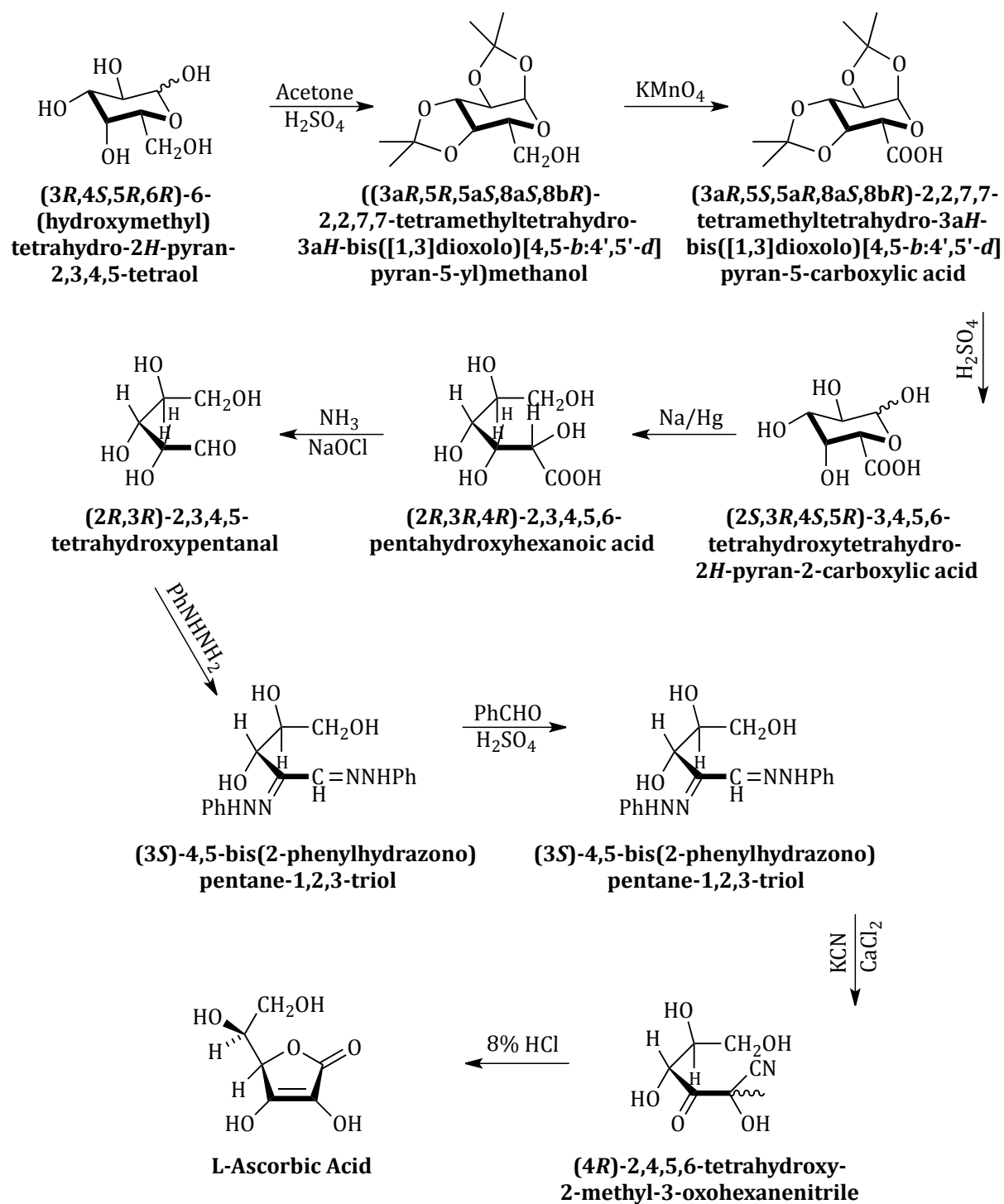
Figure 6: Synthetic ascorbic acid procedure proposed by Haworth and Hirst.[6]

The scheme shows the following compounds and reaction conditions:

(3R,4S,5R,6R)-6-(hydroxymethyl)tetrahydro-2H-pyran-2,3,4,5-tetraol

→ Acetone / H_2SO_4 →

((3aR,5R,5aS,8aS,8bR)-2,2,7,7-tetramethyltetrahydro-3aH-bis([1,3]dioxolo)[4,5-b:4',5'-d]pyran-5-yl)methanol

→ $KMnO_4$ →

(3aR,5S,5aR,8aS,8bR)-2,2,7,7-tetramethyltetrahydro-3aH-bis([1,3]dioxolo)[4,5-b:4',5'-d]pyran-5-carboxylic acid

→ H_2SO_4 →

(2S,3R,4S,5R)-3,4,5,6-tetrahydroxytetrahydro-2H-pyran-2-carboxylic acid

→ Na/Hg →

(2R,3R,4R)-2,3,4,5,6-pentahydroxyhexanoic acid

→ NH_3 / NaOCl →

(2R,3R)-2,3,4,5-tetrahydroxypentanal

→ $PhNHNH_2$ →

(3S)-4,5-bis(2-phenylhydrazono)pentane-1,2,3-triol

→ PhCHO / H_2SO_4 →

(3S)-4,5-bis(2-phenylhydrazono)pentane-1,2,3-triol

→ KCN / $CaCl_2$ →

(4R)-2,4,5,6-tetrahydroxy-2-methyl-3-oxohexanenitrile

→ 8% HCl →

L-Ascorbic Acid

18

1.2.2) 2-Iodobenzoic acid

1-hydroxyl-1-oxo-1H-1λ5-benzo[d][1,2]iodoxol-3-one, λ^5-iodane,[7] (figure 7) more commonly known as 2-Iodobenzoic acid (IBA) is amongst a range of various iodine based oxidants. Furthermore, periodanes and their oxidised derivatives (iodoso and iodoxy derivatives) have been widely used for alcohol and aldehyde oxidations with a well known example being Dess-Martin Periodane.[8]

IBA has been identified as an extremely important oxidising reagent for performing a wealth of oxidation reactions and was first created and used by Hartman and Mayer.[9] For many years, IBA was ignored for its potential applications in oxidation reactions due to its high insolubility in laboratory solvents (as a result of IBA polymerisations) and explosive characteristics.[7]
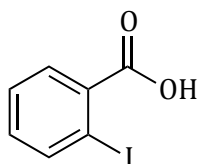
Figure 7: Chemical Structure of 2-Iodobenzoic acid.

Ninety years later, Dess and Martin harnessed the potential application of IBA. From an acetic acid facilitated reaction (Figure 8), the IBA was transformed into a hypervalent iodine oxidising reagent which had superior solvent solubility, known today as Dess-Martin Periodane (DMP).[10]

2-Iodobenzoic acid   **Cyclised intermediate**

HOAc
Ac$_2$O
100 °C

Dess-Marin Periodane
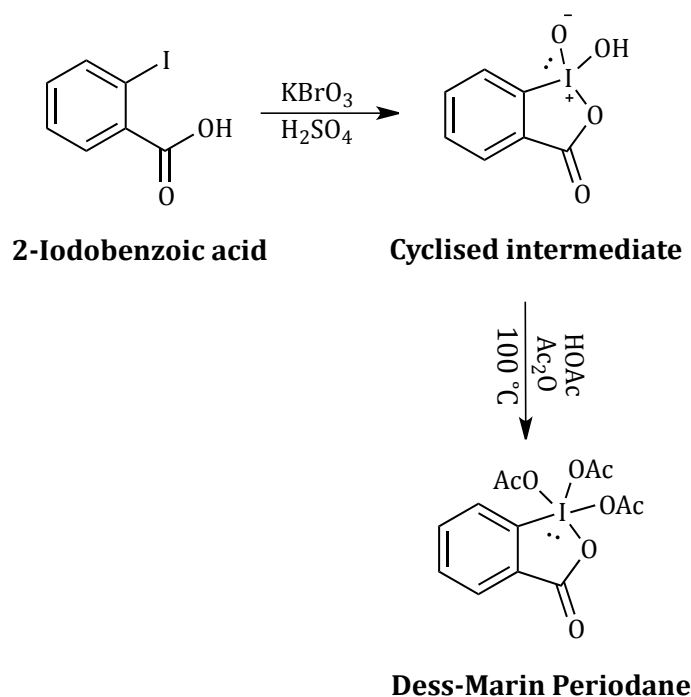
Figure 8: Reaction process performed by Dess and Martin to create the modified IBA compound 'Dess-Martin Periodane'.

DMP has been involved in numerous oxidation reactions. Due to its relative mild and non-toxic nature compared to other oxidants such as dimethyl sulfoxide (DMSO) and chromium (VI),[7] its suitability for alcohol oxidations,[11] natural product synthesis[12],[13],[14] and heterocyclic ring closures has not gone unnoticed.[15] DMP's mode of oxidative action has been identified as nearing a stoichiometric approach that liberates acetic acid and the carbonyl product. The oxidation proceeds through an intramolecular rearrangement where the hydroxyl group co-ordinates to the hypervalent iodine in a cyclised intermediate step as depicted below (figure 9).
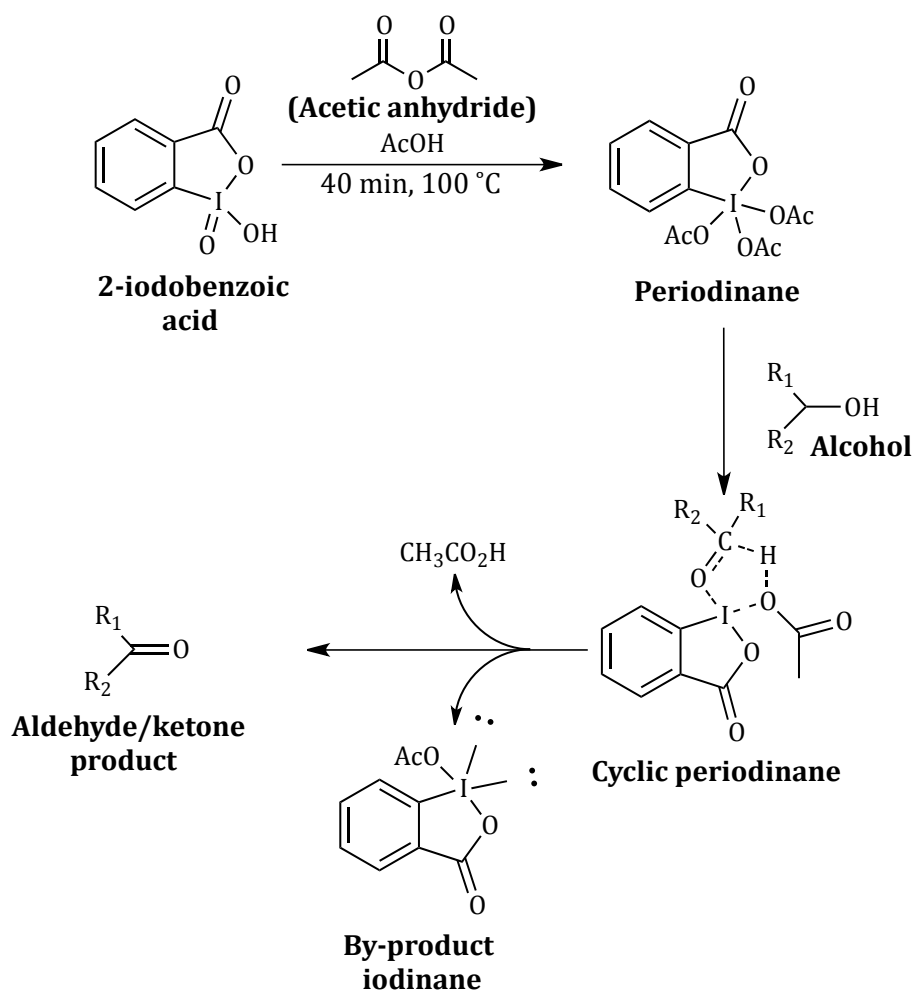
Figure 9: DMP mediated oxidation of alcohols.

1.2.3) Chromium assisted oxidations

It has been reported in the chemical literature that chromium and especially chromium (VI) oxide has been one of the most versatile chromium oxidants of primary alcohols[16] that has merited its (chromium [VI] oxide) scope being addressed in the paragraphs which follow. There is however a range of lower oxidation states of chromium that have been applied as oxidising agents for alcohol conversions. In summary, a typical chromium (VI) oxidant includes chromic acid, meanwhile chromium (V) species such as potassium chromium oxypentachloride ($CrOCl_5 \cdot 2KCl$), chromium pentaflouride (CrF_5) and chromium (V) oxide (Cr_2O_5) exist.[17] There have also been lower oxidation states of chromium (IV and III) such as chromium (IV) dioxide (CrO_2), barium chromate (IV) and chromium (III) trioxide-pyridine being reported in the oxidative chemical literature.[17]

However, since chromium (VI) has been mentioned as the most widely used chromium specie, aliphatic alcohol and solvent-less oxidation studies will be acknowledged with reference to chromium (VI).

In 1999, Riahi, *et al.,* studied alcohol oxidations through the control of a purpose designed chromium (VI)-hydroperoxide system.[18] They identified that the type of peroxide (*tert*-butyl or cumyl hydroperoxide) used would greatly impact on the yield of the constitutional isomer produced as well as the rate of oxidation (figure 10).
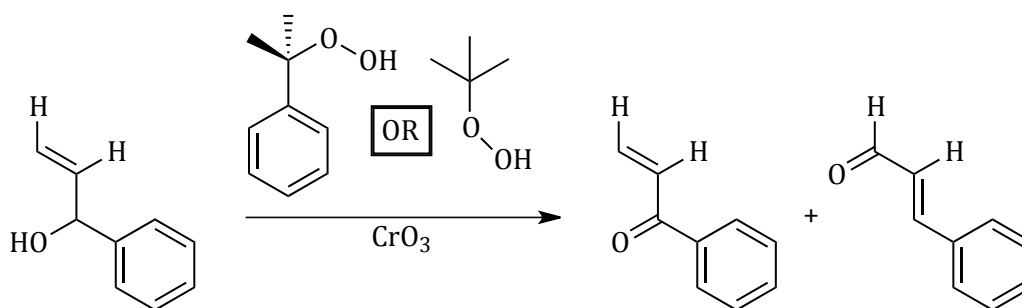

Figure 10: Alcohol oxidations using chromium-hydroperoxide oxidants.

It was proposed that there were mechanistic changes due to the alcohol's alkyl chain length, which interacted with the *tert*-butyl hydroperoxide or cumyl hydroperoxide. Twelve experiments were investigated to prove this and it was identified that *tert*-butyl hydroperoxide yielded higher alcohol conversions while cumyl hydroperoxide produced higher isomeric diversity between the two products.[18]

In other research published by Lou and Xu, chromium trioxide (CrO_3) was revealed to be an effective oxidant for solvent-less reactions.[16] It was well documented that chromium trioxide effortlessly initiates the over oxidation of alcohols to unwanted acid derivatives with several plausible solutions being mentioned in the chemical literature and these have been subsequently reviewed in this discourse. The chromium reagents researched for selective alcohol oxidation include mixtures of CrO_3 and *t*-butyl hydroperoxide,[19] complexes of 3,5-dimethylpyrazole on CrO_3[20] and CrO_3 supported on various halogen-silanes and graphite.[21],[22],[23] To subdue the potent oxidative native of CrO_3, Lou and Xu transformed six various alcohols into the corresponding aldehydes (without any over oxidation) with fair to good yields (60-90%) in short reaction times (three to

eight hours) while using a solventless approach.[24] The reactions were simple to construct, where the CrO_3 was mixed with an alcohol and stirred until the reaction was deemed complete using thin layer chromatography.

1.2.4) 2,2,6,6-tetramethyl piperidyl radicals

Scientists have discovered radical chemistry as a thought provoking field of study with its application to oxidation reactions having a similar level of interest. The following description into radical oxidants will be introduced using 2,2,6,6-tetramethylpiperidine (TEMPO) as an example. There are however numerous radical oxidants that have been identified as effective catalysts for oxidising alcohols namely *N*-hydroxyphthalimide (NHPI).[25] *N*-hydroxyphthalimide has exhibited an enhanced functionality when combined with $Fe(NO_3)_3$ and molecular oxygen for excellent secondary aliphatic and benzylic alcohol oxidations.[25] Further studies have reported benzylic, propargylic and allylic alcohol oxidations using a cooper (II) complex with a sulfonated quinoxaline scaffolding.[26]

During the latter period of the 20th century, Golubev, *et al.,* (1965)[27] discovered that the application of an oxoammonium salt (the stable form of the 2,2,6,6-tetramethylpiperidine radical [TEMPO]) could facilitate a simple oxidation reaction. They identified that the treatment of ethanol with the oxoammonium salt produced acetaldehyde during the oxidation process (figure 11).
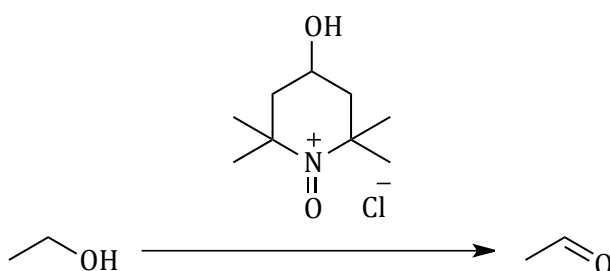

Figure 11: Oxidation of ethanol to acetaldehyde using a simple oxoammonium salt (4-hydroxyl TEMPO).

A few years later, in 1975, Cella, *et al.,*[28] identified a "one-pot process" (further elaboration of the one-pot process will be discussed in 1.4.1), where peracids were

recognised as suitable secondary oxidants that were mild enough to produce various oxidised products starting from sulfides,[29] amines[30] and olefins.[31] Cella also recognised that peracids were capable of initiating *N*-oxoammonium salt facilitated alcohol oxidations and due to their combined mild and solvent solubility nature, they were acknowledged to be potent acid-*N*-oxide mediated alcohol oxidants.[28]

In Cella's work,[28] 2,2,6,6-tetramethylpiperidine hydrochloride (TMP.HCl, **1**) was treated with a catalytic amount of *m*-chloroperbenzoic acid (MCPBA, **2**). It was hypothesised that the MCPBA functioned as a secondary oxidant, oxidising the TMP.HCl to TEMPO (**3**), which was subsequentially oxidised to the *N*-oxoammonium salt (**4**), the active primary oxidant of TMP.HCl. The active *N*-oxoammonium salt that was generated *in-situ* was then able to fulfill the alcohol oxidation within the same reaction. This is illustrated below in figure 12.
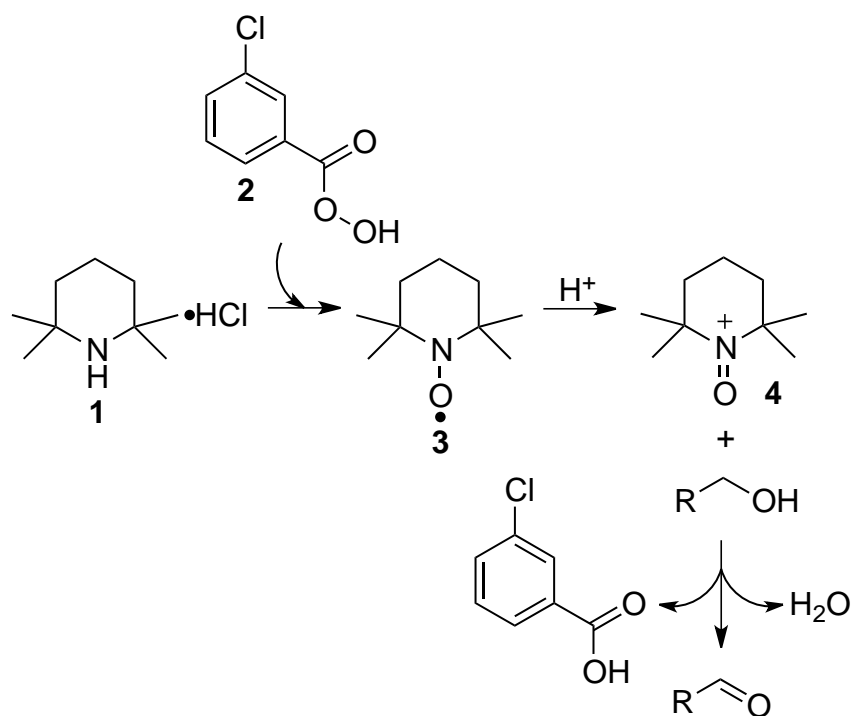

Figure 12: MCPBA facilitated oxidation of alcohols using TMP.HCl.

More recently in 2011, Richter and Garcia Manchenno[32] extended the knowledge base of TEMPO salts. Results indicated that the action of a TEMPO salt (T+BF4-), mediated the oxidative synthesis of quinoline analogs depending on the quantity of T+BF4- used.

During initial studies, glycine was reacted with styrene and only 1.2 equivalents of $T^+BF_4^-$. As expected, a poor yield of the resultant quinoline was detected due to the lesser mass of the TEMPO salt used. The low catalytic loading of $T^+BF_4^-$ only facilitated the formation of the iminium ion meanwhile the dehydrogenation of the tetrahydroquinoline intermediate by $T^+BF_4^-$ did not occur.

Further investigations identified that a minimum of two $T^+BF_4^-$ equivalents were necessary to complete the two-step oxidation of the aniline derivative and olefin to the quinoline. It was noted however, that the reaction kinetics were temperature dependent, thus a further one equivalent of $T^+BF_4^-$ aided a high conversion of the tetrahydroquinoline to the fully oxidised quinoline (figure 13).
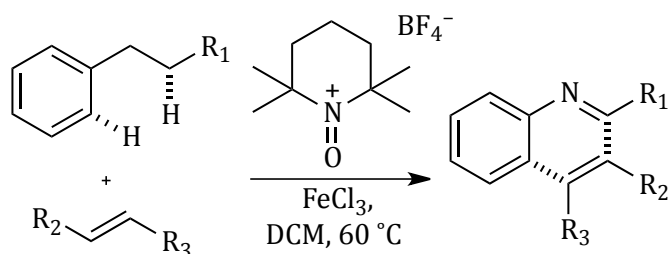
Figure 13: TEMPO Mechanistic insight proposed by Heinrich Richter and Olga Garcia Manchenno.

1.2.5) Ceric ammonium nitrate.

Following the review by Smith,[33] oxidation studies using ceric ions have rapidly increased. Various ceric ion derivatives such as cerium sulfate, cerium (IV) glycol and carbonyl complexes exist as well as ceric ammonium nitrate ([CAN], a common inorganic salt), which will be discussed in the following text. CAN has been proven to be an effective catalyst with a wide oxidative scope for the oxidation of primary alcohols to their corresponding aldehydes and for the oxidation of toluene through to phenol and other carbonyl derivatives,[34] meriting its review in this introduction. In addition, it (CAN) has also been identified to facilitate nitratoaldehyde synthesis due to the incorporation of a nitrate group from the oxidant itself.[34]

Ceric ammonium nitrate has also been recognised by Shanmugam and Perumal[35] as an important catalyst which favours the oxidative synthesis of pyrimidine parental

compounds that have powerful antagonist properties against the HIV virus by acting against the cortico-tropin receptor. The CAN method of synthesising these important biologically active molecules favour the regioselective synthesis of either ethyl 2,4-dioxo-6-phenyl-tetrahydropyrimidin-5-carboxylate or ethyl 6-methyl-4-aryl(alkyl)-pyrimidin-2(1H)-one-5-carboxylate when using solvent controlled reaction conditions.

Under moderate reaction temperatures (80 ℃), Shanmugam utilised CAN in acetic acid (due to the excellent solubility of 3,4-dihydropyrimidin-2(1H)-one in acetic acid) to yield ethyl 2,4-dioxo-6-phenyl-tetrahydropyrimidin-5-carboxylate. Initial studies presumed that the dehydrogenation would occur under the acetic acid conditions, although no dehydrogenated product formed. It was believed that this resulted from the involvement of an unstable coordination of the hydrogenated intermediate to acetic acid. However, basic conditions (sodium hydrogen carbonate, $NaHCO_3$) promoted regioselective control that led to the synthesis of ethyl 6-methyl-4-aryl(alkyl)-pyrimidin-2(1H)-one-5-carboxylate, which was the dehydrogenated product of the 3,4-dihydropyrimidin-2(1H)-one starting material (figure 14).
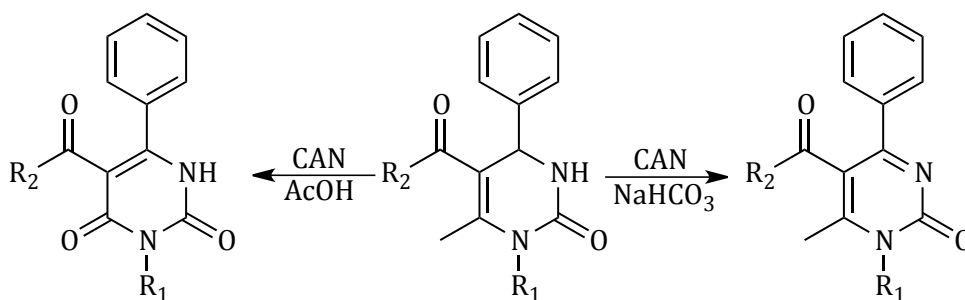
Figure 14: Regioselective oxidative control of 3,4-dihydropyrimidin-2(1H)-one.

In other reports, Madabhushi, *et al.,*[36] broadened CAN studies. They introduced an interesting study with the first documented synthesis of pyrroles using CAN as an one-electron transfer oxidant.

The CAN system was tested using a number of solvents, which included: *N,N*-dimethyl-formamide, 1,2-dichloroethane, 1,4-dioxane, tetrahydrofuran and toluene.

Optimisation procedures were achieved while using 1,4-dioxane with a one molar CAN equivalent. It is important to note that the reaction conditions (amount of CAN) appeared to be in excess because catalytic systems should only require a nominal amount of catalyst to hasten a chemical reaction. However, under standard laboratory conditions (three hour reflux in 1,4-dioxane), high yields (73%)[36] of pyrroles-2,3,4,5-tetracarboxylate derivatives were synthesised from dimethyl acetylenedicarboxylate and a collection of amine starting reactants (figure 15).

tetramethyl-pyrrole-2,3,4,5-tetracarboxylate derivatives
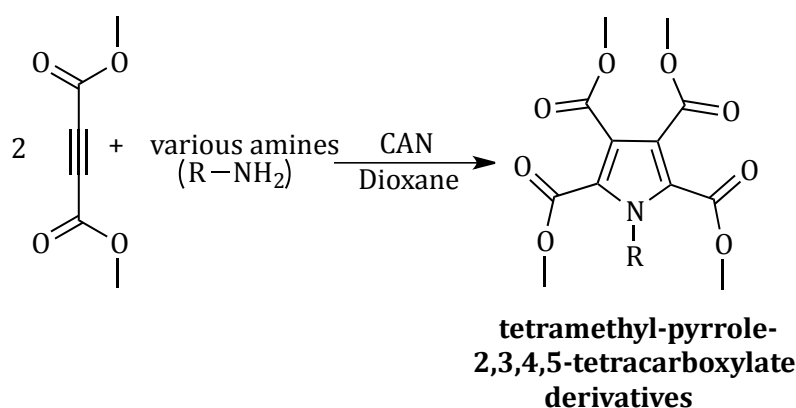
Figure 15: CAN facilitated synthesis of pyrrole-2,3,4,5-tetracarboxylates.

The CAN oxidant was confirmed to be a necessary during the optimisation study. In the absence of any CAN, the dimethyl acetylenedicarboxylate formed an un-cyclised 1:1 adduct of the dimethyl acetylenedicarboxylate and chosen amine.

1.2.6) Oxidation reactions using dimethyl sulfoxide.

Dimethyl sulfoxide (DMSO) is a common organic solvent, which has numerous applications in synthetic procedures such as the Parikh-Doering and Swern Oxidations due to its oxidative nature and high polarity index. A brief review of this versatile inorganic specie will be mentioned below to illustrate its value in alkyne oxidations.

During the past decade, a French research group coupled microwave energy with an active Lewis Acid catalyst in DMSO for the successful transformation of diarylalkynes into 1,2-diarylketones (Figure 16).[37]

Figure 16: Transformation of diarylalkynes into diarylketones using DMSO and microwave energy.

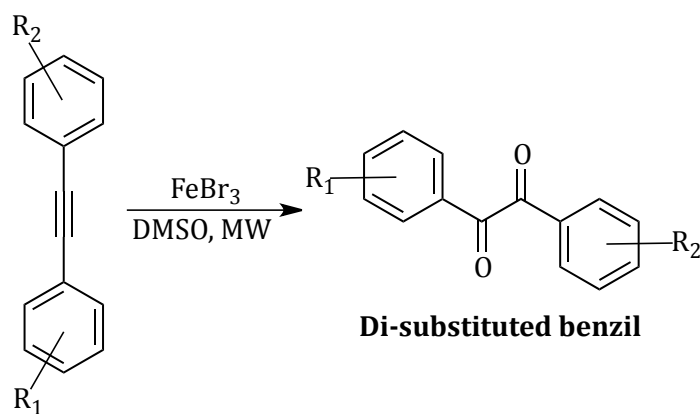An optimisation study was conducted to identify the most suitable transition metal salt to achieve a 1,2-arylalkyne oxidation to 1,2-diaryldiketones. During the investigations, both ferric bromo and chloro salts were evaluated. Chloro salts gave similar results although reaction times were significantly longer than bromo equivalents. After determining that chloro transition metal salts were less effective than bromo metal equivalents, various metals; (nickel (Ni), manganese (Mn), indium (In) and copper (Cu)) were compared to iron (Fe). While the various metals produced the desired products, the yields were lower and reaction times were extended compared to iron. After successfully identifying the optimal reaction conditions, over a dozen 1,2-diaryldiketones were synthesised with yields up to 75%.[37] Favourable catalytic parameters were met with low catalyst loadings (10 mol%) that yielded various 1,2-diaryldiketones in periods ranging from 9-120 minutes.[37]

1.2.7) Copper chloride salts

In recent years, copper has been discovered as an excellent co-catalyst for TEMPO oxidation systems. In various reports, copper and TEMPO have oxidised a range of aliphatic, cyclic, aromatic and heterocyclic alcohols with excellent yields being achieved.[38],[39] Although there has been an astonishing number of copper oxidation systems using TEMPO, a review of a simple copper chloride salt which participated in the total synthesis of (+)-Davidiin will be discussed (since TEMPO oxidation reactions have already been mentioned in 1.2.4 of the introduction).

While it was identified that bromide metal salts were ideal for the oxidation of diarylalkynes in a DMSO environment,[37] Kasai, *et al.,*[40] from Kwansei Gakuin University, Japan, introduced copper chloride (CuCl$_2$) as a mild oxidant. The recent natural product study has elevated the literature of ellagitannins. These are a class of ligand blocking agents, which inhibit ligand-receptor site binding. In Kasai's publication, the research team established a retrosynthetic procedure for the development of (+)-Davidiin ellagitannin with axial rich conformations from a simple D-glucopyranose sugar (figure 17).
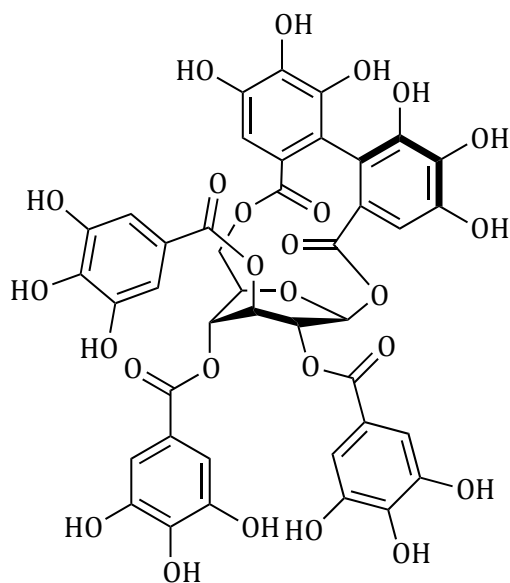
Figure 17: Chemical structure of (+)-Davidiin ellagitannins.

The synthesis fashioned a unique 'conformational lock system' to synthesise (+)-Davidiin which allowed the molecule to contain numerous thermodynamically unfavourable axial conformational positions. Under natural conditions, D-glucopuryanose sugars have a preference to be equatorial rich, although the axial rich environment was guaranteed through the introduction of a 1,6-hexahydroxydiphenyl (HHDP) bridge.

In order to satisfy the erection of the essential bridging component, an intramolecular oxidation was required during the synthetic strategy; this was neatly performed using copper (II) chloride/n-butylamine. As mentioned by Kasai,[40] it was a mild oxidant that

selectively completed the oxidation via gallate coupling to produce a 78% yield of the intermediate product (figure 18).
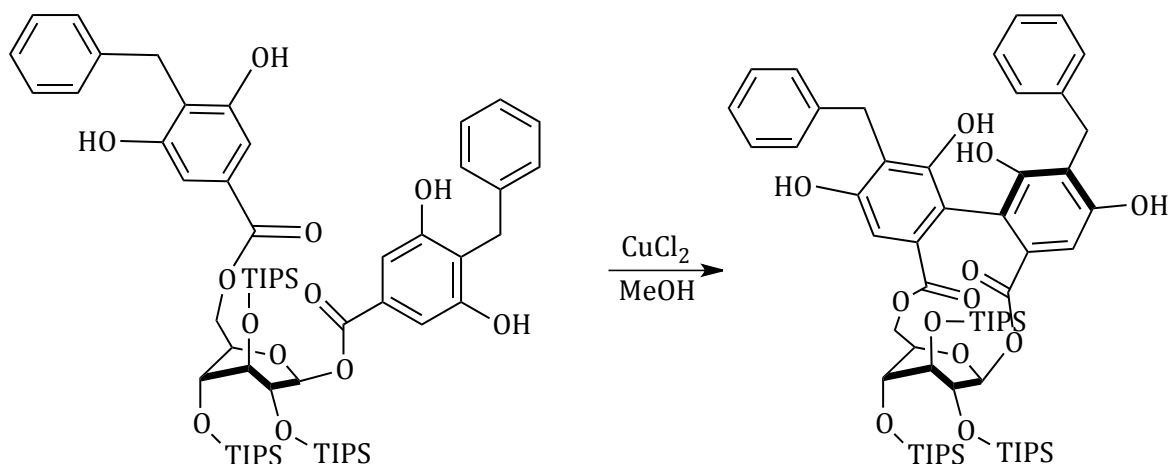
Figure 18: Cu(II)chloride facilitated aryl-aryl coupling.

As reported until now, previous studies have illustrated effective oxidative capabilities. However, their homogenous nature inhibits catalyst recycling. Contemporary 'Green Chemistry' has shifted scientists to conform to the 'Twelve Rules of Green Chemistry'[41] and utilise heterogeneous 'recyclable' catalysts for oxidation reactions that will be discussed in the paragraphs which follow.

1.3) Methods for effective catalysis

1.3.1) Tandem oxidation-one-pot processes

In the recent chemical literature, there have been a variety of oxidation studies using 'Tandem Oxidation – One-Pot Processes' for the oxidation of alcohols to aldehydes. This is a highly unique approach to complete numerous organic processes via isolated stages that are safe, non-toxic and efficient. The reaction requires initiation, sealed if required and to experience no interference until the experiment is completed (figure 19).

$$A \xrightarrow[\text{Solvent Y, °C, hrs.}]{\text{Reagents 1,2,3}} A' \xrightarrow[]{\text{'In-situ' Intermediate}} B \qquad \text{'Tandem Oxidation Process'} \qquad (2)$$
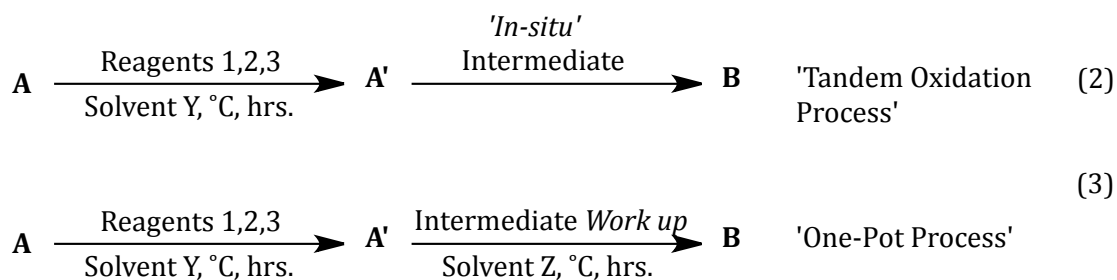
$$(3)$$

$$A \xrightarrow[\text{Solvent Y, °C, hrs.}]{\text{Reagents 1,2,3}} A' \xrightarrow[\text{Solvent Z, °C, hrs.}]{\text{Intermediate } Work\ up} B \qquad \text{'One-Pot Process'}$$

Figure 19: Depiction of tandem oxidation and one pot processes.

Fogg classified tandem oxidation reactions using two very important criteria.[42] For a reaction to be classified as "tandem," it must be performed under identical reaction conditions (no variations in; temperature, solvents, gases and or pressures) throughout the entirety of the experiment. Fogg further specified that tandem oxidation processes could either be described as autocatalytic or as orthogonal catalysis. Autocatalysis tandem oxidation processes use one catalyst (cat. 1) to complete the reaction, while orthogonal catalysis may use two or more catalysts (cat. 1 and cat. 2) to achieve the completion of the oxidation reaction (figure 20 below).
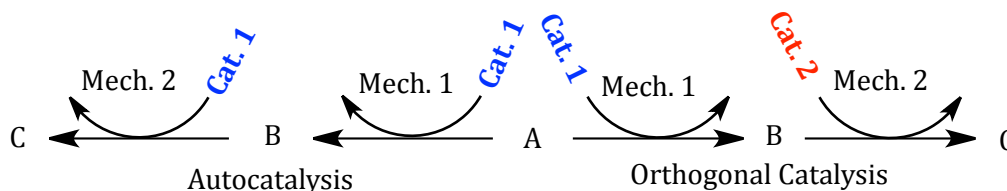
Figure 20: Autocatalysis and Orthogonal Catalysis tandem oxidation processes.

During his research, Fogg also elaborated on one-pot processes (also known as 'sequential' or 'assisted tandem' reactions) and noted that the addition of various reactants and catalysts while the reaction was in progress was in accordance with one-pot process parameters.

With an introduction into tandem oxidation and one pot processes from the findings of Fogg,[42] a review of the chemical literature will identify applicable cases where tandem oxidation and one pot processes have been used with attention being focused on metal oxide (MnO_2, TiO_2 and ZnO) semiconductor oxidants.

1.3.2) Manganese dioxide's extensive diversity

Early studies into MnO_2 had numerous chemists interested in this white metal oxide. In 1995, Elmorsy, utilised MnO_2 in combination with triazidochlorosilane under anhydrous conditions to selectively transform various aldehydes to acyl azides.[43]

The important contribution of this research was that using modern interpretations, it could be considered to be a "One-Pot Process" (Further elaboration of the one-pot process has been addressed during an introduction into the work of Taylor[44]). This work by Elmorsy coupled triazidochlorosilane with activated MnO_2 under anhydrous conditions to facilitate the transformation of various aldehydes with electrons donating and withdrawing groups to various aromatic acyl azides (figure 21).
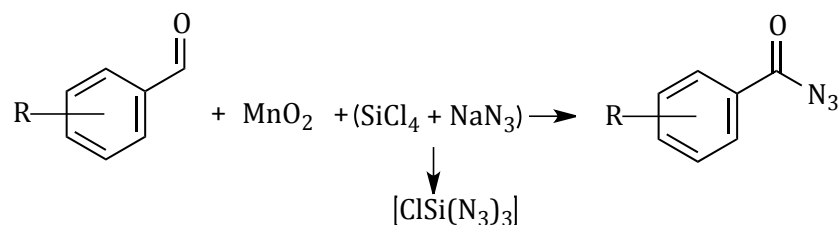

Figure 21: Triazidochlorosilane -MnO_2 facilitated azidation of aldehydes.

The isolation of the acyl azides presented in figure 21 were easily isolated after each reaction which was important to note as aromatic acyl azides are sensitive compounds that can be easily altered from Curtius Rearrangements and produce alkyl isocyanates.[43] Since the triazidochlorosilane-MnO_2 system was a mild oxidative system, the rearrangement was eluded.

In 2007, Phillips, *et al.,* studied the oxidative olefination pathways of unsymmetrical α,β-unsaturated hydroxy esters as products of various diols.[45] They indicated not only the mild nature and selectivity of MnO_2 but also its limitations as well. Never the less, MnO_2 was efficient at converting diols to the mono-oxidised hydroxy-aldehyde derivatives that were trapped using various Wittig Reagents. Phillips, *et al.,* identified during reaction work-up procedures that 1,4 and 1,5-diols proceeded through lactol cyclised intermediates,[46] which were going to be the next chapter of their further investigations.

In support of these findings, Phillips noted that Taylor[44] reported the oxidative cleavage of 1,2-diols while using MnO_2 as the oxidant[47] and also recognised that MnO_2-Wittig oxidation/olefination reactions of 1,3-propanediol only produced products of oxidative degradation.[45]

As a result, Phillips tried to synthesise dienyl-dienoates from diols but this was unsuccessful as (E)-2,4-pentadienoate was isolated from an intermediate (3-hydroxypropanal) product.[45] Therefore, Phillips believed that the elusive dienyl-diester was only achievable by controlling the oxidative nature of the MnO_2. Various model studies were performed with different grades and quantities of MnO_2; however the synthesis of α,β-unsaturated hydroxy esters were the only achievable result (figure 22).[45]
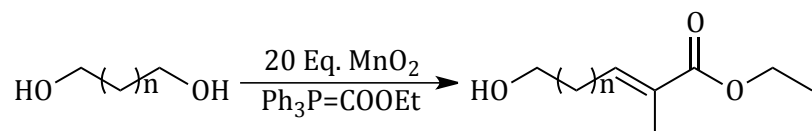
Figure 22: Mono alcohol oxidation-Wittig olefination of diols.

Furthermore, as a part of his research, Philips subjected the α,β-unsaturated hydroxy esters to additional oxidative/olefination reruns with higher temperatures and longer reaction times. However, the reactions only produced low dienyl-diester yields with the majority of species analysed being unreacted hydroxy esters.

Thus, to obtain the dienyl-diester in decent yields, Phillips approached the problem in a different direction after utilising pyridinium chlorochromate with a silica support layer and produced dienyl-diesters in good to high yields (figure 23).

Figure 23: PCC mediated dienyl-diester synthesis from α,β-unsaturated hydroxy esters.

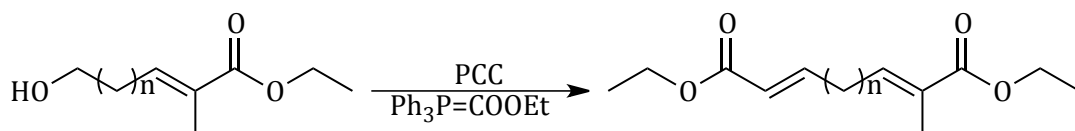In other studies, Taylor and co-workers[44] reacted activated alcohols with various stabilised Wittig Reagents in the presence of MnO_2 and dichloromethane. From the activated alcohols tested (propargylic, benzylic and allylic alcohols), the reactions progressed with great efficiency, yielding Z-enantiomers with high selectivity and yields (51-81%).[44]

The MnO_2-tandem oxidation study was also applied to modified Horner-Wadsworth Emmons (HWE) reactions during the investigation. The reactions achieved high yields and enantiomeric selectivity during the modified HWE studies (figure 24). For the success of each reaction, an *in-situ* generated carbanion was generated from either lithium hydroxide and molecular sieves or 7-methyl-1,5,7-triazabicycl[4.4.0]dec-5-ene (MTBD-guanidine base).

4-Nitrobenzyl alcohol

MnO_2, $(EtO)_2POCH(NHZ)CO_2Me$
MTBD, 6 hrs.

(*Z*)-Methyl 3-(4-nitrophenyl)-2-((phenoxycarbonyl)amino)acrylate
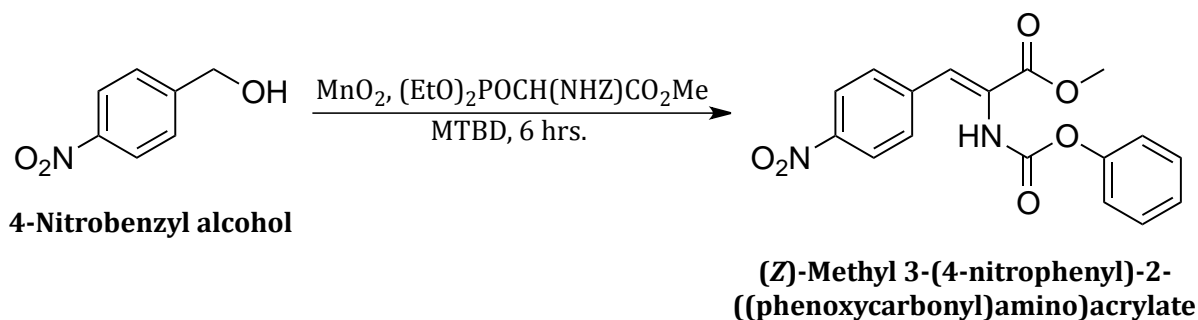
Figure 24: Tandem oxidation-Horner-Wadsworth-Emmons synthesis of alkenes.

However, additional challenges arose for the synthesis of selected benzylic, phenolic and allylic olefination compounds using unstable and semi-stabilised ylides. The reactions revealed varying degrees of success (55-92 %), although the *in-situ* generation of the unstable ylide from various phosphonium salts using 7-methyl-1,5,7-triazabicycl[4.4.0]dec-5-ene as the anion generator required longer reaction times and on occasion, the addition of titanium tetraisopropoxide (figure 25).

4-Bromobenzyl alcohol   **(*Z*)-1-Bromo-4-(pent-1-en-1-yl)benzene**

Figure 25: Horner-Wadsworth-Emmons oxidation/olefination using semi-stabilised ylides.

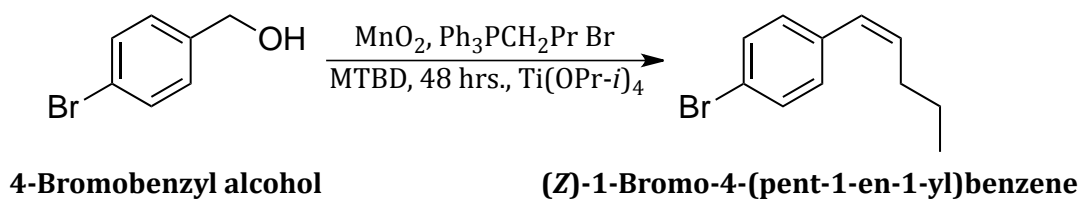Sulfur-ylide-TOPs were also investigated in cyclopropanation reactions. *α,β*-Unsaturated carbonyl adducts were formed from allylic alcohols and cyclised using sulfur ylides (figure 26).

(*Z*)-1-(Benzo[*d*][1,3]dioxol-5-yl)-   **Ethyl 2-(benzo[*d*][1,3]dioxol-5-ylmethyl)-3-**
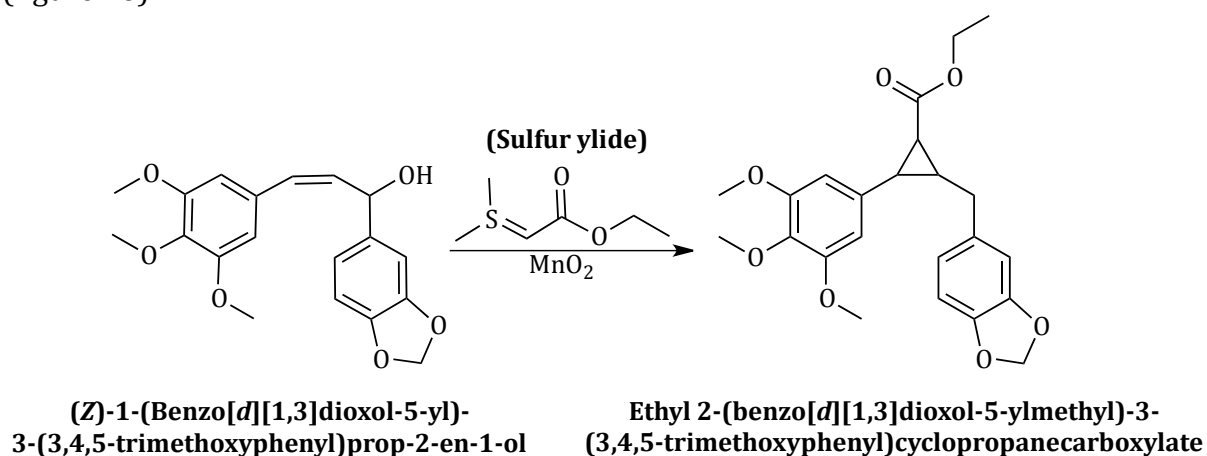**3-(3,4,5-trimethoxyphenyl)prop-2-en-1-ol**   **(3,4,5-trimethoxyphenyl)cyclopropanecarboxylate**

Figure 26: Sulfur-mediated cyclopropanation of allylic alcohols.

The addition of various Wittig reagents housed the tandem oxidation process-cyclopropanation/olefination reactions under the same tandem oxidation umbrella. The research delivered numerous cyclopropanated molecules with good yields (50-83%).[44]

In the article published by Taylor *et al.*,[44] there are still a multitude of further tandem oxidation processes that have been discovered and documented. These processes detail heterocyclic aromatic chemistry using nucleophiles with a nitrogen component. The range of products included oximes, amines, quinoxalines, dihydropyrazines, pyrimidines, nitriles and numerous other heterocyclic compounds, all of which have been synthesised using the tandem oxidation MnO_2 process.

1.4) Semiconductors

1.4.1) Conductors, semiconductors and insulators

While MnO_2 has been shown to be a highly capable oxidant in the chemical literature,[44] more contemporary and environmentally friendly oxidants have shown to be adept at demonstrating similar and even superior functionalities amongst a range of synthetic procedures.[44],[48] Therefore a shift towards metal oxide semiconductors will be pursued with a focus on photocatalysis.

In solid-state material science, there are two classes of substances that are capable of conducting electrical charge and these are known as conductors and semiconductors. Insulators belonging to a third class are considered incapable of promoting any significant degree of electrical conductivity through the solid. For the course of this thesis, semiconductor and insulator materials will be discussed in detail.

Łukasiak[49] has reported that semiconductor research began *circa* 1782 with the fundamental findings proposed by Volta. Subsequently, documentation on electrical conductivity measurements was recorded on copper and silver sulfide compounds. Although, it was not until 1874 that Karl Ferdinand Braun discovered metal sulfide rectification.

As reported by Bott,[50] semiconductor materials consist of a near infinite number of atoms and hence atomic orbitals. Within the material's structure, each atom has an associated atomic orbital that overlaps with a neighboring atomic orbital to form a new set of molecular orbitals. Considering that there are a near infinite number of molecular orbitals existing in electrically conductive materials, a simplification of band gap theory is obtained from a review of the electronic structure of solids in terms of the associated 'energy bands'. The energy bands that exist in conductive materials have a near infinite number of energy levels and are distributed according to their electron population (figure 27). Bott furthered mentioned[50] that the band level of lowest electron occupation is referred to as the valence band and the band level of highest unoccupied electron occupation is known as the conduction band. Therefore the interest of studying

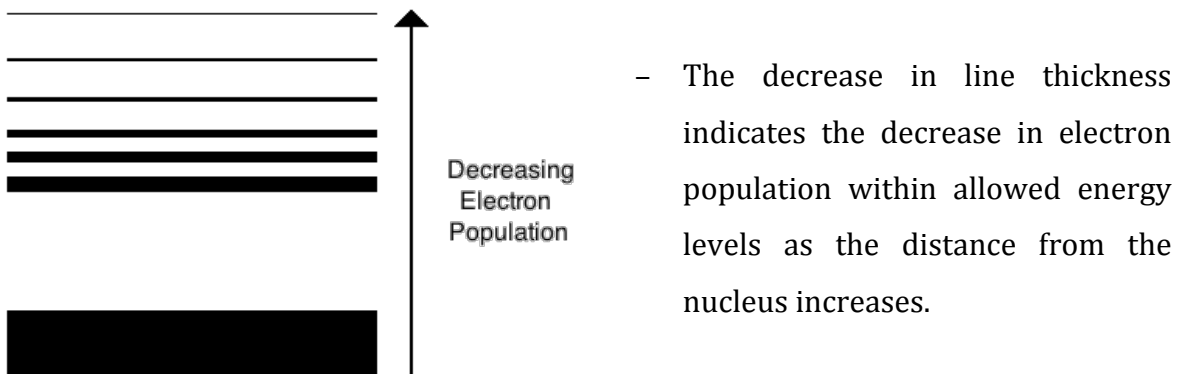conductive materials lies in the 'band gap energy' that exists between the valence band and conduction band.

– The decrease in line thickness indicates the decrease in electron population within allowed energy levels as the distance from the nucleus increases.

Figure 27: Declining electron occupations with increasing band gap energy.

Figure 28 below has illustrated that semiconductor materials and insulators have only allowed energy levels. This infers that electrons can only occupy discrete energy levels in the semiconductor and insulators' electronic structure. To emphasise this contention, simple band gap diagrams below depict the distinguishing features that catalogue materials as conductors, semiconductors or insulators.

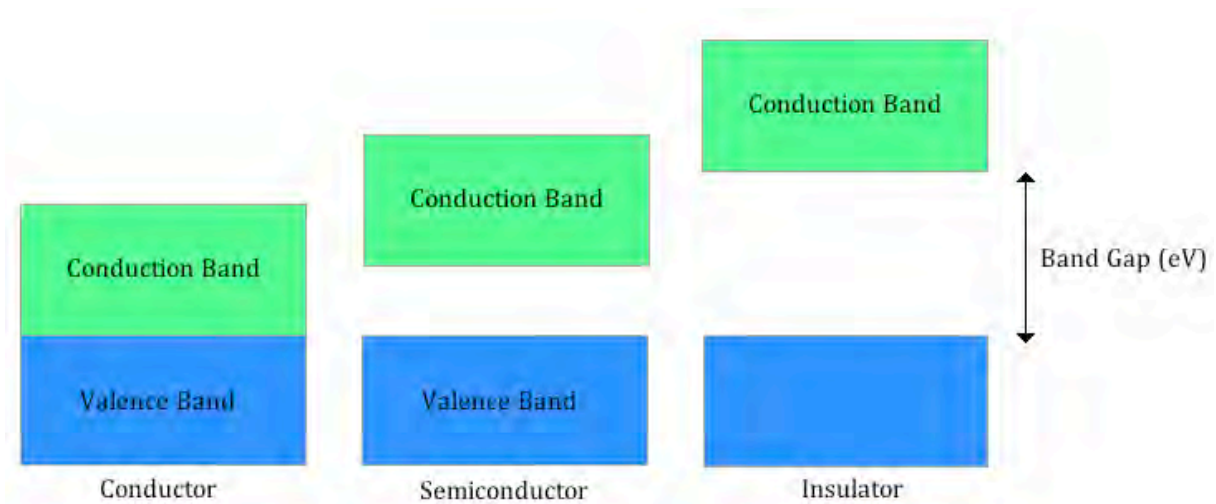**Figure 28: Band structure of conductors, semiconductors or insulators.**

As illustrated in figure 28, the noticeable difference between all three materials is the electron volt (eV) value of the respective band gaps. An electron will be promoted from one allowed energy level to the next when the energy requirement to facilitate the transition is provided (either thermally, electrically or photolytically).

The value of the band gap for a conductor is minimal. Hence materials such as copper, iron and silver are highly efficient conductors and used as conductive materials. Copper is the most widely used, finding applications for electrical wiring presented in industrial items such as impact drills and generators to household wiring. Of the remaining materials, semiconductors and insulators have band gaps larger than 1.0 eV.[51] A typical wide band gap semiconductor has an electron volt energy value of 1.0-3.4 eV with a selection of semiconductors tabulated below with their respective eV values (table 1).

Table 1: Typical eV energy values for selected semiconductors. [52],

Semiconductor	eV
WO_3	2.80
$\alpha\text{-}Fe_2O_3$	3.10
ZnO	3.20
$SrTiO_3$	3.20
TiO_2	3.20
BiOCl	3.32
ZnS	3.60

Insulators are materials that have excessively large band gaps. Species such as diamond (5.5 eV),[53] quartz(8.5 eV),[54] and cubic boron nitride (CBN, 6.4 eV)[55] are only a few examples. The energy needed to overcome the band gap is significant and therefore the requirement for very high-energy sources to convey electrical conductivity through the material is necessary.

When a semiconductor and/or insulator acquires a suitable energy source equal to or greater than the transitional band gap energy, the electron shifts into a higher energy state. The electron travels from the valence band (highest occupied molecular orbital state) to the conduction band (lowest unoccupied molecular orbital state) within the allowed energy bands of the material (figure 29).
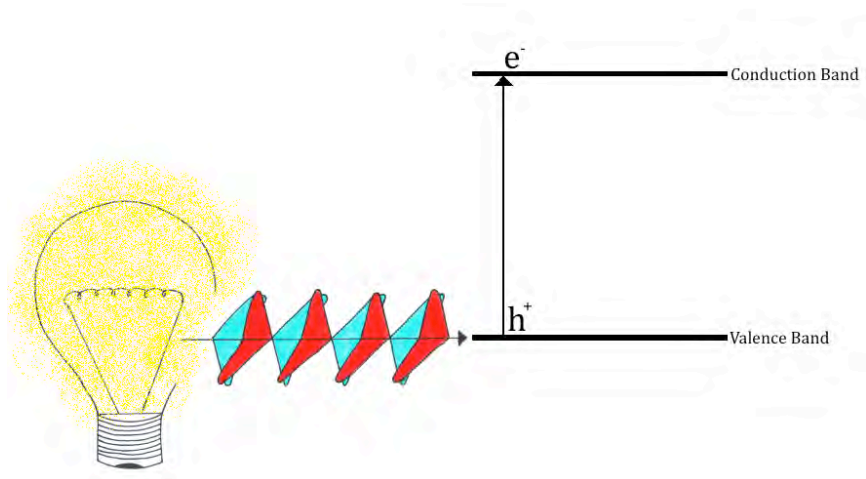
Figure 29: Valence band excitation using irradiation energy.

After the electron excitation has occurred, the presence of an electron-pair (e^-/h^+) exists.[56],[57],[58] These e^-/h^+ pairs are capable of numerous operations. Due to their strong oxidative potentials, they have found multiple oxidative applications.[59],[3],[60],[61]

In order to harness the potential of semiconductors, and to function as conductive materials, they must be exposed to an energy source capable of exciting electrons within the low (valence band) energy levels of the material and consequently into the higher-allowed (conduction band) molecular orbital states. There are various sources of energy available (electrical, convection and irradiation), however for the duration of this literature review, semiconductor activation will only be explored using irradiation sources only.

1.5) Irradiation sources

The electromagnetic spectrum is a diverse scope of frequencies (figure 30), each emitting a distinctive energy (photon), which has numerous applications from X-rays for bone scanning to radio waves for telephonic communications. The value of the frequency is measured in Hertz (*Hz*) and is described as the cycle repetition passing one identified point within a period of one second.[62]
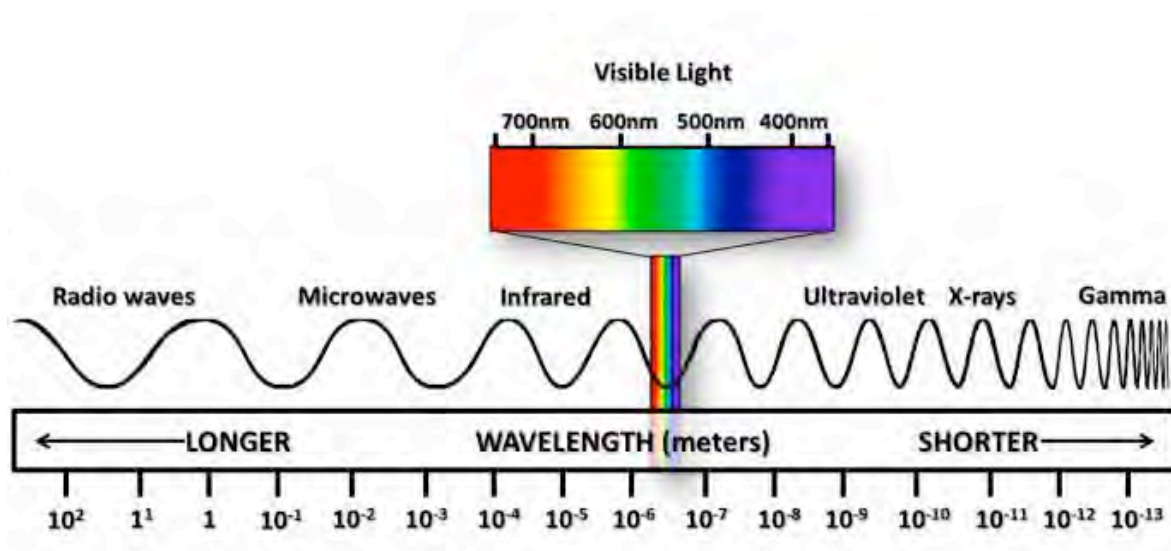
Figure 30: Electromagnetic Spectrum.[63]

There are various types of electromagnetic radiation, which include: radio waves, microwaves, infrared, visible light, ultra-violet (UV), X-ray and gamma ray radiation. As the series progresses from radio waves to gamma rays, the radiation (UV, X-rays and gamma rays) becomes ionisable. The ionisable radiation can have devastating effects on biological tissue cells, skin and allows for malignant tumor growth. However, radiation has successfully and beneficially been harnessed. X-ray radiation has found to be invaluable for bone matter screening. Due to short wavelengths and high radiation energy, soft tissue does not absorb the radiation, which allows for a clear image to be recorded. Gamma radiation has also found widespread applications as a highly favoured power supply. As a result of the intense discharge of energy from the fissure of radioactive isotopes, an abundance of energy can be harvested and used to supply national power grids.

Based upon the characteristics of high-energy radiation, it has been proposed that semiconductors have the potential to produce highly reactive photocurrents when irradiated with a suitable photon-energy source that is a match to the value of the band gap. With reference to the band gap and methods to activate it, an evaluation of the chemical literature will assist in demonstrating how semiconductors have been used for alcohol oxidations.

1.6) Techniques for alcohol oxidation using semiconductors

Proposed by Kirsh, a photocatalytic process involves the conversion of light into chemical energy (equation **[1]**, figure 31).[64] Once activated, the semiconductor (TiO_2^*, equation **[2],** figure 31) has the capability of either deactivation[52] or initiating numerous redox operations (equation **[3]**, figure 31).[53],[65],[66] The continued state of activation allows for the transformation of starting materials (see SM in figure 31) into complex organic molecules (SM_1^*, equation **[3]**, figure 31) due to the strong redox potentials of both the positive hole (h^+) and free electron (e^-)[67] as illustrated below.

$$TiO_2 \xrightarrow{\;hv\;} h^+ + e^- \qquad\qquad \textbf{(1)}$$

$$TiO_2^*\,(e^-/h^+) \xrightarrow{\;Time\;} TiO_2 \;\;(\text{Semiconductor deactivation}) \qquad \textbf{(2)}$$

$$TiO_2^*\,(e^-/h^+) + SM_1 \xrightarrow{\hspace{2cm}} TiO_2 + SM_1^* \qquad\qquad \textbf{(3)}$$

$$SM_1 = \text{alcohol to aldehyde}$$

$$\text{OR}$$

$$O_2 \twoheadrightarrow O_2^-$$
$$Ag^+ \twoheadrightarrow Ag^0$$
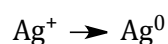$$Dye \twoheadrightarrow Dye^*$$

Figure 31: Semiconductor (X) excitation from electromagnetic irradiation.

However, caution of specific catalyst poisoning species should be noted at all times when conducting photocatalytic studies. As reported by Skupien[68] and Moulijn,[69] carboxylic acids are known catalyst poisoning substrates as the acid terminates the e^-/h^+ pair, hindering its activated state and quenching any further redox processes. In other investigations, Kirsh reported that oxygen is also capable of terminating positive holes found on the surface of activated semiconductors.[64] Molecular oxygen causes the semiconductor to undergo a distinctive energy transfer movement when oxygen is reduced by the conduction band electrons to a superoxide ion. The superoxide ion is then further mono-oxidised to singlet oxygen in an one-electron oxidation. The disadvantage of this transformation occurs while the oxygen is being oxidised. The positive holes are temporarily hindered for their oxidative functions until they are re-activated by a suitable energy source.

1.6.1) TiO$_2$ water splitting

Electrochemical decomposition of water requires a potential that must be more than 1.23 V between electrodes. Since 1.23 V equates to 1000 nm, the potential for water splitting is feasible using visible light (400-700 nm). However due to water's high transmittance of almost all wavelengths in the visible spectrum, it cannot be split, unless energies lower than 190 nm are used.

Fujishima and Honda attempted to investigate and to research this novel concept of water splitting into oxygen and hydrogen gas. They explored this by constructing a simple galvanic cell (figure 32) of a TiO$_2$ and a platinum black cathode.
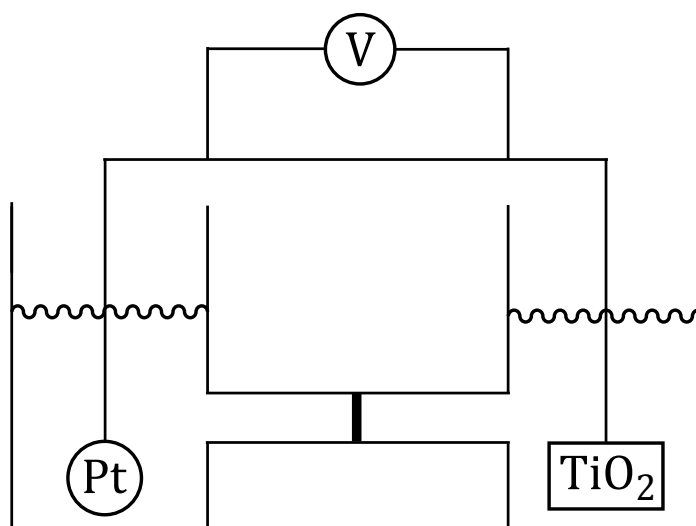

Figure 32: Galvanic cell used by Fujishima and Honda.

The TiO$_2$ anode was irradiated with a 500 W xenon (Xe) lamp and water splitting was detected. There was a need to identify the band gap of TiO$_2$ that was evaluated using current-voltage curves while illuminating TiO$_2$ using various wavelengths. From measurements recorded with a static potentiometer, it was possible to detect an anodic photo current below 415 nm (3.0 eV) and hence the band gap of titanium dioxide. Further evidence was collected that suggested hole (h$^+$) formation on the anodic TiO$_2$ surface.

Titanium dioxide is an effective semiconductor,[70] which may be used to perform oxidation reactions with the aid of a free electron scavenger. The TiO_2 can be easily excited with an energy source equal to its bang gap (3.2 eV), however after the electron excitation, electron-hole (e^-/h^+) recombination will inevitably occur due to charge attractions, thus producing heat or photon emissions causing an ineffective use of (e^-/h^+) pairs.[71] This can be circumvented by the action of a scavenger, such as silver ions[67] or molecular oxygen.[71] They function by removing free electrons in the conduction band of the semiconductor and inhibit any recombination of the electrons and holes. The advantage of inhibiting the (e^-/h^+) pair recombination lies in greater photocatalytic efficiency for numerous semiconductor-mediated reactions.

One further advantage of preventing (e^-/h^+) recombination is in the production of hydrogen (H_2) gas as identified by Yoong.[72] The group successfully achieved hydrogen gas evolution using a 500 W halogen lamp setup. They prepared copper doped TiO_2, which functioned as a photocatalyst to accomplish hydrogen gas evolution. During their studies, they formulated two separate copper doping techniques. The first was a precipitation method using a complex glycerol procedure (m-CuTa-b), while the second was a typical wet impregnation method (CuT). In both evaluations, hydrogen gas evolution (8.5 ml h^{-1} and 4.0 ml h^{-1}) was higher when compared to commercially available Degussa P25 TiO_2, which had a hydrogen gas evolution of only 2.5 ml h^{-1}.

In 2008, Zhang, *et al.,*[2] published a noteworthy TiO_2-Alizarin Red, TEMPO, molecular oxygen (O_2) and visible light irradiation system. Visible light irradiation activated an absorbed dye species to initiate the oxidative pathways (figure 33) that was successfully applied to a number of alcohol (benzyl alcohol, cinnamyl alcohol, hexanal, cyclohexanol and 3-methyl-2-buten-1-ol and 3-pyridinemethanol) oxidations. Low catalyst loadings (8 mg, 6.5 x 10^{-4} mmol Alizarin Red) yielded excellent selectivity's (93-99%) amongst all of the alcohols tested.
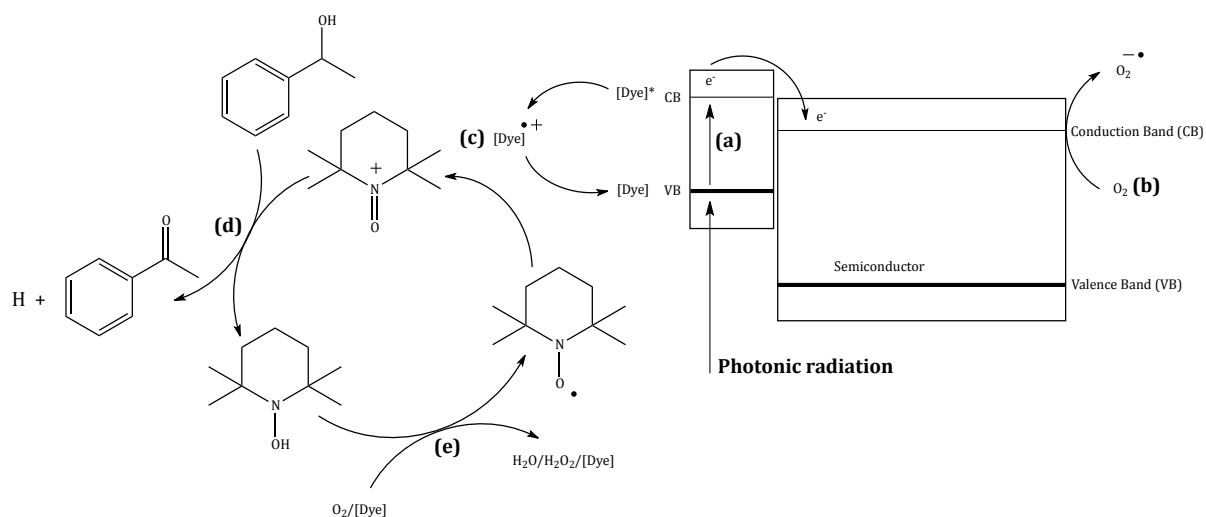
Figure 33: Dye-sensitised TiO₂ for visible light oxidation of alcohols.

The alcohol oxidation system proceeded through five steps. Initially in step (**a**), a photonic emission excited the surface bound dye molecules (bound to the TiO₂), where an electron was promoted from the valence band into the conduction band of the dye. As the dye had a conduction band potential higher than the conduction band of TiO₂, the electron fell into the conduction band of TiO₂ and was trapped by the electron scavenger (molecular oxygen, step [**b**]). Once the dye was activated, it subsequently oxidised the TEMPO radical to the active *N*-oxoammonium salt (step [**c**]), which was capable of oxidising the alcohol (step [**d**]). Excess molecular oxygen completed the oxidative cycle by reducing the hydroxylamine back to the TEMPO free radical (step [**e**]).

Subsequently, Jeena and Robinson improved the oxidative system.[73] By identifying that silver was a superior electron scavenger to molecular oxygen, the oxidative cycle was enhanced using the zinc oxide (ZnO)-Alizarin Red-Silver-TEMPO system. Since silver had a higher electron scavenging affinity than oxygen, it greatly improved the kinetics of the alcohol oxidation. The catalytic system was also evaluated using both titanium dioxide and zinc oxide, while zinc oxide exhibited consistently superior results in each of the evaluation studies. Through a process of reasoning, it was identified that titanium dioxide exhibited a strong back electron transfer mechanism with the application of alizarin red which inhibited the electron ejection into the conduction band of titanium dioxide. The evidence supported the findings of low alcohol oxidations when using the titanium dioxide/dye/silver system. A comparison study to Zhang's[2] work explored the

oxidation of similar alcohols with high alcohol conversions (82%) being achieved, however reaction times were significantly lower (three hours compared to eighteen). The mechanism for the zinc oxide oxidation system was postulated to concur with that identified by Zuang and was shortly confirmed thereafter.[74]

Titanium dioxide and zinc oxide have proven not only to be widely applicable photocatalysts that are robust and applicable to a number of semiconductor investigations but have also shown to be excellent solid-state catalytic media. Data has been published by Kegnæs,[75] which has shown that gold supported TiO_2 catalysts are highly effective for alcohol oxidations. Gold was chosen to effectively enhance the absorption of oxygen onto the semiconductor support that allowed the molecular oxygen to remove free conduction band electrons. Within their experimental report, the aldehyde adducts were condensed in a basic methanolic solution yielding methyl esters and subsequently aminolysed in the same solution yielding amides with both high ester and amide yields. The technique operated smoothly while using one-pot parameters and allowed for an efficient retention of the aldehyde and methyl ester adducts without any loss caused through separation and extraction work up procedures. Aldehydes are well-known to be highly volatile and hard to isolate which marks their findings as highly commendable (figure 34).[76],[77],[78]
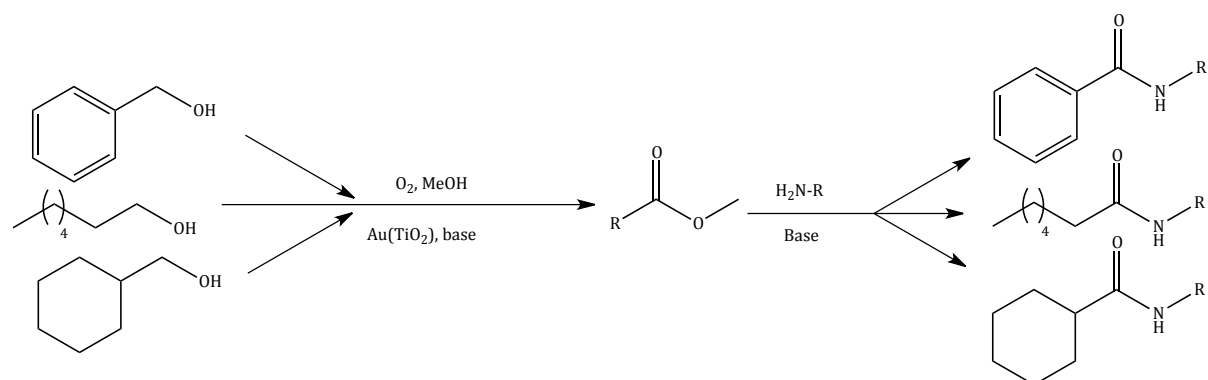

Figure 34: Titanium dioxide support for gold mediated one-pot synthesis of amides.

In other studies, Higashimoto, *et al.,*[1] investigated the photocatalytic oxidation of various benzylic alcohols using titanium dioxide under both ultraviolet and visible light irradiation with molecular oxygen as a terminal oxidant.[1] They explored the surface bound interactions between TiO_2 and benzyl alcohol and identified that benzyl alcohol absorbed onto the TiO_2 surface shifted the 3.2 eV band gap into the visible region. The

justification to support their findings explained that benzyl alcohol possessed a unique surface charge transfer that existed on the surface of the benzyl alcohol-TiO$_2$ complex.

Additional titanium dioxide studies by Rao, *et al.,*[79] have developed a novel approach to synthesising dihydropyrazines from a TiO$_2$ mediated photocatalytic system. The experiments required a zeolite-TiO$_2$ slurry that was activated (300 °C for four hours) and calcinated (400 °C for six hours). The data did not mention the scale of each reaction, however one hundred milligrams of the TiO$_2$ supported catalyst was suspended in 20 ml of acetonitrile suggesting catalyst loadings were high. The percentage yields of the dihydropyrazines were low (maximum yield of 20.4%) that further suggested that the catalytic technique needed refinement.

TiO$_2$ was used to photocatalytically reduce molecular oxygen to the strong oxidising superoxide ion that completed the oxidation of propylene glycol to its methylglyoxal derivative on the zeolite support. The zeolite was identified to be far superior over solid phase acids (SiO$_2$) and aqueous acids. There was a definite mechanistic influence of the zeolite that not only enhanced the synthesis of dihydropyrazines but also selectively controlled the absorption of propylene glycol instead of ethylene diamine. This was highly favourable for the TiO$_2$ to be in close proximity of the alcoholic functional group as rapid oxidation was promoted.

The zeolite also stabilised a key cationic intermediate (as identified through their literature review[80]) of the dihydromethyl pyrazine adduct which was later identified as undergoing demethylation via a functional group interconversion from an aldehyde to a carboxylic acid following decarboxylation and dehydrogenation yielding the dihydropyrazines.

1.6.2) Palladium-wool complex of cadmium sulfide

In other studies, Wang, *et al.,* fashioned an unusual palladium-biopolymer supported cadmium sulfide photocatalyst[81] to evaluate its effectiveness towards rhodamine B dye degradation (a common water pollutant). Cadmium sulfide was the chosen photocatalyst due to its low band gap value (2.4 eV, corresponding to the visible region)

and its excellent–wide substrate applicability in oxidation, reduction and amine condensation reactions.[82],[83]

During their investigations, 200 mg of the fabricated Pd-wool photocatalyst was saturated in a rhodamine dye solution (45 ml of 10 mg/l solution). Following a three and a half hour absorption equilibrium period between the wool and the rhodamine dye in the dark, the sample was irradiated at 420 nm using a 300 W xenon (Xe) lamp. During the investigation, dye degradation was tested without any photocatalyst and it revealed that the dye would not succumb to self-photolysis under visible light exposure. Furthermore, monitoring the effects of the palladium: cadmium sulfide (Pd:CdS) ratios revealed that photocatalytic activities were constantly superior to undoped cadmium sulfide reactions. The research revealed that a 0.5% wool-Pd/CdS sample effectively reduced the total organic carbon from 279.6 mg/l to 26.72 mg/l (a 87% reduction after 210 minutes).

The results were recorded by monitoring the decrease in the 554 nm absorption band due to the N-deethylation of the dye. It was stated that the Pd-wool/CdS functioned as a superior separator of photogenerated charge carriers due to the contributing n-type doping character of the palladium species that actively promoted the degradation of the investigated dye.

1.7) Boron doped synthetic chemical vapour deposition diamond

1.7.1) A contemporary semiconductor

Within the domains of this study, the main anticipated outcome was focused on applying boron doped synthetic chemical vapour deposition (CVD) diamonds to function as semiconductors to effect the oxidative transformation of alcohols and organic dyes into their oxidised derivatives.

Diamond is probably most widely known for its commercial value in the jewelry industry. However in the past two decades, it has been extensively researched which has made it one of the most studied solid-state materials within the scientific community.

Amongst the various discoveries, diamond has been used for its high chemical[84] and mechanical robustness,[85],[86],[87] thermal conductivity,[88],[89],[90],[91],[92] wide potential widow over the visible region,[88] electrochemical applications[87],[93],[94] and biological studies.[85],[93]

It is well known that undoped-natural and synthetic diamonds are highly efficient insulators[95] and therefore the contemplation of applying synthetic CVD diamonds to an oxidation study appears highly questionable. However, if a suitable irradiation source is provided (figure 35),[96] diamond may be capable of producing a photocurrent for oxidative purposes.
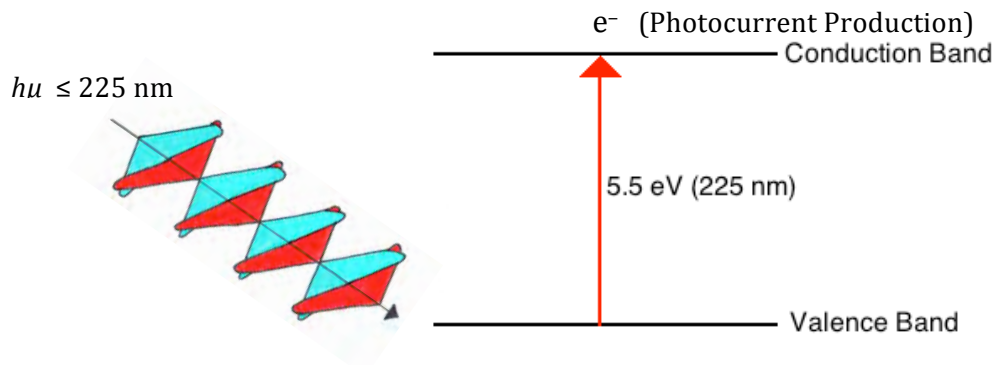
Figure 35: Band gap depiction of synthetic diamond.

Due to diamond having a sp^3 hybridised array of tetrahedral coordinated carbon atoms, diamond has an intrinsic insulating property[92],[97] When the carbon atoms of the diamond vibrate due to distortions in the equilibrium ground states, the lattice is capable of absorption heat. However, since polycrystalline diamond has grain boundaries and numerous defect sites, the lattice vibrations (phonons) are scattered.[88] This causes the diamond to withstand extreme thermal conductivities, approximately a five-fold higher thermal conductivity figure compared to copper at 2000 W m^{-1} K^{-1}.[88] Not only is nature and synthetic CVD diamond an excellent insulator in its native form, but the physical hardness of natural and synthetic CVD diamond is superior to all known natural and synthetic materials.[98]

However, in order for synthetic CVD diamond to emit a photocurrent, it requires an extrinsic dopant that will impart electrical conductivity within the diamond lattice.

Numerous research groups[89],[94],[99],[100] have focused on doping diamond using hydrogen, oxygen, phosphorus, nitrogen, sulfur and boron in an attempt to measure the electrochemical properties of the crystal.

Of all the potential dopants including; phosphorus, nitrogen, lithium, sulfur, boron and phosphorus, boron has been commonly used because of its low charge carrier activation energy (E_A) (for example: 370 meV for boron versus 600 meV for phosphorus and 1.6-1.7 eV for nitrogen).[92] The covalent radius of boron (8.8×10^{-2} Å) is also highly favourable with that of carbon (7.7×10^{-2} Å), thus facilitating a smooth integration of boron into the sp^3 diamond lattice.[92] The other potential dopant agents mentioned above have larger atomic radii that make their incorporation into the diamond lattice difficult (except for nitrogen will a smaller atomic radius than carbon [7.4×10^{-3} Å]).[101] Since boron has a low activation energy, it has shallow electron acceptor sites and *p*-type charge conductivity can be introduced into the diamond with relative ease as shown in figure 36.

EA = 370 meV   EA = 1.6-1.7 meV
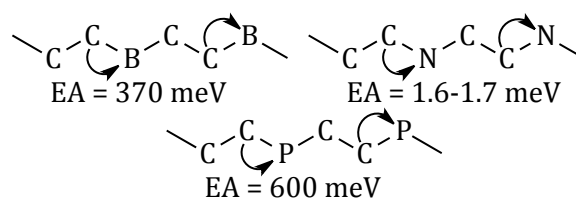
EA = 600 meV

Figure 36:   One-dimensional surface depiction of boron (B), nitrogen (N) and phosphorus (P) dopant activation energies.

As boron is a trivalent atom, substitutional incorporation into the diamond lattice produces uncompensated bonds next to neighbouring carbon atoms, hence causing *p*-type conductivity within the diamond lattice.[92] Nitrogen was previously mentioned to have a smaller atomic radius (7.4×10^{-3} Å), however it has an extra valence electron, which does not impart *p*-type charge conductivity in the diamond (and was not the focus of this study). High boron concentrations generate metallic-like conductivity, while low boron doping is desired for avoiding defects in the doped material. This has allowed scientists to realise that synthetic CVD diamonds can be tailor made to meet the requirements of the experiment. Therefore, a brief review of how synthetic chemical vapour deposition diamonds are produced will be discussed in the following section.

1.7.2) Synthetic diamond synthesis and growth

Synthetic diamonds are grown in numerous ways within a laboratory. Different methodologies include hot chemical vapour deposition (HCVD), high pressure-high temperature (HTHP) or by controlled detonation.[102] When using the hot chemical vapour deposition technique (figure 37), methane-hydrogen ratios (CH_4/H_2) of 0.3-1.0:1, 0.8-1.0 kW, 35-65 Torr and temperature above 2000K enter a hot vapour deposition chamber.
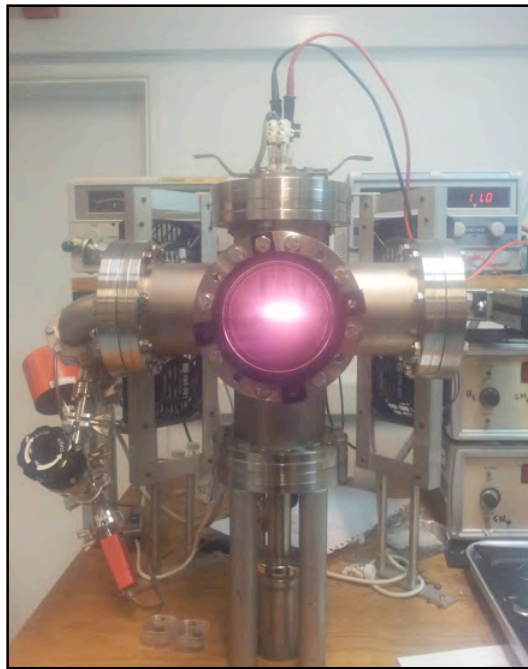

Figure 37: Hot chemical vapour deposition diamond growth at The University of Bristol.

Within the chamber, methyl radicals facilitate surface growth while hydrogen gas serves two main functions. Firstly, hydrogen acts to abstract chemisorbed hydrogen from surface methyl groups, thus facilitating diamond film growth through the promotion of active site formation. Hydrogen is also crucial for surface passivation, especially after the diamond film growth is complete. Preceding the diamond growth, the methane and dopant (boron, nitrogen, phosphorus or sulfur) gases are switched off while leaving the hydrogen gas to terminate any dangling carbon bonding sites, thus inhibiting sp^2 carbon bond growth. Typically, diborane (B_2H_6) and not trimethylborane (TMB) gas is used as it

promotes homogenous diamond crystal growth. Triemthylborane contains extra carbon atoms that could cause unnecessary film abnormalities.[103]

The second method of growing diamonds is by using high temperature-high pressure (HTHP) conditions (1500 °C, 2 GPa) that support thermodynamically favourable synthetic diamond growth (figure 38).[88]
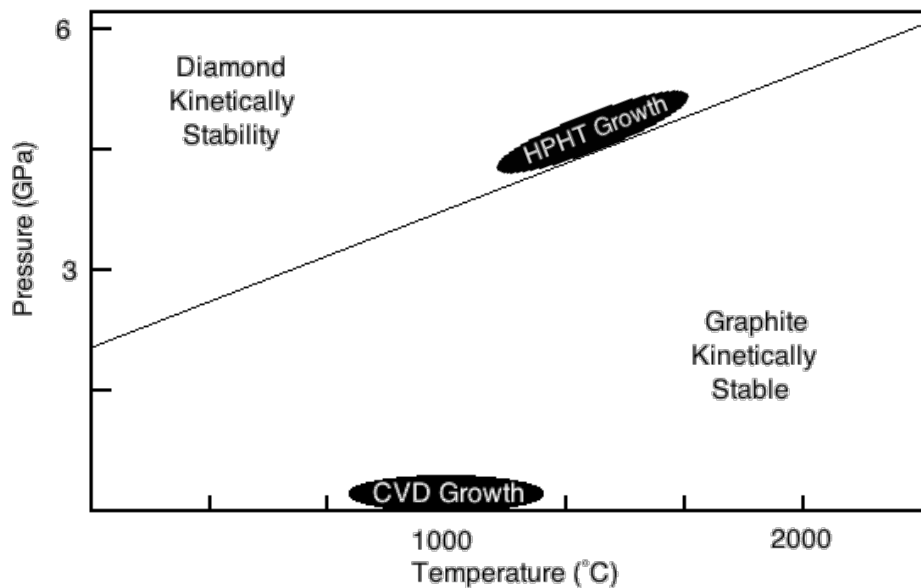

Figure 38: High pressure-high temperature diamond growth under controlled conditions.[88]

Balmer, *et al.,*[88] reported that high temperature-high pressure synthetic diamond growth is favoured when initiating nucleation sites on metal substrates such as nickel, iron or cobalt.[88] It was further noted by Balmer that high pressure-high temperature synthetic diamond growth produces high quality synthetic diamond structures up to eight millimeters in diameter with only trace impurities.

The last technique commonly used to synthesise synthetic diamonds is by detonation. A mixture of heterocyclic reagents (trinitrotoluene [60%] and hexogen [40%]) are added to a metal reaction chamber containing water, carbon dioxide and molecular nitrogen.[104] The trinitrotoluene is then detonated and the temperature and pressure rise rapidly to a point known as the 'Jouguet Point'. At this transient state, the temperature and pressures gradually start to decrease, after which nanodiamonds begin

to crystallise from a liquid phase until they are separated from the soot material at standard atmospheric conditions.[105] Synthetic diamond surfaces produced from detonation are highly functionalised and the presence of carboxylic acids act as anchors for the attachment of biologically important molecules such as doxorubicin anticancer drugs (figure 39).
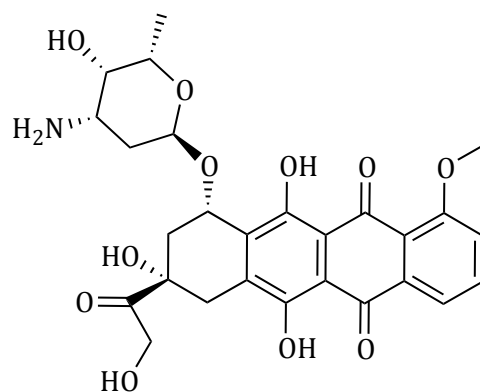
Figure 39: Chemical Structure of doxorubicin.

There are however several disadvantages to using this technique. Firstly, synthetic detonation diamonds tend to agglomerate during the cooling period. Since detonation synthetic diamonds cluster into varying aggregates, they are not suitable for the application of refined synthetic diamond seeding. Secondly, superfluous amorphous graphite soot is produced during the detonation and hence the overall yield of crystalline synthetic diamond is low compared to synthetic diamonds grown using the chemical vapour deposition or high temperature-high pressure methods.

1.7.3) Electrochemical applications of synthetic diamond

Diamond's natural chemical inertness requires a dopant to achieve electrical conductivity. It has been reported that a hydrogenated synthetic diamond surface promotes a conductive surface.[88],[89],[106] However, doping species are either capable of introducing a *p*-type (acceptor) or *n*-type (donor) characteristic into the diamond lattice. Boron is a *p*-type dopant and is electron deficient (Group three of the periodic table). It has been identified to be a highly favourable *p*-type dopant due to its shallow ionization energy, which has a dopant energy level slightly above the valence band of synthetic diamond.[92] *p*-Type conductivity of synthetic diamond depends on the boron doping

concentration level. As the boron concentration increases, the conductivity on the synthetic diamond's surface changes from an insulator, to a semiconductor (moderate boron doping [10^{19}-10^{23} atoms cm^{-2}]) and lastly to a metallic conductor (in excess 10^{23} atoms cm^{-2}).[107]

Nitrogen and phosphorus are also common doping agents. However, they have *n*-type dopant characteristics that produce an *n*-type doped semiconductor. *n*-Type doped synthetic CVD diamonds have an excess of free electrons and is caused by nitrogen and phosphorus being electron rich species that donate electrons into the conduction band of the diamond. The doping of semiconductors produce varying results and can have significant effects on the chemical synthetic pathways. For example, hydrogenated boron doped diamond has shown to be highly favourable in electrochemical research,[108],[109] while either nitrogen or phosphorus co-doped with boron diamonds have shown excellent applications as photovoltaic cells.[110] A few examples of doped synthetic diamonds will be discussed below which detail the advantages of doping synthetic diamonds with either boron, nitrogen or phosphorus.

Bhattacharyya, *et al.,*[111] reported a large conductivity enhancement when undoped ultrananocrystalline synthetic diamond was doped with nitrogen. It was recorded that the conductivity rose from 0.016 Ω^{-1} cm^{-1} to a sizeable 143 Ω^{-1} cm^{-1} at 0.02% total molecular nitrogen concentration with the measurement being recorded at room temperature. The nitrogen-doped synthetic diamonds possessed similar conductivity figures to data findings of heavily boron doped synthetic diamond samples that are well regarded in the chemical literature as highly conductive.[111] Similar findings were also published by Liu, *et al.,*[112] who mentioned that nanocrystalline as well as ultrananocrystalline synthetic diamonds had superior electrical conductivity responses at room temperature and also featured enhanced electric field specifications.

During the synthetic manufacturing of polycrystalline diamonds using the chemical vapour deposition technique, numerous defects are inherent in the lattices when compared to a minimal number found in single-crystal chemical vapour deposition diamonds.[113] These defects are known as 'grain boundaries' and have been recorded as potential sites of electrical conductivity when using both *p*-type (boron) and *n*-type

(nitrogen/phosphorus) doping conditions.[111],[112] On the surfaces on the synthetic polycrystalline diamonds, there are numerous grains which compose the diamonds' surfaces and these grains are essentially individual synthetic diamond crystals.

Nitrogen (introduced into the plasma as di-nitrogen gas [$N_{2(g)}$]) is believed to be a prominent species in altering the electrical properties of grain boundaries.[114],[115] Grain boundaries have been shown to contain non-diamond hybridised sp^2 carbon atoms as well as dangling carbon bonds,[111] that have been identified as being highly strained. The incorporation of nitrogen allows for semi-metal like characteristics to be extrinsically housed in the synthetic diamond through chemi-electrical modifications of the grain boundaries. It was postulated by Bhattacharyya[111] that electrical conductivity occurred in these boundaries due to nitrogen being a deep energy level donor (1.7 eV) and together with the favourable modelling calculations (3-5 eV for grain boundary doping), nitrogen was expected to be in the grain boundaries (figure 40).[113]
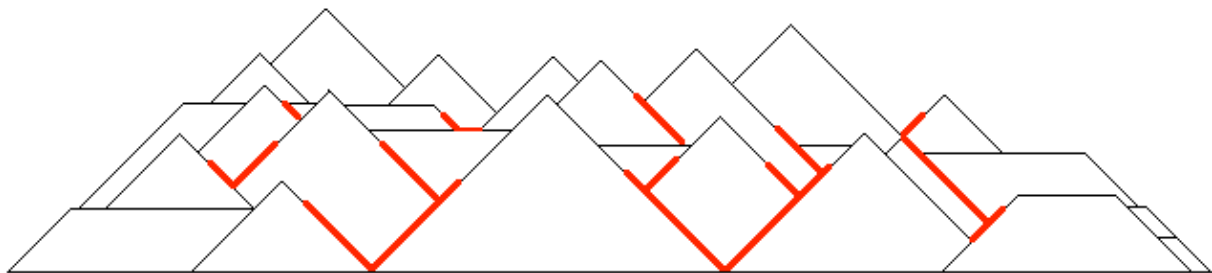
Figure 40: Crystalline representation of diamond surface topology with grain boundaries (bold red lines).

Phosphorus has also been identified[112] to be a potential *n*-type dopant, however due to its high-activation energy (0.6 eV), poor room temperature conductivities (less than 10^{-4} Ω^{-1} cm^{-1}) and low e$^-$/h$^+$ values (less than 250 cm^2 V^{-1} S^{-1} at 30 K), nitrogen has been used as a superior *n*-type synthetic diamond-doping agent.

The chemical literature has also shown that phosphorus (P) is problematic in synthetic diamond doping due to its positive charge which couples with negatively charged hydrogen (H) atoms (hydrogen being negatively charged in *n*-type synthetic diamonds), thus forming neutral P-H species. This expresses that synthetic diamond hydrogenation (which occurs during synthetic diamond growth) needs to be suppressed during

phosphorus doping. However hydrogen is a known requirement to impart electrical conductivity in synthetic diamonds, hence the limited study of phosphorus doped synthetic diamonds.[116] To conclude this introduction, a review of boron and hydrogen doping studies of synthetic diamonds will be mentioned followed by the objectives of the project.

A recent synthetic diamond study has reported interesting findings while using boron doped synthetic diamonds that were grown on titanium substrates.[117] The titanium substrates were chosen for their porous nature, which opened avenues for synthetic diamond electrochemical studies. There were concerns regarding poor titanium-diamond adhesion forces from the *in-situ* produced titanium carbide interlayers. It was identified that a balance was required as titanium carbide interlayers provided the necessary electrical conductivity between titanium and synthetic diamond. The titanium carbide layer was also required to resolve thermal expansion differences between the titanium and the synthetic diamond. However, while the synthetic diamonds grew and were being simultaneously boron doped, the boron was identified to mediate the titanium carbide: diamond adhesion ratio by controlling the boron flow rate.

Maier reported that synthetic diamond hydrogenation promotes surface conductivity while synthetic diamond oxygenation does not.[114] It was further postulated that hydrogen was contracted for the surface production of conductive holes which were present in grain boundaries and other defect sites.[97],[118] Evidence has suggested that hydrogen-terminated synthetic diamond electrodes exist with a valence band potential that is greater than $H^+_{(aq)}|H_{2(g)}$.[108] The result of this phenomenon is synthetic diamond which actively promotes solvated electron ejection into aqueous media.[108] This data is also in excellent agreement with the recent findings of Zhu and co-workers[119],[120] who published in Nature Materials (2013) describing the production of solvated electrons which were produced from irradiated synthetic diamond squares while being harnessed for the reduction of nitrogen gas to ammonia. Zhu also published in Angewandte Chemie (2014) for carbon dioxide (CO_2) reduction to carbon monoxide (CO).[119],[120]

1.8) Aims

Previous findings within this group have explored a wide scope of alcohol oxidations that have been mediated by various TiO_2 and ZnO photocatalytic systems. In an attempt to further the understanding of these alcohol oxidation techniques, the primary objective of this project was to expand upon the TiO_2 and ZnO foundations to affect alcohol oxidation processes and organic dye degradations while using synthetic CVD diamonds. In addition, an effort to explore the presence of any boron doping in the synthetic CVD diamond powders and to understand the fundamental semiconductor chemistry of the synthetic CVD diamond's bang gap was envisaged to be an interesting subsection to explore. Lastly, an evaluation of published findings within the group offered an opportunity to improve a zinc oxide photocatalytic system with the aim of publishing the results in an internationally recognised ISI rated journal.

CHAPTER 2: Results and Discussion

2.1.1 Preface

The literature review has reported a study of synthetic chemical vapour deposition (CVD) diamond that will be the focus of this investigation. During the course of the study, various solvents, radiation wavelengths, irradiation periods and conduction band electron scavengers will be explored in an attempt to compose an understanding of synthetic CVD diamond chemistry. The research gathered during the study will be applied towards the oxidation of various organic compounds.

From the initiation of the study, our experimental outcome was to achieve a successful alcohol oxidation while using various synthetic CVD diamond samples. After completing the optimisation study, the aim was focused on expanding the study for a wide substrate scope analysis. The chemical literature has noted that boron doped synthetic diamond is highly conductive[120] and therefore a further outcome was to explore the effect of various boron concentrations on the rate of benzyl alcohol oxidation.

After composing a review of the literature findings in the introduction of this report, it appeared plausible for synthetically grown chemical vapour deposition diamond to produce a photocurrent when irradiated with a suitable ultraviolet irradiation. Therefore, the main objective of the study was to expose CVD diamond powders to ultraviolet irradiation and evaluate the efficiency of the synthetic CVD diamonds towards the oxidation of benzyl alcohol.

2.2) Introductory oxidation studies.

2.2.1) Benzyl alcohol oxidation

Before initiating the synthetic CVD diamond alcohol oxidation studies with almost no reports on photo-activation of synthetic CVD diamonds, a well-researched alcohol that had been oxidised with known semiconductors was required to start the oxidation studies. The objective was to find such an alcohol being reported in the chemical literature, which could be tested while using the synthetic CVD diamonds and ultraviolet radiation.

Various solid-state materials (titanium dioxide [TiO_2] and zinc oxide [ZnO]) have been thoroughly investigated and reported in the literature as highly efficient semiconductors in photocatalytic systems.[75],[121] Particular attention has been focused on benzyl alcohol oxidation which has been researched for countless years in an attempt to improve these semiconductor controlled reactions.[75] Recent detailed studies have investigated the oxidation of benzyl alcohol and various benzylic alcohols using gold nanoparticles supported on titanium dioxide.[75] Kegnæs reported[75] that gold-doped titanium dioxide nanoparticles effectively oxidised acryl alcohols while using molecular oxygen as the terminal oxidant. High conversions within 24 hours were achieved while unactivated alcohols (1-heptanol) only managed sluggish transformations (34%). Discussions in the literature have revealed gold to be an efficient semiconductor dopant that promotes the surface adsorption of molecular oxygen which facilitates the removal of conduction band free electrons on the surface of semiconductors.[122]

In another report by Kegnæs,[121] a similar approach was implemented for the oxidative conversion of benzyl alcohol with 1-hexylamine towards the synthesis of *N*-benzylidenehexan-1-amine. Mohamed[53] also described the oxidation of aromatic alcohols while using mercury lamp irradiation sources and oxygen-saturated mixtures of acetonitrile and titanium dioxide. The concluding remarks of the study mentioned that titanium dioxide produced conduction band free electrons while being irradiated which promoted superoxide radical ion formation to effect the alcohol oxidations.

Based on the studies of Kegnæs and Mohamed,[53],[75],[121] benzyl alcohol appeared to be an appropriate reactant to initiate the synthetic CVD diamond oxidation studies.

However, molecular oxygen had also been reported to act as the terminal oxidant in the previously mentioned studies. Therefore, for the purpose of fully understanding the synthetic CVD diamond catalytic system, the role of molecular oxygen in semiconductor oxidation reactions will be explained.

As reviewed in the introduction (Section 1.4), semiconducting materials consist of a near infinite number of molecular orbital energy levels. Amongst the energy levels, 'allowed energy states' have stored potential energies, which can be harnessed for various chemical transformations. In a photocatalytic environment, when the semiconductive material receives an energy source (photons) that is capable of promoting allowed energy transitions (step **a**, figure 41), the semiconductor is equipped to initiate a photochemical reaction. Once the semiconductor has been 'activated,' an electron exists in the conduction band (step **b**, figure 41). However, after the electron has been promoted, there are two distinctive pathways that the electron can follow. The electron may 'relax' back into the ground state of the valence band (step c, figure 41) and thus deactivate the semiconductor. Otherwise, if an 'electron scavenger' (for example, molecular oxygen) is present to trap the free conduction band electrons, then the electron is permanently removed from the semiconductor's surface (step **d**, figure 41). When the electron is permanently removed, the molecular oxygen is reduced to a superoxide radical (step **d**, figure 41) and the formation of a positive hole remains in the valence band. When the free electron-positive hole (also known as an 'excitron') and superoxide radical (both species have strong oxidation potentials[123]) are in existence, the semiconductor is capable of oxidising various organic compounds (steps **f** and **g**, figure 41).
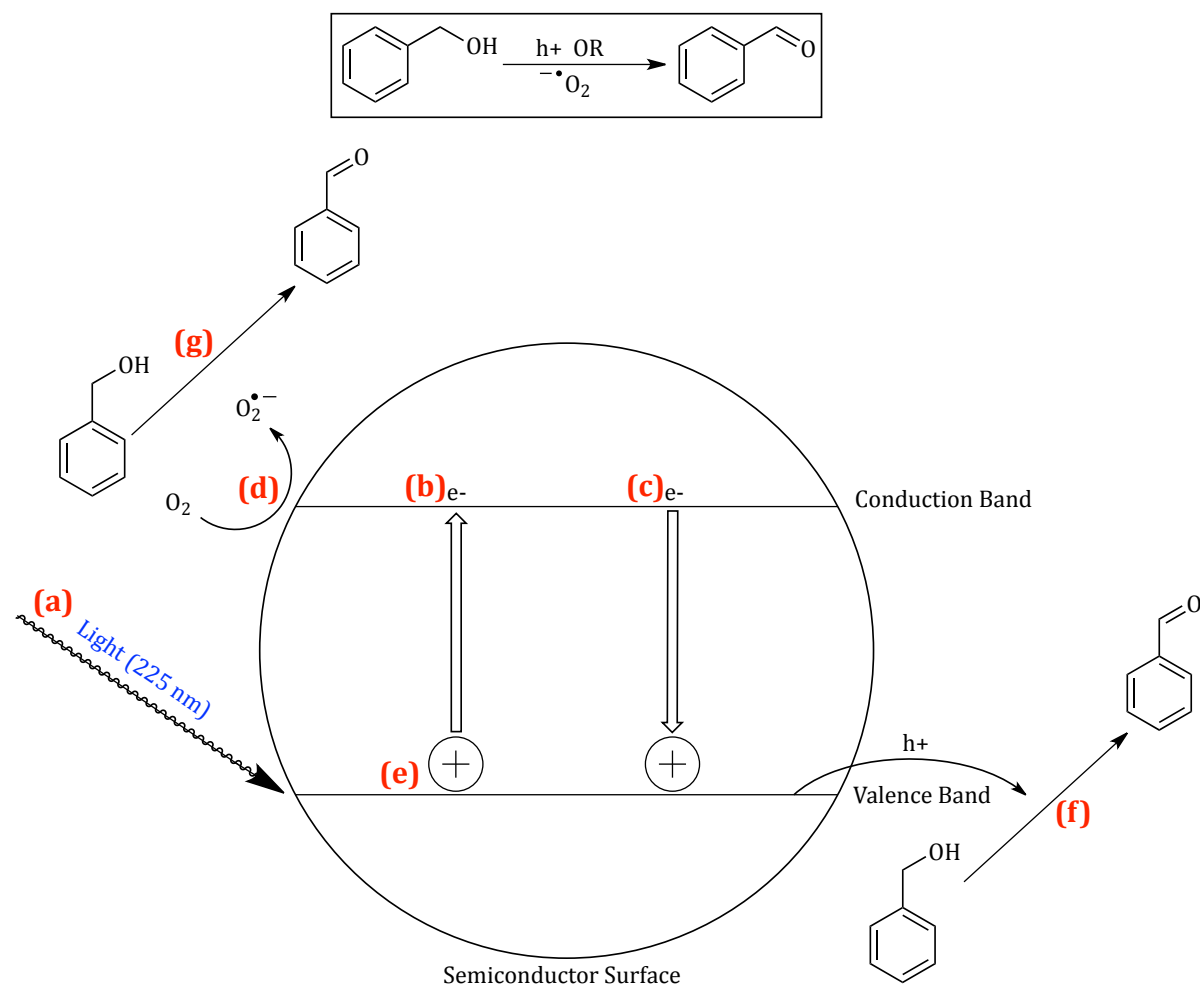
Figure 41: Superoxide ion formation after synthetic CVD diamond activation.

Therefore, to remove free electrons that would be promoted into the conduction band of the synthetic CVD diamond after ultraviolet irradiation, molecular oxygen would become the terminal oxidant. However, not only was the molecular oxygen identified as being a suitable terminal electron scavenger that would inhibit the electron-hole recombination, it would also participate in alcohol oxidations. Literature articles have shown that molecular oxygen absorbs free electrons and is excited to superoxide radicals that exhibit strong oxidation potentials.[1],[124] Therefore, it was envisaged that a combination of synthetic CVD diamond positive holes and superoxide free radicals would be effectively generated under ultraviolet irradiation for the oxidation of benzyl alcohol (figure 41).

From a review of the literature to identify the appropriate alcohol (benzyl alcohol) and terminal oxidant (molecular oxygen), benzyl alcohol oxidation was investigated using a

commercially available synthetic CVD diamond grinding powder. The first sample purchased was a synthetic CVD diamond powder with a grading of 0-1 microns (figure 42). The particle size (0-1 microns) was believed to be appropriate to the reaction scheme due to its larger surface area to volume ratio than the other catalogued products.

Figure 42: 0-1 micron graded synthetic CVD powder.

In the preliminary reactions, one millimol (mmol) of benzyl alcohol was added to a mixture of acetonitrile (CH_3CN, 2 ml) and synthetic CVD diamond power (0-1 micron graded, 15 mg), hereafter referred to as boron doped diamond (BDD 0-1) in a quartz test tube.

The test tubes were purged with oxygen gas above the reaction mixture for two and a half minutes to oxygenate the reaction mixture, which were then sealed. Following the oxygenation, the test tubes were housed around a 2000 W OSRAM® ultraviolet lamp and irradiated (table three). The OSRAM® lamp was chosen for its strong ultraviolet radiation flux and was housed in a quartz cylinder that was submerged under water to prevent the lamp from over-heating due to extended periods of use. A copper coil in the water bath enhanced the cooling process by circulating 5 ℃ water from a water chiller (figure 43).
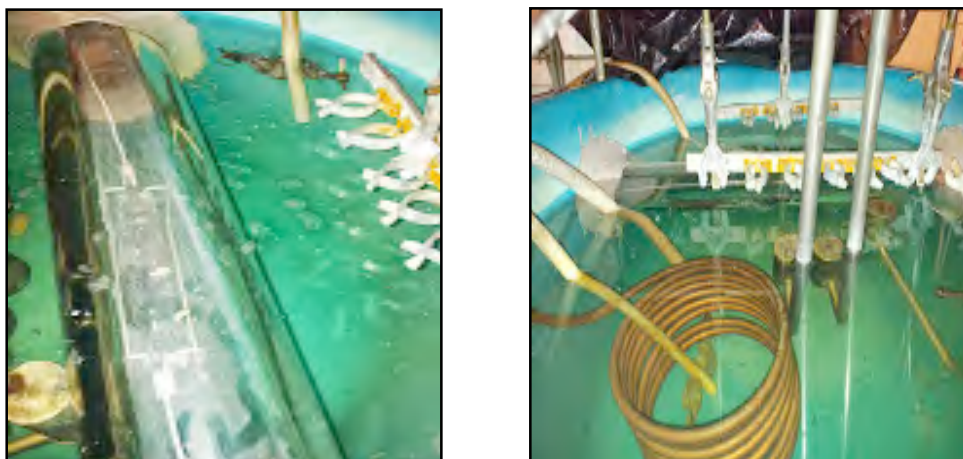
Figure 43: Ultraviolet setup for irradiation of quartz test tubes.

From the preliminary investigations presented in table two below, the oxidative system using the synthetic CVD diamond powder exhibited promising results. There were however, inconsistencies in the results with entry one showing no benzaldehyde yield while entries two, three and four listing benzaldehyde yields of varied percentages. One of the important objectives of the project was to obtain selective oxidation of the chosen alcohol to either benzaldehyde or benzoic acid. The literature has reported that selective oxidation control is highly valuable;[1] therefore an emphasis was focused on achieving high yields of either benzaldehyde or benzoic acid with continued modification of the synthetic CVD diamond oxidative system until this was obtained.

Table 2: Preliminary findings of benzyl alcohol oxidation.[a]
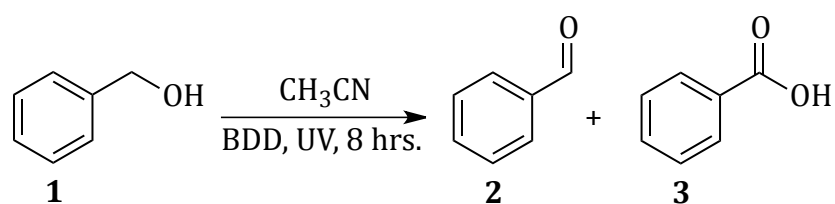
Entry	BDD (0-1) (mg)	Product **2** yield (%)	Product **3** yield (%)
1	25	0	0
2	20	18	0
3	15	12	0
4	10	24	0

[a] Benzyl alcohol (1 mmol) **(1)** and acetonitrile (0.5 ml) were added to test tubes prior to purging with oxygen gas for two and a half minutes followed by 8 hours of ultraviolet irradiation (UVA/UVB). The yields of **2** and **3** were determined using the integral ratios from ^{1}H NMR spectroscopic data.

Once each reaction in table 2 had run for the designated period, a noticeable thin diamond film had deposited on the walls of each quartz test tube, which may have accounted for the observed results. This finding was of concern since the thin synthetic CVD diamond film was sus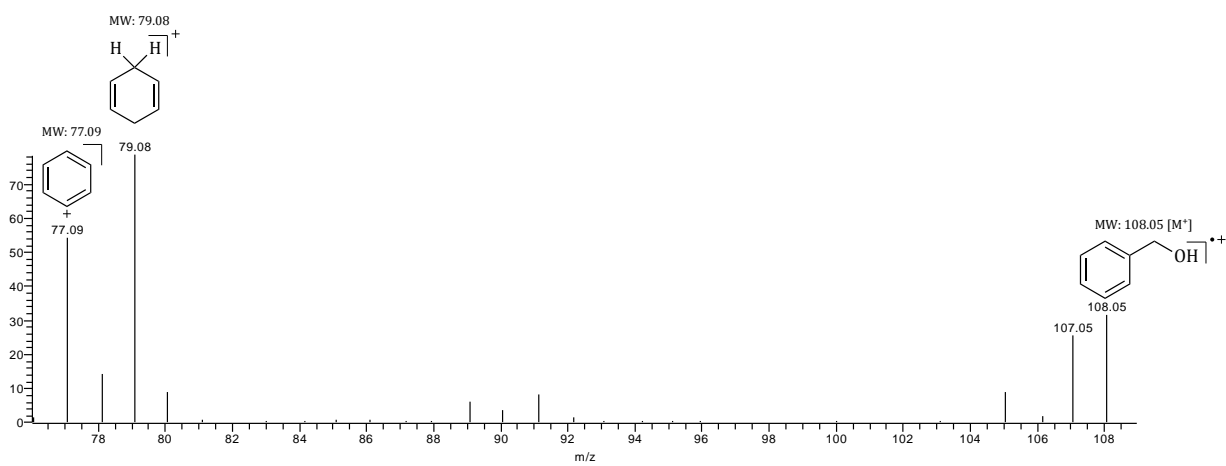pected of inhibiting the ultraviolet light from entering the test tubes and promoting the full activation of the bulk synthetic CVD diamond powder.

Similar observations have been reported in the literature where a phenomenon known as 'stagnant film theory' has explained how a limitation in the transfer of reactants (such as a organic waste-water pollutant) from the bulk medium to the catalyst's surface (lower analyte concentration) causes a reduction in catalytic efficiency.[125] This statement has shown validity in the benzyl alcohol study since the thin synthetic CVD diamond film was suspected of decreasing the reactant-catalyst interaction by inhibiting light transmittance to the organic solution. Therefore, the reaction conditions needed to be adjusted in order to reduce or limit the formation of the thin synthetic CVD diamond film.

After identifying that the reaction conditions were producing a thin synthetic CVD diamond film, the diamond loadings were reduced and the benzyl alcohol oxidations were repeated. The volume of solvent used for each reaction was also lowered, so as to increase the catalyst-reactant interaction period (table 3).

Table 3: Modified reaction conditions for benzyl alcohol oxidation.[a]
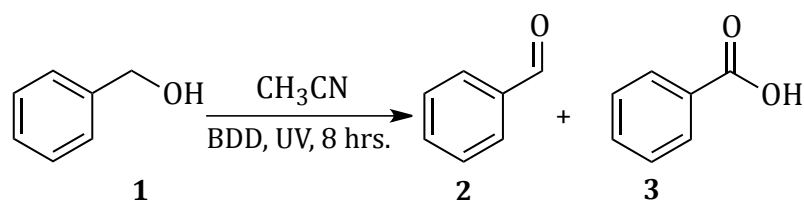
Entry	BDD (0-1) (mg)	Product **2** yield (%)	Product **3** yield (%)	Other side products (%)
5	4	10	13	20
6	3	17	50	9
7	2	15	46	10
8	1	8	65	7

[a] Benzyl alcohol (1 mmol) **(1)** and acetonitrile (0.5 ml) were added to test tubes prior to purging with oxygen gas for two and a half minutes followed by 8 hours of ultraviolet irradiation (UVA/UVB). The yields of **2** and **3** were determined using chromatographic peak areas on a Thermo Finnigan GC-MS.

The outcome of reducing the amount of solvent and catalyst significantly improved the results of benzyl alcohol oxidation as evident in table 3 above. The results illustrated that the mass of synthetic CVD diamond powder added to reactions five through eight had limited effects on controlling its oxidative capabilities with a wide scope of oxidised products being produced. Hence, in an attempt to evaluate the potential oxidising efficiency of the synthetic CVD diamond, the four reactions in table 3 were repeated with the results tabulated in table 4.

Table 4: Rerun of reactions presented in table 3.[a]
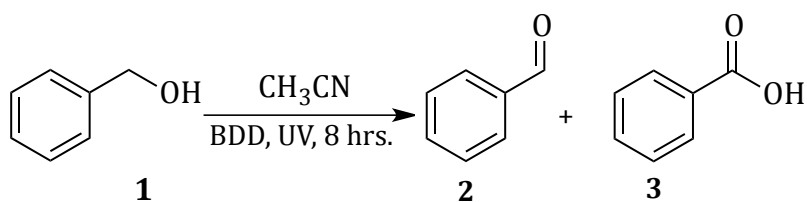
Entry	BDD (0-1) (mg)	Product **2** yield (%)	Product **3** yield (%)	Other side products (%)
9	4	14	42	5
10	3	10	21	26
11	2	13	25	19
12	1	9	54	13

[a] Benzyl alcohol (1 mmol) **(1)** and acetonitrile (0.5 ml) were added to test tubes prior to purging with oxygen gas for two and a half minutes followed by 8 hours of ultraviolet irradiation (UVA/UVB). The yields of **2** and **3** were determined using chromatographic peak areas on a Thermo Finnigan GC-MS.

The yields presented in table 2 were measured with ^{1}H nuclear magnetic resonance (NMR) spectroscopy. However, gas chromatography was introduced to simplify the quantification of the complex reaction mixtures after inspecting the multitude of over-lapping NMR peaks. An Elite-5MS column was utilised during preliminary quantifications, which was later exchanged (due to poor peak resolution) after purchasing a more applicable free-phase fatty acid column. While the free-phase fatty acid column was being sourced, a Thermo Finnigan Trace gas chromatograph and PolarisQ mass spectrometer provided the necessary instrumentation for data collection (figure 44).

a) Gas chromatogram of complex reaction mixture.

Benzyl Alcohol

RT: 5.68
AA: 97504527

Benza
ldehy
de

Side Product

RT: 15.24
AA: 35328627

Benzoic Acid

RT: 4.50
AA: 17382361

RT: 7.99
AA: 22564407

Time (min)

b) Benzy   cohol (5.66   in.)

MW: 79

H   H

MW: 77.09

79.08

70

MW: 108.05 [M$^+$]

60

OH$\rceil^{\bullet+}$

77.09

50

40

30

108.05

20

107.05

10

0

m/z

c) Benzaldehyde (4.56 min.)

MW: 77.07

MW: 105.05 [M$^+$]

100

105.05

O$\rceil^+$

90

80

70

77.07

60

50

40

30

106.01

20

10

0

m/z

66
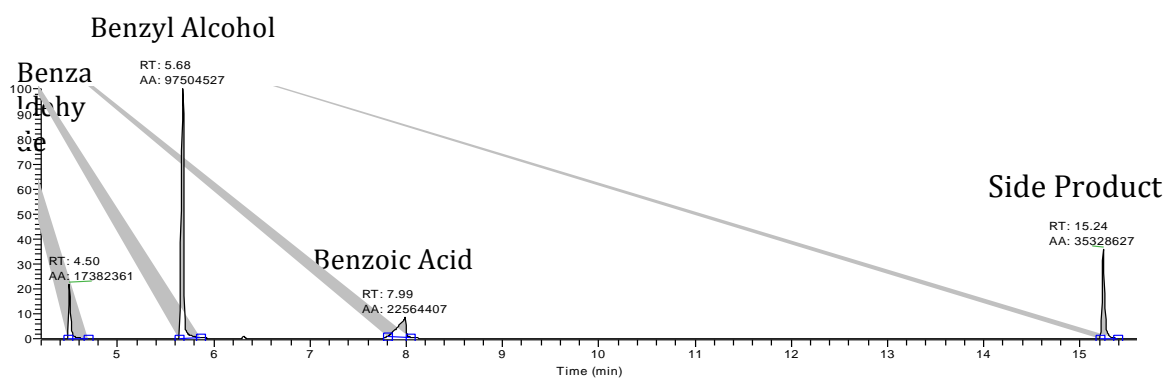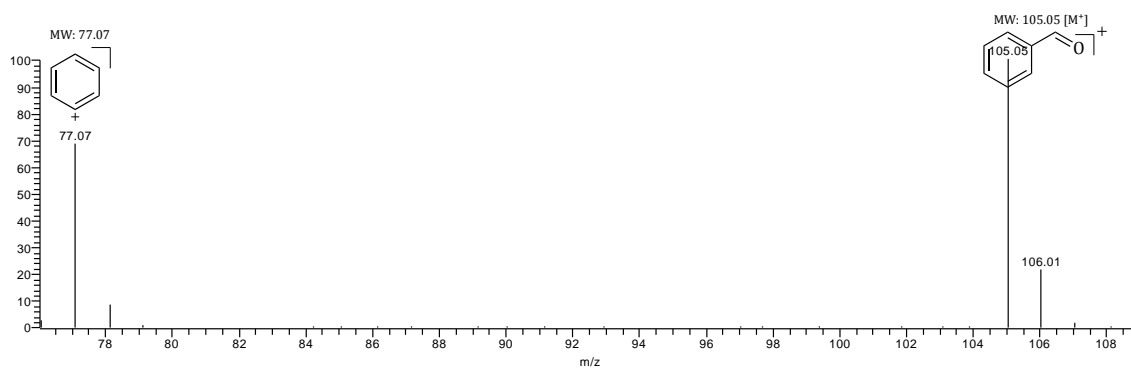
d) Benzoic acid (7.83 min.)
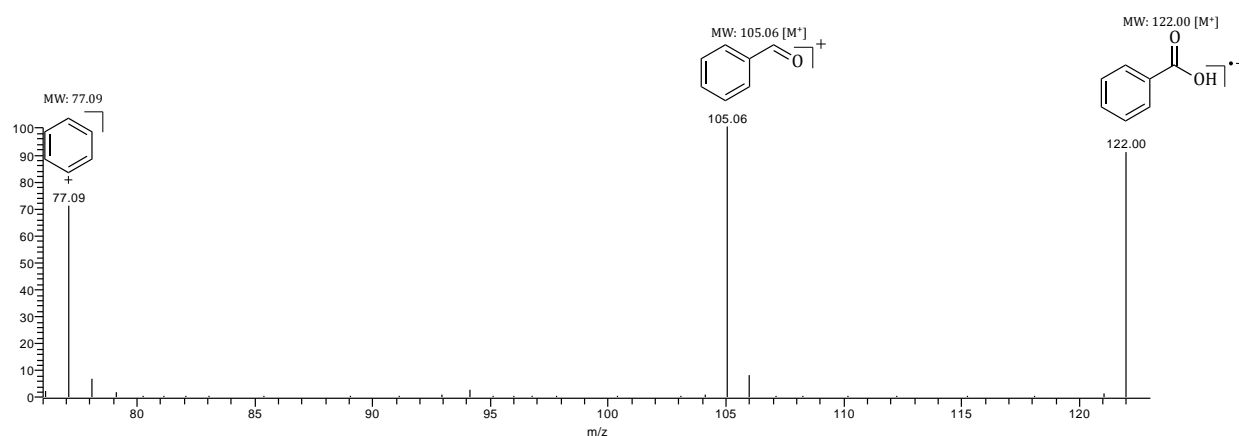
Figure 44: Gas chromatograph – mass spectrometry data of entry twelve, table four.

Sample Calculation:

OH PA:	Benzyl alcohol peak area
CHO PA:	Benzaldehyde peak area
COOH PA:	Benzoic acid peak area
SP PA:	Side product peak area

$$\text{Benzaldehyde yield} = \left(\frac{\text{[CHO] PA}}{\text{[OH+CHO+COOH+SP] PA}} \right) \times 100$$

$$\text{Benzaldehyde yield} = \left(\frac{17382361}{17382361+97504527+22564407+35328627} \right) \times 100$$

$$= 10\%$$

From a comparison of the data presented in tables 3 and 4, there was no apparent oxidative trend and the selective oxidation of benzyl alcohol was unclear. It was evident though, that the quartz test tubes (as shown in figure 46 **[a]**) were located at different sites relative to the central horizontal position of the lamp. This was conjectured to be a possible source of inconsistent oxidation results due to variations in radiation intensities emitted to each test tube. Later confirmation from the OSRAM® lamp specification sheet indicated that the lamp had a maximum burning angle of 30° (relative to the horizontal, figure 45). The information obtained from the specification sheet lead to suggest that the radiation emissions and test tube array were potentially contributing to the unpredictable conversions of benzyl alcohol.
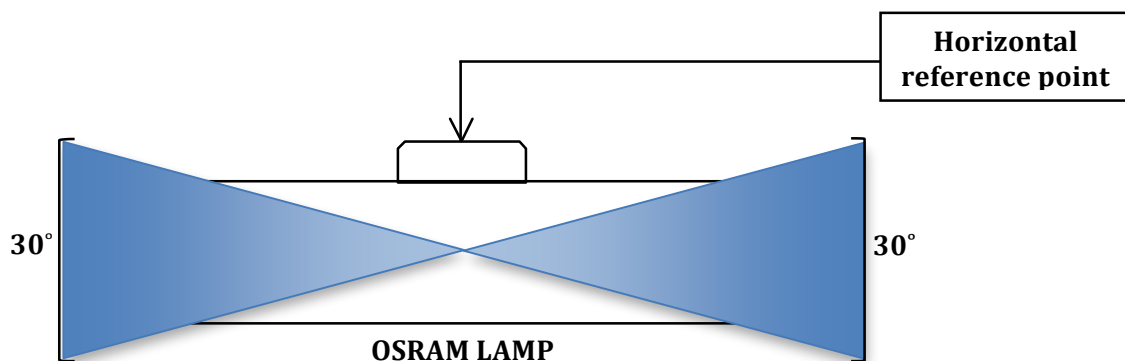
Figure 45: OSRAM lamp horizontal burn angle (30˚).

Therefore, the positioning of each test tube was altered in an attempt to achieve an optimal light exposure for each test tube to the lamp source. From the preliminary investigations (tables 2,3,4), the test tubes were arranged in a half moon arrangement around the lamp (figure 46 **[a]**. Although it was suspected that the distribution of photonic emissions were not being fully utilised after considering the data represented in figure 45. A further analysis of the test tube arrangement suggested that the foreground test tubes were shielding the ultraviolet radiation from reaching the rear test tubes ($\otimes$) (figure 46 **[a]**). Therefore, the test tube arrangement (figure 46 **[a]**) currently being used was believed to be the cause of inconsistent oxidation yields, which may have been attributed to the shielding effects of the foreground test tubes. Subsequently, the setup was modified to house three test tubes that were each clamped in a straight line that were all equidistant from the lamp. Two setup apparatus were erected; one on each side of the lamp to support six reactions being irradiated during each reaction run (figure 46 **[b]**).

a)
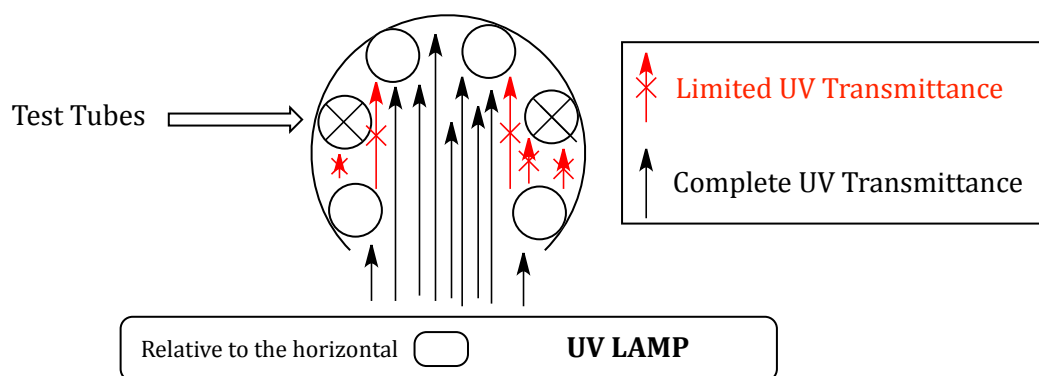
b)
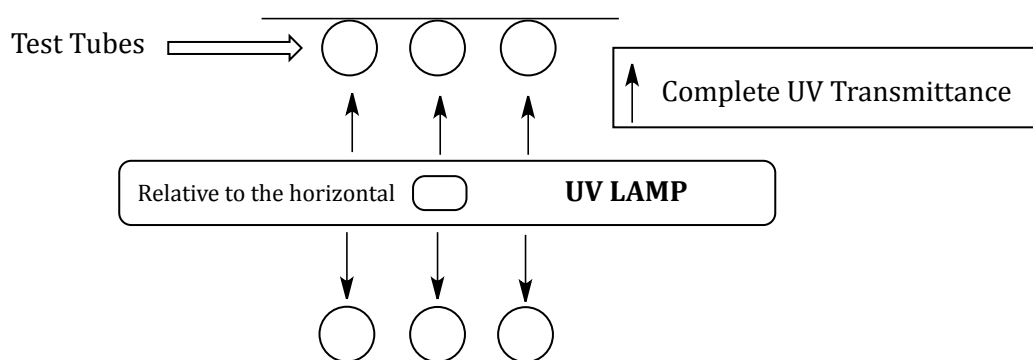
Figure 46: Half moon (a) and linear (b) reaction rack setups used in the irradiation bath.

As indicated in figure 46, the curved lamp setup was suspected of causing a shielding effect for the radiation reaching the background test tubes.

During this stage of the study, further evaluation with respect to catalyst loading and test tube arrangement were investigated to assess the selective oxidative control of the synthetic CVD powder. For a third attempt, the same reactions from table 4 were repeated once more, while reducing the synthetic CVD diamond loadings significantly with the new 'linear' test tube array (table 5).

Table 5: Benzyl alcohol oxidation using 0.1-0.4 mg synthetic CVD diamond catalyst loadings.[a]
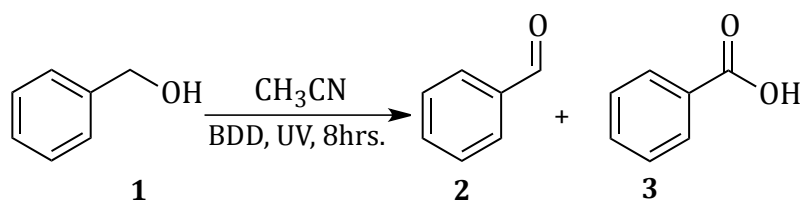
Entry	BDD (0-1) (mg)	Product **2** yield (%)	Product **3** yield (%)	Other side products (%)
13	0.4	4	87	3
14	0.3	11	55	28
15	0.2	6	74	5
16	0.1	7	56	13

[a] Benzyl alcohol (1 mmol) **(1)** and acetonitrile (0.5 ml) were added to test tubes prior to purging with oxygen gas for two and a half minutes followed by 8 hours of ultraviolet irradiation (UVA/UVB). The yields of **2** and **3** were determined using chromatographic peak areas on a Thermo Finnigan GC-MS.

Further data was collected and tabulated in table 5 which revealed that the synthetic CVD diamond semiconductor mediated nonselective alcohol oxidations even after altering the test tube positioning. Table 5 did *howbeit* introduce a compelling near total conversion of benzyl alcohol. The conversions ranged from 76% (entry 16) to an almost quantitative conversion (94%, entry 13) of benzyl alcohol to benzaldehyde, benzoic acid and other side products. The results in table 2 presented a limited oxidation of benzyl alcohol while tables 3,4 and 5 had improved results, although with no reproducibility. Inspection of the data collected in table 3,4 and 5 illustrated that the majority of the product was benzoic acid. The yields of benzoic acid (from tables 3,4 and 5) revealed great prominence to the data presented in table 2. This suggested that the photocatalytic system's 'proof of concept' stage was near completion (in terms of selectivity); however it was decided necessary to continue the optimisation of the synthetic CVD diamond oxidative system before attempting to oxidise a wider scope of alcohols.

2.2.2) Nucleophilic coupling of benzyl amine

While investigating sources of information to promote reproducible–selective benzyl alcohol oxidation, the experimental study focused on the introduction of a nucleophilic trapping agent. Since aldehydes are known to be valuable key intermediates in synthetic procedures,[126] an attempt at regulating the synthetic CVD diamond oxidative system was attempted while using benzyl amine to trap benzaldehyde (figure 47).
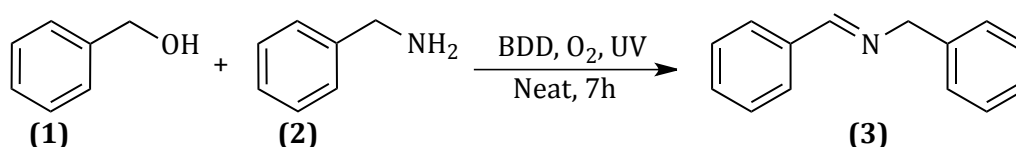
Figure 47: Trapping of benzaldehyde using benzyl amine in an one-pot synthesis.

Besides using benzyl amine (figure 47, **[2]**) as a nucleophilic trapping agent, the addition of an amine was introduced to impart a Le Châtelier *'like'* principle that would promote the exclusive production of benzaldehyde over benzoic acid. As the production of *N*-benzylidenebenzylamine (Figure 47, **[3]**) would only occur in the presence of an aldehyde, the addition of benzyl amine was chosen to selectively produce benzaldehyde formation while using the synthetic CVD diamond.

In addition, the choice of using benzyl amine as a trapping agent arose from a literature study reported by Burdzhiev and Stanoeva.[127] *N*-benzylidenebenzylamine was reacted with glutaric anhydride to produce 1-benzyl-6-oxo-2-phenylpiperidine-3-carboxylic acid (figure 48 **[6])**, which contained a piperidine parent structure. It was mentioned that piperidine chemistry has shown promising results in anti-inflammatory and anticonvulsant studies.[127]
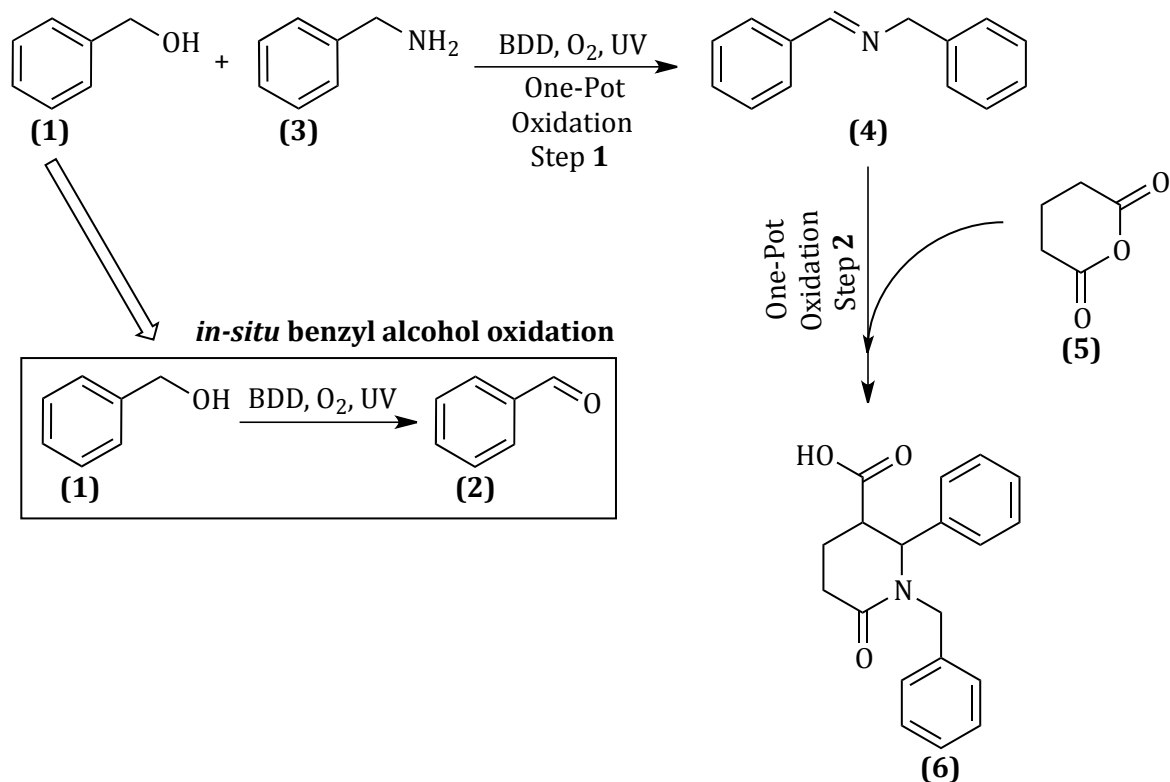
Figure 48: Synthesis of *trans*-1-benzyl-6-oxo-2-phenylpiperidine-3-carboxylic acid.

Due to the reported biological activity of piperidines, an interesting opportunity arose to potentially apply an advanced one-pot oxidation process to the benzyl alcohol oxidation study for the synthesis of these important biologically active molecules once the nucleophilic coupling-optimisation was complete. The tandem oxidation route was designed to oxidise benzyl alcohol (figure 48 **[1]**) to benzaldehyde (figure 48 **[2]**), which would be trapped with benzyl amine (figure 48 **[3]**) to afford *N*-benzylidenebenzylamine (figure 48 **[4],** one-pot oxidation step **1**). The proposed concept would then couple *N*-benzylidenebenzylamine further with glutaric anhydride (figure 48 **[5]**) for the synthesis of 1-benzyl-6-oxo-2-phenylpiperidine-3-carboxylic acid (figure 48 **[6],** one-pot oxidation step **2**). However, as will be discussed later in the Results and Discussion (Chapter 2 ([2.3.6])), pertinent findings on the reactivity of imine chemistry under ultraviolet light and the activation of the synthetic CVD diamond surface prohibited the coupling study from being pursued further.

In table 6, quantitative measurements were computed using the Thermo Finnigan GC-MS that served to quantify *via* average peak area measurements (as illustrated in figure 49 below).

a) Gas chromatogram of complex reaction mixture.
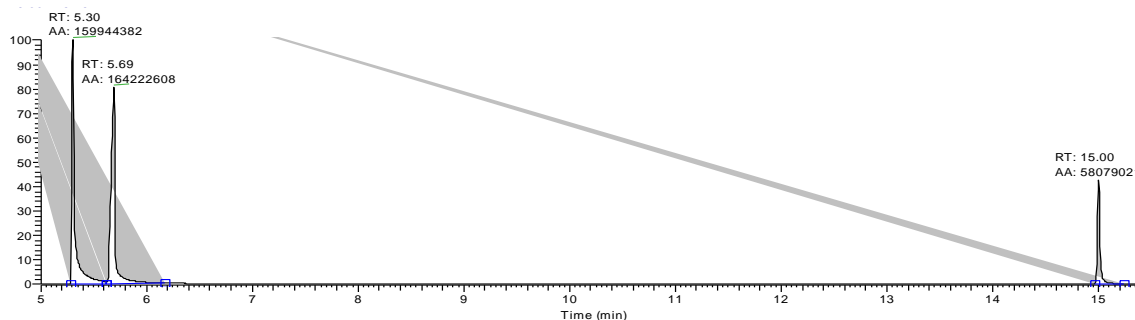
b) Benzyl alcohol (5.69 min.)
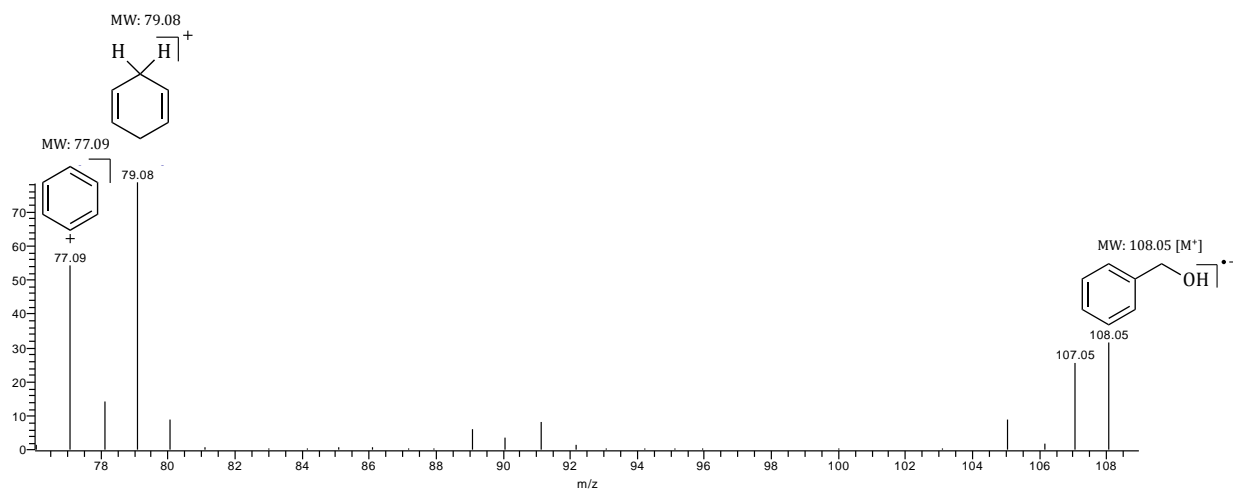
C) Benzyl amine (5.30 min.)
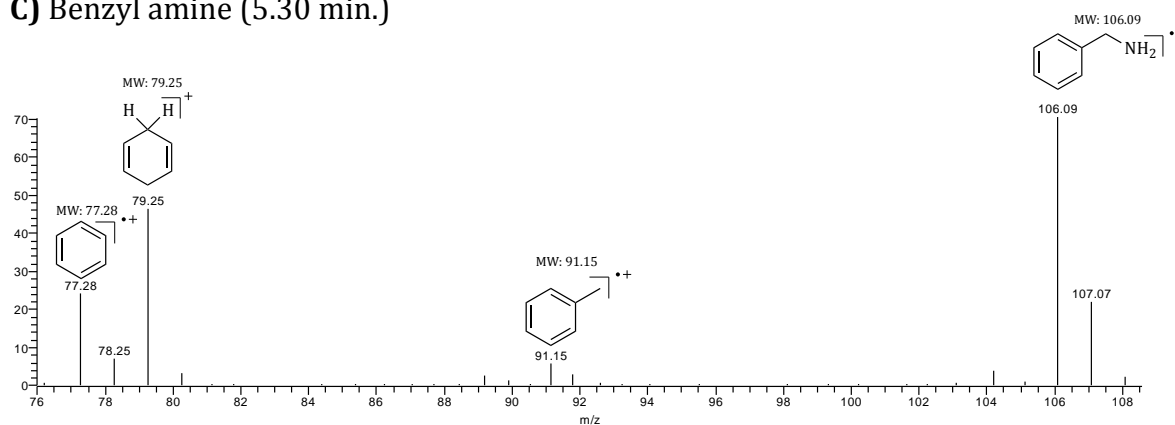
D) *N*-benzylidenebenzylamine
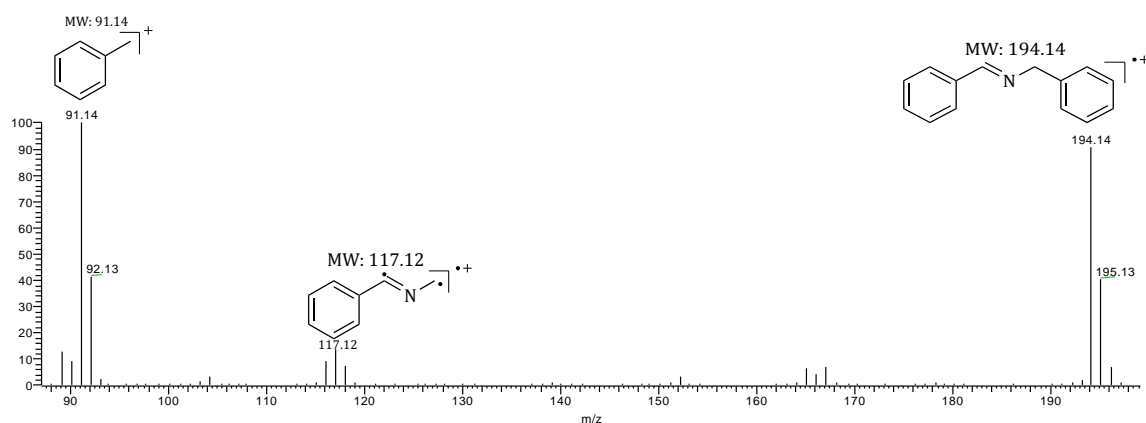
Figure 49: ***N*-benzylidenebenzylamine identification and chromatographic yield determination.**

The amine coupling was repeated with five identical reactions being completed and tabulated below (table 6).

Table 6: Alcohol oxidation-nucleophilic trapping of aldehydes.[a]
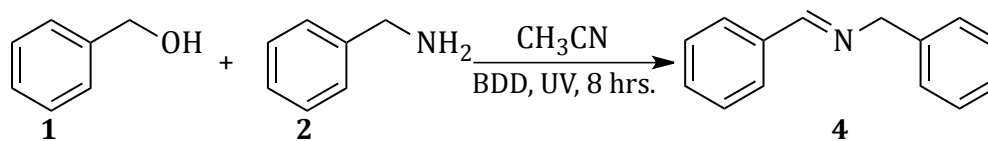
Entry	Product **4** yield (%)
17	8
18	8
19	99
20	38
21	35
22	28

[a] Benzyl alcohol (1 mmol) **(1)**, benzyl amine (2 mmol) **(2)** and BDD ([0-1 micron graded] 10 mg) were added to test tubes prior to purging with oxygen gas for two and a half minutes followed by 8 hours of ultraviolet irradiation (UVA/UVB). The yields of **(4)** were determined using chromatographic peak areas on a Thermo Finnigan GC-MS.

Until this stage in the project, the benzyl alcohol oxidation studies had proven to be highly erratic and produced various oxidised products and yields. Therefore, to assess if a similar uncontrollable trend would be detected during the nucleophilic coupling reactions, entry 17 of table 6 was repeated multiple times. The various reagents and catalyst (0-1 micron grading synthetic CVD diamond powder) were added to each of the test tubes at the start of the reactions and were not interfered with until deemed complete and ready for quantitative analysis in accordance with standard one-pot procedures.[44] In an attempt to achieve reproducible results, the nucleophilic attack of benzyl amine on the benzaldehyde intermediate was run under neat conditions without any solvent present. The newly designed linear test tube setup (figure 46 **[b]**) was used to promote uniform irradiation of each test tube.

Once again, the results obtained in table 6 were similar to those recorded for the benzyl alcohol oxidation (tables 2-5). The yield of *N*-benzylidenebenzylamine varied significantly from a near quantitative 99% (entry 19) to a low 8% yield (entry 17). Despite all the modifications made to the reaction setup (test tube array) and performing the reactions with the absence of any solvent, the differences amongst the yields of *N*-benzylidenebenzylamine were still evident. A great deal of research had been conducted to ensure that the yields of *N*-benzylidenebenzylamine were high and consistent. However the data collected from the experiments performed in table 6 confirmed that a major dissimilarity in product yield existed between the succeeding reactions. Upon analysis of table 6, two variables were considered to be a potential cause of these inconsistencies. Firstly, the position of each test tube relative to the ultraviolet lamp was believed to be a cause of the erratic yields. However, after inspecting the data from tables 5 and 6, the theory of unequal radiation flux was no longer appearing to be a valid cause for the poor selective control while using the synthetic CVD diamond photocatalytic system.

The second variable that had been assessed for inhibiting high yields of *N*-benzylidenebenzylamine was the deprotonation of the benzyl alcohol. Attention was directed towards the assessment of benzyl alcohol and its conversion into benzaldehyde. Various literature sources have reported that alcohol oxidation could be hastened from the addition of a base.[128],[129] In addition, Jiang, *et al.*, reported excellent imine yields while using catalytic quantities of potassium hydroxide.[130] The base functioned to deprotonate the alcohol by extracting the hydroxy proton and therefore in this investigation, enabled the removal of an α-benzylic proton on the benzyl alcohol to affect the oxidation to benzaldehyde, which would promote the nucleophilic addition of benzyl amine. Therefore, benzyl alcohol oxidation was investigated by comparing potassium hydroxide (KOH) and sodium hydroxide (NaOH) as strong nucleophilic bases to favour *N*-benzylidenebenzylamine synthesis (table 7).

Table 7: Base mediated alcohol oxidation using BDD.[a]
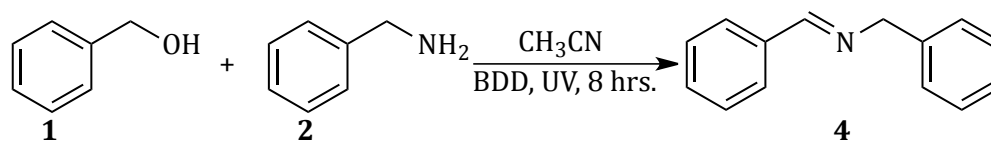
Entry	Base (mol%)	Product 4 yield (%)
23	KOH (10)	26
24	KOH (10)	35
25	KOH (10)	31
26	NaOH (130)	52
27	NaOH (130)	51
28	NaOH (130)	65

[a] Benzyl alcohol (1 mmol) **(1)**, benzyl amine (2 mmol) **(2)** and BDD ([0-1 micron graded] 10 mg) were added to test tubes prior to purging with oxygen gas for two and a half minutes followed by 8 hours of ultraviolet irradiation (UVA/UVB). The yields of **(4)** were determined using chromatographic peak areas on a Thermo Finnigan GC-MS.

The addition of the bases showed noticeable improvements, not only in the yield of *N*-benzylidenebenzylamine but also in the reproducibility of the results. The potassium hydroxide promoted imine yields in excess of 20%, which was a considerably more stable mean when compared to the data present in table 6. There was also a further improvement in these results (entries 26-28, table 7) when information was gathered from an article published by Cano and co-workers[131] who used sodium hydroxide for similar studies. After inspecting the article by Cano, 130 mol% sodium hydroxide was used to synthesis *N*-benzylidenebenzylamine with three consistent yields above 50%. This newly found evidence motivated that both potassium and sodium hydroxide were

indeed promoting the production of *N*-benzylidenebenzylamine; however the catalytic system was still to be optimised.

Further hypotheses were obtained from the chemical literature after analysing the previous reaction tables (table 2-6). This information resulted in a trial to identify the low oxidative potential of the synthetic CVD diamond powder by testing the newly found literature findings. Solvents were reported to contain stabilisers which limit the degradation of solvents such as chloroform.[132] However, the possibility for solvent degradation (under ultraviolet irradiation) was a concern and feasibly a contributing factor towards the irregular oxidation patterns of benzyl alcohol from interactions between the degraded solvent products and benzyl alcohol. Other findings, which were identified after inspecting the data of tables 2-6, suggested that differences in oxygen saturation existed during the period when each test tube was purged with oxygen. The differences in oxygen saturation levels may have contributed to the variation amongst the yields of *N*-benzylidenebenzylamine. Lastly, after reviewing the chemical literature, the data suggested that the imine bond was sensitive to environmental and chemical conditions.[133] The current electromagnetic radiation reaction setup utilised strong ultraviolet radiation and was suspected to be the cause of the possible imine degradation. Therefore, each of the newly found viewpoints were assessed with various reactions being performed to evaluate their value.

2.3) Adjusting reagent parameters.

2.3.1) Solvent degradation.

The concern of solvent degradation was investigated, as it appeared possible that the solvents that had been used in this project could have been subject to chemical transformations in the presence of electromagnetic radiation. This was speculated since the short-wavelength ultraviolet radiation possessed a significant amount of energy that had the potential to break chemical bonds in the solvent molecules. Suna, *et al.*,[134] reported that toluene was capable of being degraded in the presence of a Fe-TiO$_2$ catalyst that was prepared using a sol-gel method.[134] During their investigation, toluene was identified to degrade into various products, which were identified to cause

catalyst poisoning. In other literature reports, Addamo and co-workers investigated acetonitrile decomposition studies but identified that acetonitrile was less prone to degradation, especially while in the liquid phase.[135] These findings presented a strong relevance to the current study and hence the evaluation of solvent degradations was investigated for toluene and acetonitrile (CH_3CN) (figure 50). To test these findings, three milliliters of each solvent were placed in clean quartz test tubes in the absence of any diamond powder. The test tubes were also sealed off to prevent the solvent being exposed to atmospheric oxygen and to stop any evaporation over the course of the irradiation period. From the data presented in figure 50, toluene appeared to be unaffected during the course of the irradiation (figure 50 has illustrated the toluene solvent study. ^{1}H NMR spectroscopic analysis of acetonitrile is available in the supporting appendix).
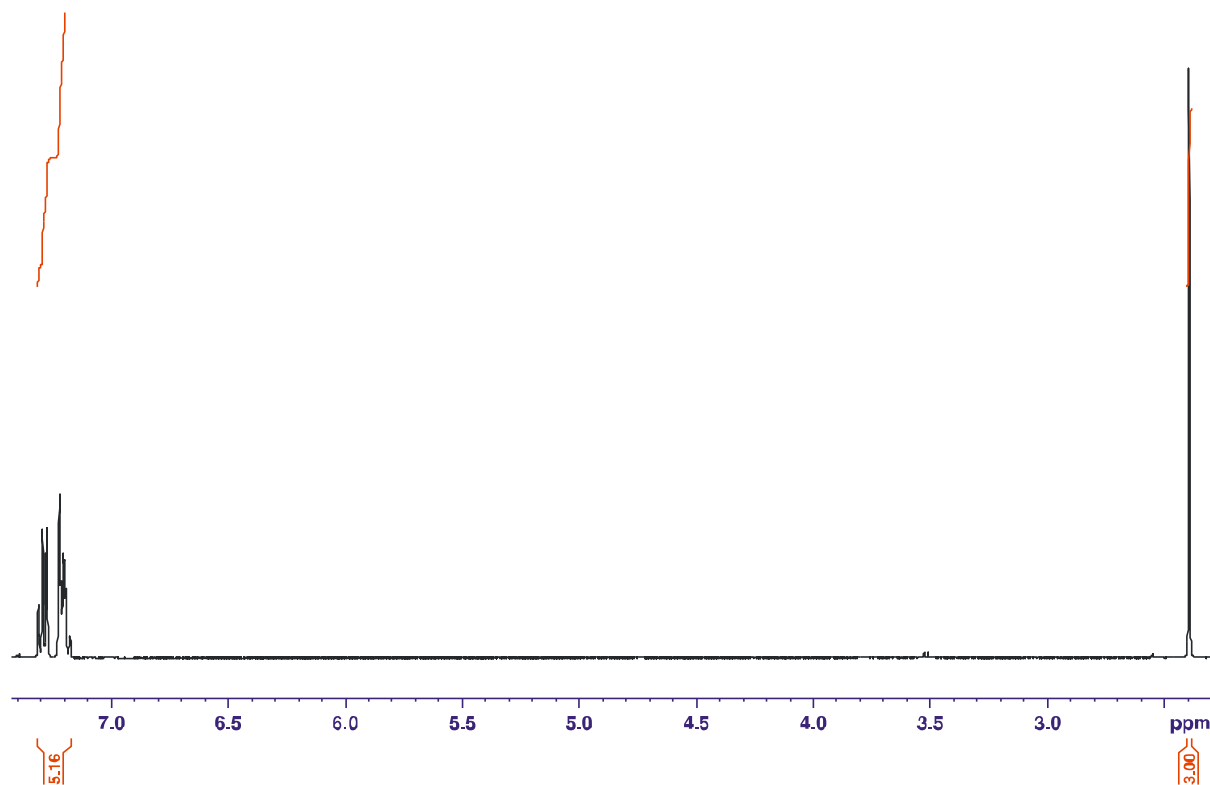
Figure 50: Irradiation of toluene to investigate solvent degradation.

After investigating the two solvents for evidence of decomposition, the data suggested that the solvents were not contributing nor inhibiting the oxidations, as the evidence marked no signs of decomposition in the peaks presented in the two spectra.

While investigating the effects of solvent degradation in the literature for the possibility of preventing synthetic CVD diamond activation, Marko´, *et al*.,[128] reported that polar solvents such as acetonitrile were incompatible for alcohol oxidations. The research identified that polar solvents exhibited inhibiting oxidation attributes, a*lbeit* non-polar solvents such as trifluoromethylbenzene, toluene and benzene were superior choices that quickened reactions significantly. This new evidence indicated that additional reactions needed to be scheduled with the addition of increased oxygen saturations.

2.3.2) Oxygen saturation

Literature findings revealed numerous studies where pure oxygen gas was bubbled through reaction mixtures for an efficient catalyst-terminal oxidant interaction[124],[79] with similar results being achieved while using high pressure oxygen environments (10 atmospheres).[136] The literature reasoned that an increased oxygen-catalyst interaction would promote the removal of free elctrons in the conduction band of semiconductors as well as increase the terminal oxidant concentration in the reaction medium. After completing the solvent study of toluene and acetonitrile, which proposed that, the solvents did not appear to degrade under ultraviolet radiation; benzyl alcohol oxidation was attempted while using toluene with constant oxygen saturation through the test tubes. In order to achieve constant oxygen saturation, the following setup was devised to deliver oxygen to each of the six test tubes for up to eight hours (figure 51).
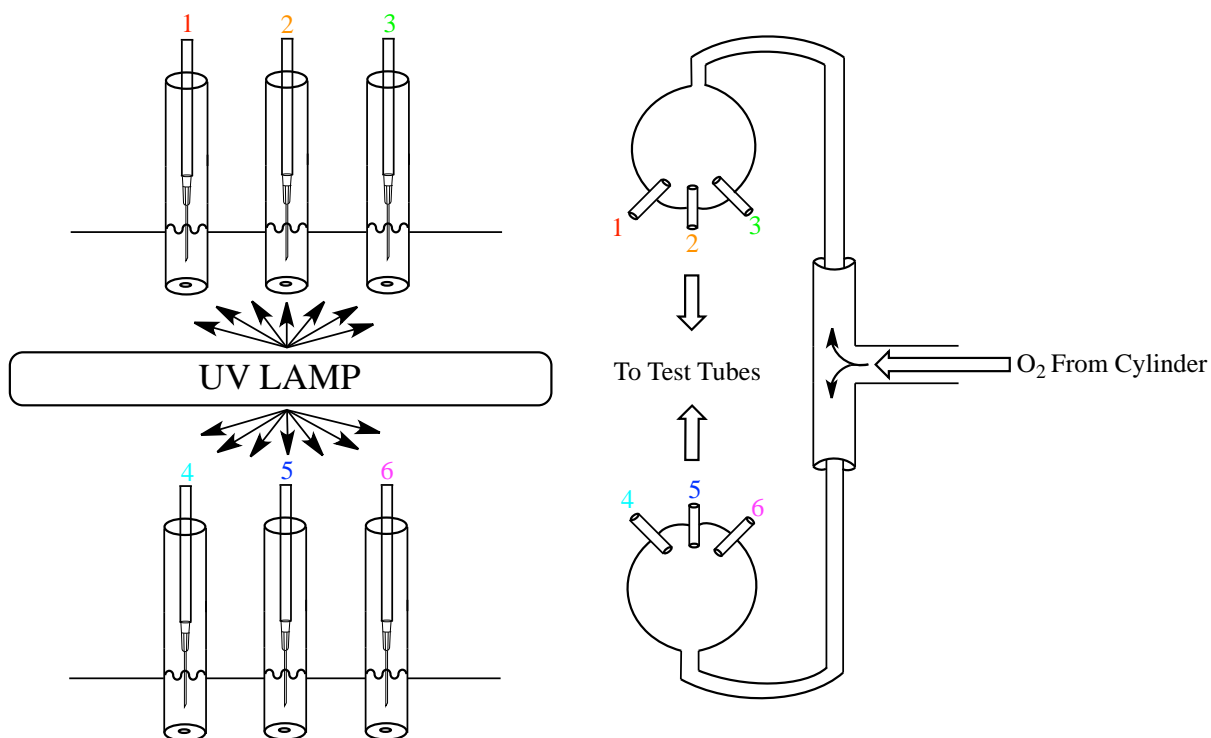
Figure 51: Oxygen bubbling system for alcohol oxidations.

Benzyl alcohol oxidation was tested while using synthetic CVD diamond powders, toluene and the newly designed oxygen saturation system (figure 51). However after multiple attempts, reaction yields were very low (the maximum benzaldehyde yield was 6% and there was no detectable benzoic acid). Therefore the benzyl alcohol oxidation system needed further refinement. In an attempt to achieve a benzaldehyde yield greater than 6%, an increased oxygen supply was employed to trap a greater magnitude of conduction band electrons on the surface of synthetic CVD diamonds, however no notable improvement was noted. Toluene had also been discussed by Marko′, *et al.*,[128] to be an appropriate choice for alcohol oxidations but the extra gaseous oxygen and toluene had no apparent beneficial effects.

After completing the oxidation reactions using toluene and continuous oxygen saturation, it was evident that the synthetic CVD diamond mediated oxidative system was more complicated than originally expected. An electron paramagnetic investigation was suggested to evaluate whether superoxide species were present in the acetonitrile and toluene reactions. However, it was considered to be beyond the scope and aims of

this thesis. In hindsight, it was also later discovered that a test reaction using acetonitrile, sodium hydroxide and oxygen saturation was advisable. However, as will be discussed later in the Results and Discussion, this had no influence on the benzyl alcohol oxidation study due to pertinent findings on the band gap structure of synthetic CVD diamond.

2.3.3) 20-80 micron-graded Synthetic CVD diamond powder

After thoroughly assessing the results from tables 2-7, the oxidative system was found to be highly complex and considerably more so than expected. Therefore, the entire contents of the oxidation study were reviewed and in particular, one variable that had not been addressed was the 0-1 micron graded synthetic CVD diamond powder. It has been previously reported in the Results and Discussion (Section 2.2) that the synthetic CVD diamond powder was forming thin films that coated the insides of the quartz test tubes. Consequently, as this was one variable that had not been studied, an opportunity arose to purchase two supplies of synthetic CVD diamond powders with larger grading sizes (20-40 and 54-80 micron graded, figure 52). It was postulated that the larger synthetic CVD diamond grains would not adhere to the surface of the test tubes, thus promoting full exposure of the lamp's emissions to the semiconductor and the reactants housed in each test tube.
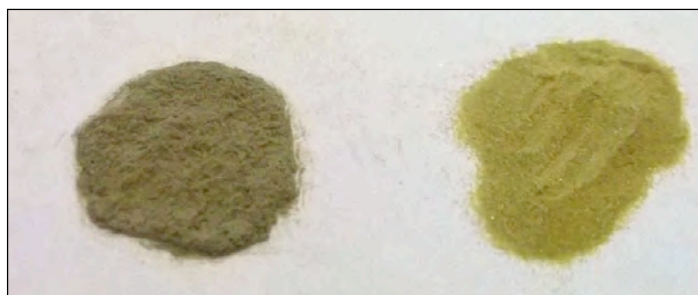
Figure 52: 20-40 (left) and 54-80 (right) micron graded synthetic CVD diamond powders.

Once the synthetic CVD diamond powders had been purchased, another proposal to evaluate benzyl alcohol oxidation was introduced while attempting to scrutinise various solvents and continuous oxygen saturation. However, before attempting the alcohol

oxidation, spectrophotometric studies were required to determine which solvent and glass would be an optimal choice for this investigation. Previous solvent choices were based on reported literature findings[128] yet none were identified to be suitable for oxidising benzyl alcohol in this study.

Twelve organic solvents were identified to possess intrinsic absorption properties after UV/Vis spectrophotometric analysis. Depending of the solvent, absorption outset wavelengths were experimentally determined to vary from 100 nm (water) to 380 nm (toluene). This was an important discovery to the synthetic CVD diamond alcohol oxidation reactions as if the solvent outset (in nanometers) exceeded the excitation band gap energy of diamond (5.5 eV, 225 nm), the solvent would absorb a portion of the ultraviolet radiation and prohibit the photo-activation of the synthetic CVD diamond.

In order to assess suitable solvents, a solvent study examined the absorption outset edge of 12 solvents, which allowed for the determination of the optimal medium to test the oxidation reactions. To measure the solvent absorbance between 200-800 nm, optical grade quartz (HOQ 310H) cuvettes were necessary. This was because the fused quartz would allow for the complete transition of all wavelengths down to 180 nm and be suitable to handle the harsh solvent properties whereas plastic cuvettes would not. For the analysis, a range of solvents was investigated. As shown below is an illustrative example of the absorption spectrum collected from acetone (figure 53).

Figure 53: Acetone absorption spectrum.

After analysing the absorption spectrum of acetone, an additional eleven common laboratory solvents were investigated to determine their ultraviolet adsorption outset windows. In the spectroscopic absorption spectrum of acetone above, the arrow indicated the outset of radiation absorption in the ultraviolet region. An absolute calculated value for the outset was deemed unnecessary since qualitative measures were only required to identify a solvent that had an absorption outset below the band gap of synthetic CVD diamond (5.5 eV, 225 nm).[96] If the solvent absorbed electromagnetic radiation above 225 nm, it was considered to be unsuitable for the oxidation study using synthetic CVD diamonds due to the solvent absorbing a portion of the ultraviolet emissions. This would lower the catalytic efficiency of the synthetic CVD diamond semiconductor.

Once the solvent study was completed, most of the twelve solvents revealed a strong ultraviolet absorption. Therefore, with the aid of the acetone spectrum and the tabulated data (table 8), evidence suggested how various solvents absorb at different wavelengths.

Table 8: Solvent absorbance outset between 200-800 nm. [137],[138]

Entry	Solvent	Approximate Solvent Outset (nm)
29	Acetonitrile	210
30	Chloroform	265
31	Tetrahydronfuran	340
32	Acetone	350
33	Water	< 200
34	Ethyl Acetate	290
35	Ethanol	245
36	Methanol	245
37	Diethyl Ether	270
38	Toluene	315
39	Hexane	245
40	Dichloromethane	245

From the summary presented in table 8, the only logical solvent options were acetonitrile and water due to their low ultraviolet absorbance (220 and < 200 nm respectively).

After inspecting the twelve laboratory solvents, various glasses (from test tubes and NMR tubes) that included standard glassware quartz, HOQ 310H quartz as well as borosilicate NMR tubes were examined for their absorption properties.

In comparison to standard borosilicate glass showing strong absorption between 200-320 nm, the quartz exhibited excellent transmittance of almost all-ultraviolet

radiation in the region, confirming it to be applicable to the study (the borosilicate absorption spectrum has been recorded in the supporting appendix).

With these new findings (solvents and glasses) brought under scrutiny, the study of *N*-benzylidenebenzylamine was re-evaluated (table 9). For the oxidation/nucleophilic-coupling attempts presented in table 9, each of the three micron graded (0-1, 20-40 and 54-80 microns) synthetic CVD diamond powders were tested in duplicates while using continuous oxygen saturation and 18 Ω de-ionised water.

Table 9: *N*-benzylidenebenzylamine synthesis using new operational parameters.[a]
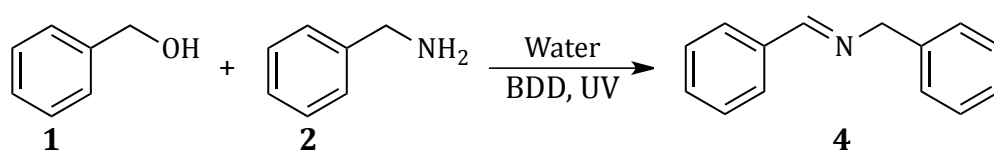
Entry	BDD [micron] (mg)	Time (hrs.)	Product **4** yield (%)
41	[0-1] (15)	1	20
42	[20-40] (15)	1	19
43	[54-80] (15)	1	19
44	[0-1] (10)	0.5	11
45	[20-40] (10)	0.5	10
46	[54-80] (10)	0.5	11

[a] Benzyl alcohol (1 mmol) **(1)**, benzyl amine (2 mmol) **(2)**, ultra-pure 18 Ω water (3 ml) and BDD (0-1, 20-40 and 54-80 micron graded respectively) were added to test tubes prior to continuous oxygen saturation followed by 8 hours of ultraviolet irradiation (UVA/UVB). The yields of **(4)** were determined using chromatographic peak areas on a Thermo Finnigan GC-MS.

Before attempting the reactions of table 9, the chemical literature on imine chemistry identified the imine bond to be acid sensitive and hard to isolate, thus suggesting it to be very delicate.[133] Reaction times were lowered to prevent the intense ultraviolet light from degrading the imines that was questioned after reviewing the chemical literature. However, after the quantitative data for table 9 had been collected and processed, inconclusive evidence lead to suggest that the route of *N*-benzylidenebenzylamine production was unclear. This gave a plausible explanation for low *N*-benzylidenebenzylamine yields that may have been due to the light assisted decomposition of the imine bond after it was formed.

While trying to further investigate literature methods to favour *N*-benzylidenebenzylamine production with high yields while preserving the imine bond, the work undertaken by Marko′, *et al.*,[128] was still highly appealing. The catalytic system designed by Marko′ utilised a copper-azo complex which effectuated excellent aryl alcohol oxidations in toluene. Based on the findings of Marko′, another investigation was explored to assess the statement once more.

2.3.4) 1,1,2-trichloroethane

As mentioned earlier, Marko′, *et al.*,[128] reported polar solvents such as acetonitrile were unsuitable for alcohol oxidations whereas non-polar solvents such as toluene were more favourable. However, after initially investigating the statement made by Marko′ using toluene, the evidence suggested that the solvent choice (toluene) was unsuitable for benzyl alcohol oxidation. To further assess the validity of non-polar solvents, a second attempt using another non-polar solvent (1,1,2-trichloroethane) was tested. From the solvent absorbance spectra reported earlier, a non-polar solvent such as dichloromethane was suspected of being a plausible alternative to acetonitrile, since all of the above reactions yielded low, irreproducible and uncontrollable results. The wavelength outset of dichloromethane (245 nm) was problematic as it was expected to cause a reduction in the synthetic CVD diamond efficiency although it was identified to be the most appropriate non-polar solvent amongst the tested media and was deemed a viable option to explore. Therefore, a re-evaluation of benzyl alcohol oxidation was investigated using a chlorinated solvent.

Initially, dichloromethane was seen as the solvent of choice, however due to its low boiling point (39.8-40 °C),[139] a decision to use an alternative chlorinated solvent seemed appropriate. 1,1,2-trichloroethane with a higher literature boiling point (110-115 °C)[132] appeared to be a better choice (it was less likely to evaporate over the three hour irradiation period), however it contained a stabiliser. According to the literature, the stabiliser was 2-propanol (boiling point: 82 °C)[140] that was easily removed using short-path distillation. The stabiliser needed to be removed by short-path distillation to prevent it from inhibiting the oxidation reactions. After finding a potentially suitable solvent for the oxidation reactions, benzyl alcohol was investigated once again using a continuously saturated non-polar solvent with the 54-80 micron graded synthetic CVD diamond powder under ultraviolet irradiation. The result of these reactions are summarised below.

Table 10: Oxidation of benzyl alcohol with revised reaction conditions.[a]
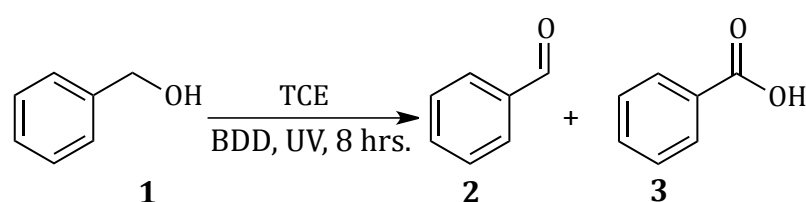
Entry	Product **2** yield (%)	Product **3** yield (%)	Other side products (%)
47	14	65	7
48	9	75	8
49	3	88	6

[a] Benzyl alcohol (1 mmol) **(1)**, trichloroethane (TCE) (3 ml) and BDD (54-80 micron graded, 45 mg) were added to test tubes prior to continuous oxygen saturation followed by 8 hours of ultraviolet irradiation (UVA/UVB). The yields of **(2)** and **(3)** were determined using chromatographic peak areas on a Thermo Finnigan GC-MS.

Finally, it was evident that there was a strong indication that the oxidative system was functioning and what appeared to be, efficiently. Entry 47 of table 10 showed a pleasing 65% yield of benzoic acid. One concern with the latest finding was whether the result

could be selectively reproduced. Previous attempts (tables 2-7 and 9) had shown very little reproducibility, therefore entry 47 needed to be re-run while using the new operational parameters in order to verify entry 47, table 10 a success. Two subsequent reactions were conducted under identical conditions. The results of entry 48 and 49 of table 10 presented promising results when 75% and 88% benzoic acid were recorded with the newly designed synthetic CVD diamond photocatalytic system. In addition, there was an additional note of appraisal as the results revealed selective oxidative control by the synthetic CVD diamonds towards benzoic acid formation with minimal amounts of benzaldehyde and side products being produced. The new solvent choice suggested that the solvent revision based on Marko''s article[128] was the keystone to harnessing the selective oxidative capability of the synthetic CVD diamond powder.

Until this point in the study, numerous concepts had been evaluated for selective benzyl alcohol conversion. Amongst the concepts tested, test tube positioning, catalyst loadings, solvents changes, the addition of bases and continuous oxygen saturation were all investigated that all produced various ambiguous results. The only positive evidence to suggest otherwise was the application of 1,1,2-trichlorethane. There was however, a concern with the use of 1,1,2-trichloroethane in the study of photochemical reactions. Dichloromethane had been experimentally determined to have a solvent cut-off of 245 nanometers although 1,1,2-trichlorethane was not evaluated for such data and should have been experimentally determined before the photochemical studies. Hence, while researching solvent choices with their respective absorbance cut-off wavelengths, a number of substantial findings became evident as described in the text below.

2.3.5) Halogenated solvent radicalisation under UV irradiation.

Halogenated compounds are known to undergo substitutional and/or elimination reactions.[141] When the organic molecule contains a halogen (fluorine, chlorine, bromine, iodine) bonded to a carbon atom, an intrinsic dipole moment exists due to electronegativity differences in the molecular structure (figure 54).[141]
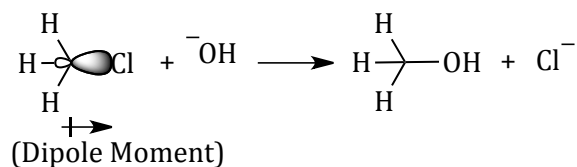
(Dipole Moment)

Figure 54: Dipole moment inherently present in chloroform promoting nucleophilic substitution.

The result of such a dipole moment would allow for nucleophilic substitution reactions to produce chlorine ions as by-products. This was pertinent to the study, as the question of exposing 1,1,2-trichloroethane to ultraviolet light had not been addressed. It was hypothesised that if chlorine was capable of being substitutionally replaced (as in the example of figure 54 above), there could have been a similar event occurring in the light activation study. The literature suggested that chlorinated molecules were capable of forming ionic species under suitable conditions; therefore it was considered justifiable to evaluate whether similar trends would occur when exposed to ultraviolet irradiation. From a literature review, this hypothesis was provided with ample support. When chlorine molecules such as chlorofluorocarbons (CFC's) are exposed to ultraviolet emissions, the molecules decompose and produce organic chloro-flouro and chlorine radicals.[141]

Another point of concern in the present study was the oxygen rich environment (which was chosen for its free electron scavenging properties). Ultraviolet light effects di-oxygen (O_2) radicalisation to atomic oxygen (O) and after di-oxygen has been cleaved, atomic oxygen is capable of attacking neighbouring di-oxygen molecules to produce ozone (O_3).

With reference to the study, the presence of an array of reactive species (atomic oxygen and chlorine radicals) would produce a cascade of oxidative damage to organic molecules. (figure 55).

$$O_2 \xrightarrow{h\nu} 2O \qquad (2)$$

$$O + O_2 \longrightarrow O_3 \qquad (3)$$

$$O_3 + Cl^\bullet \longrightarrow O_2 + ClO^\bullet \qquad (4)$$

$$O_3 + ClO^\bullet \longrightarrow O_2^\bullet + {}^\bullet ClO_2 \qquad (5)$$

$${}^\bullet ClO_2 \longrightarrow O_2 + Cl^\bullet \qquad (6)$$
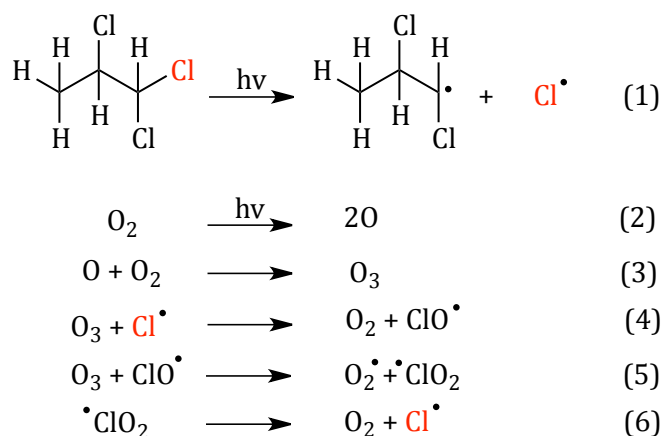
Figure 55: Production of ozone and chlorine oxides under ultraviolet irradiation.[141]

The data found in the literature[141] illustrated how the presence of oxygen and chlorine radicals produced in an ultraviolet radiation environment would be a powerful combination to potentially oxidise benzyl alcohol. Figure 55 revealed that (for example) 1,1,2-trichloroethane could be radicalised to halogenated hydrocarbon and chloride radicals in the presence of ultraviolet emissions (figure 55, step one). Secondly, when molecular oxygen was exposed to ultraviolet light, it too would radicalise. The products of oxygen radicalisation would be a singlet oxygen specie (figure 55, step two) that could react further with molecular oxygen to form ozone (O_3) (figure 55, step three). Subsequently, the newly formed chlorine and oxygen radicals would possess the ability to react (if in the same environment) and produce various hypochlorite (figure 55, step four) and chlorite (figure 55, step five) species respectively. If an excess supply of molecular oxygen was present, the chlorine could decompose back into chlorine radicals and molecular oxygen, where the radical cycle may begin again (figure 55, step six).[141]

As reported by Giorgio, *et al.,*[142] oxygen is one of the most naturally powerful oxidising agents. In addition, as oxygen effectuates its oxidative capabilities on reactants within close proximity, it transforms through various states of reduction (superoxide, peroxide and hydroxide). These transitional oxygen species produced during the oxidation process are known as 'reactive oxygen species' (ROS).[143]

Furthermore, Giorgio mentioned[142] that any specie with a low reduction potential has a high electronegativity, which makes them excellent oxidising agents. From these findings, it was hypothesised that the high yields presented in table 10 were the result of the *in-situ* generation of various oxygen and chlorine radicals that were produced during the irradiation of the test tubes with the ultraviolet lamp. Preliminary literature investigations revealed this to be highly plausible when the oxidative potential of various oxygen and chlorine radicals were researched (table 11). The data presented in table 11 verified that the oxygen and chlorine radical species possessed strong oxidising potentials that had the capability to oxidise benzyl alcohol.

Table 11: Redox potentials of various radical species.[123]

Entry	Specie	Redox Pot. (V)
50	H_2O_2	0.32
51	O_2	0.81
52	$O_2^{-\bullet}$	0.94
53	$Cl^{\bullet}$	1.36
54	$Cl\dot{O}_2$	1.49
55	$^{-\bullet}OH$	2.31

In order to verify that this was true, two test reactions were used to validate these findings. The initial study was to explore benzyl alcohol oxidation while using natural and incandescent light. For each new source of irradiation, an aliquot of benzyl alcohol and boron-doped synthetic CVD diamond powder in 1,1,2-trichloroethane was placed in the respective radiation environments. After the two reaction periods were complete, the solutions were analysed with a tabulation of the findings being reported in table 12 below.

Table 12: Benzyl alcohol oxidation in natural and incandescent light.
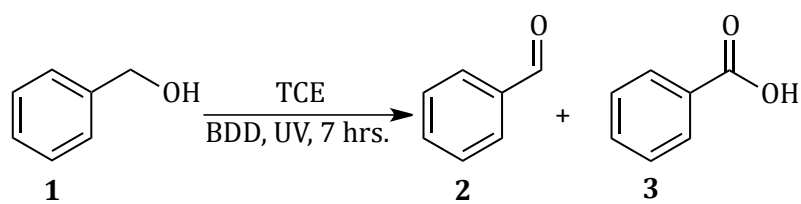
Entry	Product **2** yield (%)	Product **3** yield (%)
56[†]	4	<1
57[‡]	<1	<1

[a] Benzyl alcohol (1 mmol) **(1)**, trichloroethane (TCE) (3 ml) and BDD ([54-80 micron graded] 15 mg) were added to test tubes prior to purging with oxygen gas for two and a half minutes followed by 7 hours of ultraviolet irradiation (UVA/UVB). [†]Reaction exposed to natural sunlight, [‡]Reaction exposed to incandescent radiation. The yields of **(2)** and **(3)** were determined using chromatographic peak areas on a Thermo Finnigan GC-MS.

Results collected from table 12 confirmed that in the absence of ultraviolet irradiation, the products of benzyl alcohol oxidation were minimal when the reactions were run under natural sunlight conditions (entry 56) and incandescent irradiation (entry 57). The data advised that in order for chlorine and oxygen radicals to be produced, a strong short-wavelength radiation source was required. Furthermore, the outcome of these two reactions verified that the oxidation of benzyl alcohol would not occur under non-ultraviolet conditions due to the energy not being capable of radicalising oxygen and chlorine. In addition, the activation of the synthetic CVD diamond would not occur at the present ultraviolet wavelengths due to the energy not being suitable to activate the band gap of synthetic CVD diamond. After realising that the band gap of synthetic CVD diamond was indeed significantly large, an attention to the band gap value of synthetic CVD diamond was noted for further discussion. (The synthetic CVD diamond was identified to be incapable of oxidising benzyl alcohol due the chemistry of the band gap, which has been discussed later in the chapter). A brief statement has been recorded where the reactions of tables 12 and 13 were exposed to seven hours of electromagnetic radiation whereas the previous benzyl alcohol oxidation studies were conducted for

eight hours. The benzyl alcohol oxidation reaction in table 12, entry 56 was only irradiated for seven hours while the natural irradiation was available on the day. Therefore the remaining reactions of tables 12 and 13 were also irradiated for seven hours with the respective radiation sources to maintain a consistent irradiation period amongst the reactions.

The second method to test the effectiveness of the oxygen and chlorine radicals was to re-run the benzyl alcohol oxidation with the absence of the boron doped diamond powders, 1,1,2-trichloroethane, oxygen and ultraviolet light respectively. This was performed sequentially to assess the effect of each of the variables on the rate of alcohol oxidation and to verify that oxygen was indeed effectuating the oxidation process. To evaluate these conditions, six test reactions were run to complete this study of benzyl alcohol oxidation (table 13).

Table 13: Effect of reaction conditions on alcohol transformation while in the presence of ultraviolet radiation.[a]
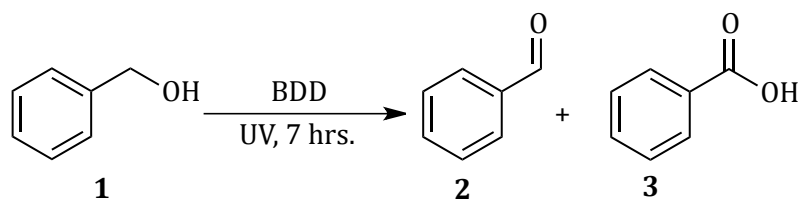
Entry	BDD [54-80] (mg)	Product **2** yield (%)	Product **3** yield (%)
58[†,§]	15	<1	<1
59[†,§,‖]	0	<1	76
60[‡,§,‖]	0	3	96
61[†,§]	15	<1	97
62[†,‖,*]	0	8	8
63[‡,‖,*]	0	1	6

[a] Benzyl alcohol (1 mmol) **(1)** was added to each reaction. †Trichloroethane was used as the reaction's solvent; ‡acetonitrile was used as the reaction's solvent. §Reaction was run with continuous oxygen gas saturation. ‖ The reaction was performed without any BDD (54-80 micron graded) powder. *An argon environment was applied by using the freeze-thaw method. Reaction 40 was performed in the absence of ultraviolet radiation. UVA/UVB radiation was utilised to irradiate the reactions for 7 hours. The yields of **(2)** and **(3)** were determined using peak areas on a PerkinElmer GC.

Immediately, the results from table 13 indicated that numerous findings were of significant importance. Entry 58 revealed that in the absence of ultraviolet light, benzyl alcohol oxidation ceased with a minimal conversion being detected. Entries 59 and 60 showed that in the absence of any boron doped synthetic CVD diamond powders, the alcohol conversions varied as typically noted throughout the course of this thesis. For comparative purposes, entry 61 was run with fifteen milligrams of 54-80 micron graded synthetic CVD diamond powder under identical conditions. The benzoic acid yield was almost matching to entry 60, thus proving that the synthetic CVD diamond powders were not necessary to perform the benzyl alcohol oxidations.

Entry 61, table 13 was a very important discovery and required further elaboration. The findings of entry 61 were of peculiar interest as the synthetic CVD diamond powder revealed no oxidative function for benzyl alcohol oxidation when compared to entry 60. The data of entry 61 (table 13) correlated with the reactions that were performed under natural and incandescent radiation (entries 56 and 57 of table 12). The data presented in table 12 clearly indicated that the absence of ultraviolet radiation prevented benzyl alcohol from being oxidised. Therefore, the newly generated information (table 12 [entries 56 and 57] and table 13 [entry 61]) led to an interesting conclusion with regards to the OSRAM® Ultramed ultraviolet lamp activating the synthetic CVD diamond powders. Despite the synthetic CVD diamond powder in entry 61 (table 13) being exposed to the OSRAM® ultraviolet radiation, it was evident that the synthetic CVD diamond was not being activated and must have been due to a problem associated with the ultraviolet lamp. Subsequently, entries 62 and 63 of table 13 were run in an oxygen-degassed environment to evaluate whether oxygen was the active oxidant of the benzyl alcohol oxidations.

To acquire an oxygen free environment, a specially modified test tube was constructed for the application (figure 56).
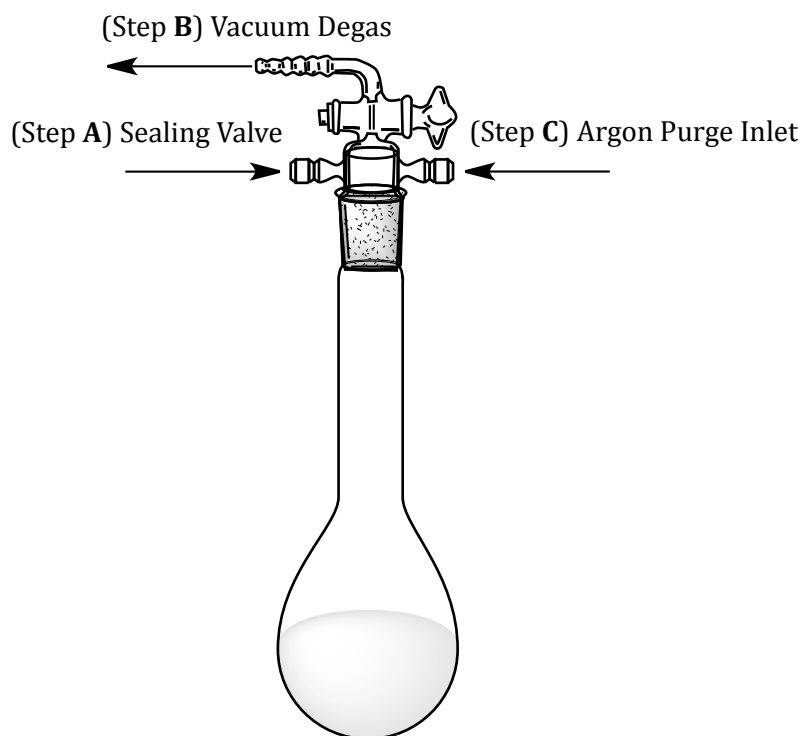
Figure 56: Modified test tube apparatus introduced for oxygen free-Argon purged environments.

The glassware item, as shown in figure 56 was introduced to remove both gaseous and dissolved oxygen from the reaction medium by a freeze thaw method that was recommended on the literature.[144] The purpose of removing the presence of dissolved oxygen was to assess the effect that dissolved oxygen had on the rate of benzyl alcohol oxidation.

To create an oxygen free-argon purged environment using the freeze-thaw method, the modified test tube was filled with the solvent and reactants and sealed off at the sealing valve (Step **a**). After sealing, the test tube was submerged in liquid nitrogen and left until the solvent had frozen. Once frozen, the test tube was removed from the liquid nitrogen the solvent was allowed to melt. After allowing the solvent to reach its melting point, the vacuum degas (Step **B**) line was opened to a rotary pump to remove gaseous oxygen for a period of five minutes. The procedure was repeated three times and was then back filled through the argon purge inlet (Step **C**) using gaseous argon for one minute. Lastly, all of the valves were sealed off and the test tube was then exposed to the ultraviolet radiation to start the reaction.

In the two experiments of table 13, (entries 62 and 63) that used an argon-purged environment, benzaldehyde and benzoic acid were produced in very poor quantities. Entry 62 still contained 1,1,2-trichloroethane that was known to radicalise under ultraviolet light,[141] yet the products of oxidation were still low. This was highly favourable to the study as these findings identified the most probable oxidant in the benzyl alcohol oxidation reactions was gaseous oxygen. The results from tables 12 and 13 suggested that possible variations in oxygen saturation in each test tube reaction caused the large derivation amongst the benzyl alcohol conversions and *N*-benzylidenebenzylamine syntheses.

To conclude the study at this point in the investigation, the results of entries 58 to 63 of table 13 gave evidence to support the following deductions which were in agreement with reported literature findings[141] on oxygen and chlorine radicalisation. These discoveries accounted for the variations amongst the yield of oxidised products and were conjectured to be for to the following reasons:

1) Controlled oxygen flow to each test tube was delivered *via* oxygen carrier lines as illustrated in figure 51. With the variation in light emission with distance (for each test tube) from the lamp body, a discrepancy in oxygen radicalisation was expected to occur, accounting for the variance in product yields.

2) Removal of 1,1,2-trichloroethane appeared to show small falling in benzoic acid yields (of approximately 2-13% amongst the reactions tested).

3) An addition of oxygen saturation significantly affected the yield of benzaldehyde and benzoic acid. The removal of oxygen terminated the production of these oxidised products with great effect.

The results of table 13 were in good agreement with the literature[141] and supported the second hypothesis (solvent degradation, oxygen saturation and imine degradation under ultraviolet radiation). In the absence of ultraviolet light, the yields of both benzaldehyde and benzoic acid were very low (while using incandescent and natural sunlight). Secondly, after oxygen and 1,1,2-trichloroethane were removed from the

reactions respectively, the yields of the expected products fell drastically. At the beginning of this study, synthetic CVD diamonds were researched for mediating benzyl alcohol oxidation reactions. However from all of the research data collected, oxygen was portrayed to be the active oxidant that yielded irreproducible benzyl alcohol oxidation results while exposed to the OSRAM® ultraviolet lamp. Therefore, as the primary aim of the project was to explore the oxidation of benzyl alcohol using synthetic CVD diamonds under ultraviolet irradiation, the course of benzyl alcohol oxidation was concluded unnecessary to research further while using the current OSRAM® ultraviolet lamp.

After concluding that benzyl alcohol oxidation had been facilitated *via* oxygen activation based on the experimental findings and the analysed literature data,[141],[142] the findings gave plausible reasoning to suspect that imines were indeed susceptible to various environmental (ultraviolet) and chemical (oxygen and chlorine radicals) conditions too. This would support the theory that imine degradation under ultraviolet light irradiation could indeed be a possibility that may have been accelerated in the incorrect solvent.

2.3.6) Ultraviolet assisted structural alterations to *N*-benzylidenebenzylamine.

At such a period in the synthesis of *N*-benzylidenebenzylamine, it was speculated upon the degradation of the imine bond. However if evidence existed to suggest that the postulated case could happen then it would give credence for low *N*-benzylidenebenzylamine yields. The investigation would require the NMR spectroscopic monitoring of *N*-benzylidenebenzylamine over time while being exposed to ultraviolet irradiation in different deuterated solvents.

The imine degradation study was investigated after a sample of *N*-benzylidenebenzylamine was prepared from benzaldehyde and benzyl amine that was purified and structurally verified using ^{1}H NMR spectroscopy. The decomposition investigation probed three deuterated solvents (chloroform, acetonitrile and dimethylformamide) that were spiked with two drops of *N*-benzylidenebenzylamine in a quartz NMR tube. After the required irradiation period, the samples were directly analysed using ^{1}H NMR spectroscopy. The aim of this structural modification study was to assess if a chlorinated solvent would produce an enhanced degradation effect on the

imine bond of *N*-benzylidenebenzylamine as well as evaluating if the ultraviolet light was causing any structural changes to the *N*-benzylidenebenzylamine molecule.

A spectroscopic sample illustrating the degradation of *N*-benzylidenebenzylamine has been depicted in figure 57 below.

a)
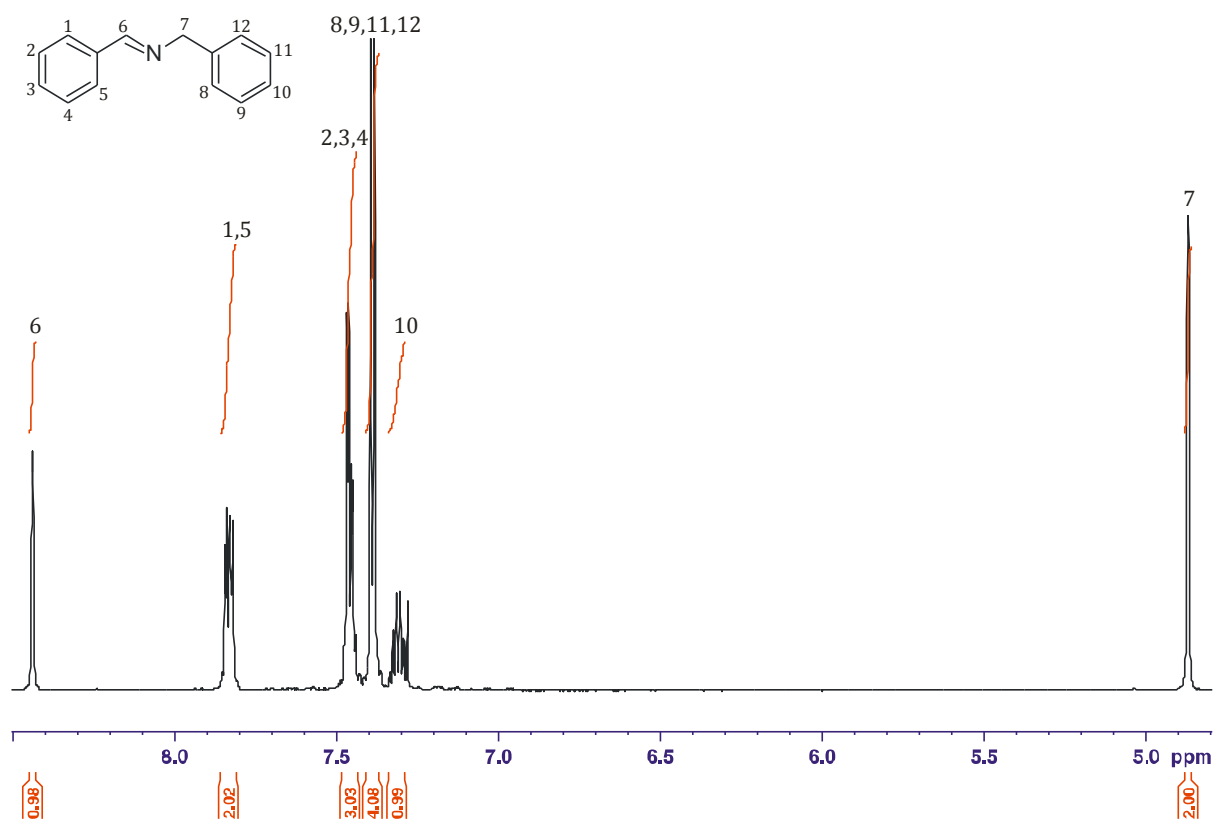
b)
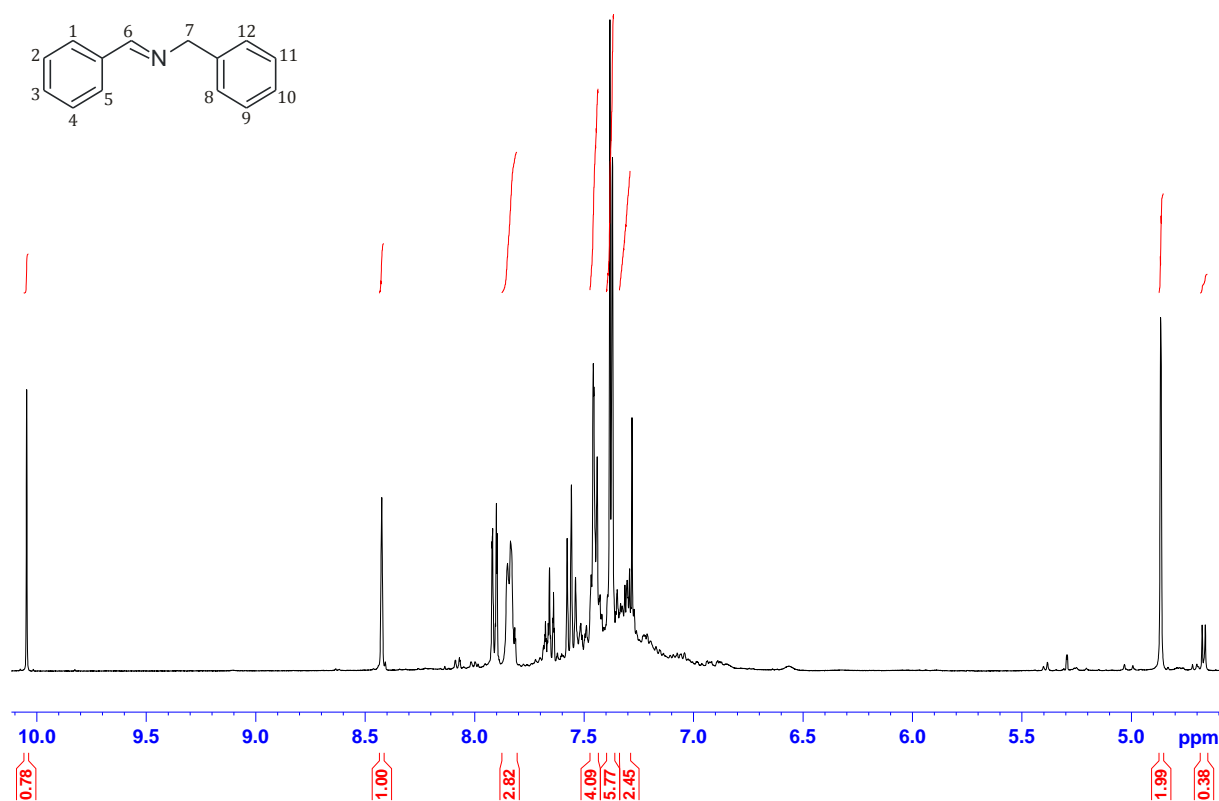
Figure 57: *N*-benzylidenebenzylamine degradation before (A) and after irradiation in deuterated chloroform (B).

Figure 57 has illustrated that *N*-benzylidenebenzylamine lent itself to exist in an equilibrium-type system post irradiation in deuterated chloroform. Figure 57 (**a**) has depicted a clean sample of *N*-benzylidenebenzylamine, which had not undergone any structural changes. However, after the sample in deuterated chloroform was exposed to ultraviolet radiation, the information suggested that the imine existed in a *quasi* state with the arrival of a strong aldehyde peak (10.05 ppm) in figure 57 **(b)** that limited an accurate spectroscopic identification.

After monitoring the system of *N*-benzylidenebenzylamine in deuterated chloroform, two other deuterated solvents were tested to assess if a reduced or enhanced solvent affect would occur in either deuterated acetonitrile or dimethylformamide. The data that has been tabulated in table 14 expressed a lesser change of *N*-benzylidenebenzylamine while in non-chlorinated solvents.

Table 14: *N*-benzylidenebenzylamine decomposition in deuterated solvents after irradiation.

Entry	Solvent	BDD (20-40 micron)	Time (hrs)	Decomposition Percentage (%)
64	Chloroform	10	7	60
65	Acetonitrile	10	7	25
66	Dimethylformamide	10	7	25

This brief solvent investigation indicated a possible cause for low *N*-benzylidenebenzylamine yields. Table 14 confirmed the pattern that a chlorinated solvent was causing an enhanced decomposition of the imine bond over non-chlorinated solvents, therefore establishing an equilibrium-type system between *N*-benzylidenebenzylamine production and decomposition. After identifying plausible reasoning for uncontrollable benzyl alcohol oxidation and *N*-benzylidenebenzylamine production, a shift in experimental proceedings were directed towards the activation of the synthetic CVD diamond surface.

2.4) Benzyl alcohol oxidation using UVC.

After confirming that controllable benzyl alcohol oxidation was not possible using chlorinated solvents in an oxygen rich environment with an ultraviolet lamp that was incapable of activating the synthetic CVD diamond powder; an intensified study of the physical properties of synthetic CVD diamond was investigated. Whilst reviewing technical data specifications of the ultraviolet lamp used during the course of the oxidation reactions, it was identified that the lamp was not suitable for the photo-activation of synthetic CVD diamond (figure 58). The problem arose because a synthetic CVD diamond photocurrent would only be produced when enough energy was available (ultraviolet radiation of the correct wavelength) to excite an electron into the conduction band of the synthetic CVD diamond. However, the present lamp had ultraviolet emissions that ceased below 275 nm and for synthetic CVD diamond to be photo-excited, a wavelength of 225 nm or less was required to excite the synthetic CVD

diamond's band gap. This lack of suitable electromagnetic radiation has been presented in figure 58 below.
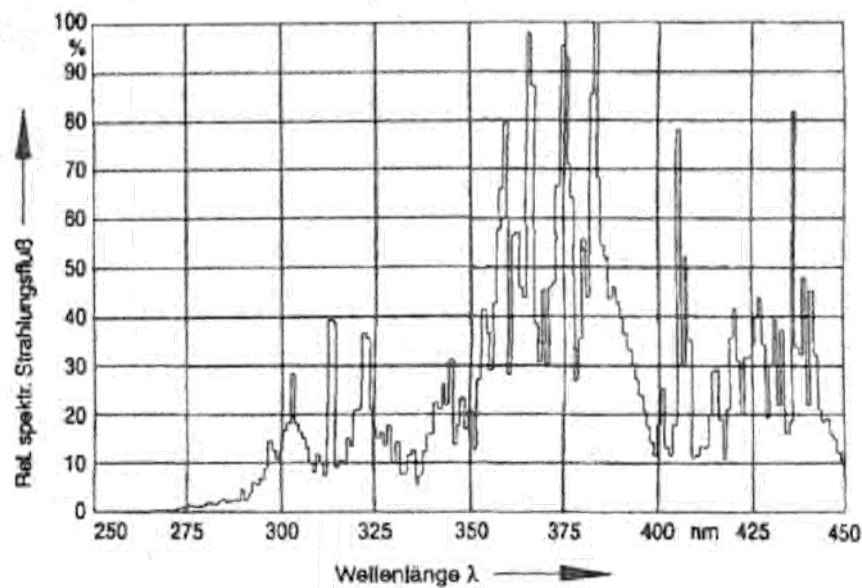
Figure 58: Emission spectrum of OSRAM® Ultramed UH-High Pressure Lamp.[Sourced from product brochure]

As evident from figure 58, the wavelength emissions for the OSRAM® Ultramed ceased below 275 nm. During the later course of the project, the emission spectrum of the lamp was obtained. Despite the lamp possessing an intense 2000 W flux, the UVC emissions were extremely low. The lamp's capabilities were initially believed to provide an adequate photonic energy to photo-activate the synthetic CVD diamond, however it was later identified to be unsuitable for synthetic CVD photocurrent activation-alcohol oxidation studies due to the absence of UVC emissions.

With insufficient photonic energy available from deep UVC (100-280 nm) emissions to photo-activate the synthetic CVD diamonds, a lamp that emitted shorter ultraviolet radiation in the UVC region (100-280 nm) was required.

Following successive communications with various optical specialists, a deuterium lamp was sourced from a Shimadzu high performance liquid chromatography (HPLC) detector.

The literature researching prior to acquiring the lamp identified deuterium lamps to emit strong UVC emissions that would be appropriate to activate the synthetic CVD diamond.

Illustrated below is a replicate data set of a deuterium lamp from Heraeus Noblelight (figure 59).
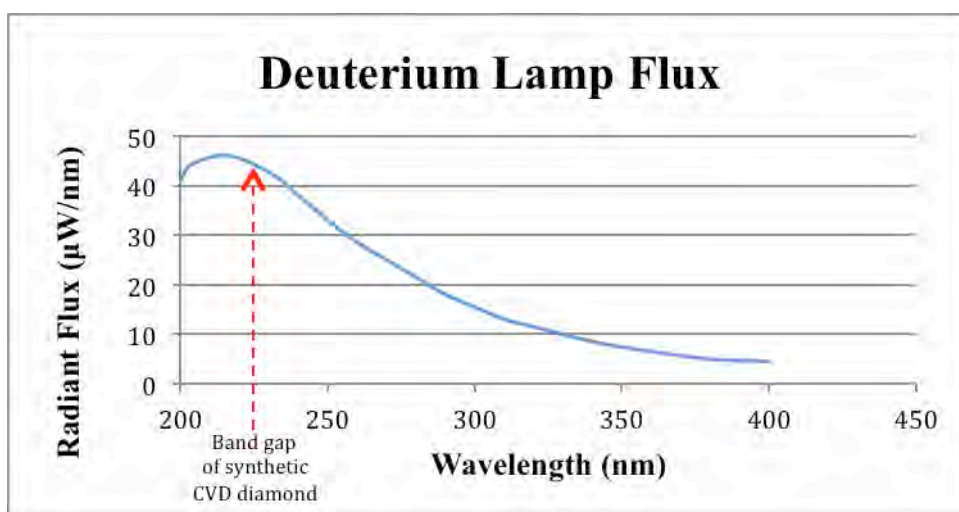
Figure 59: Deuterium lamp emission from Heraeus Noblelight.[145]

The deuterium lamp's spectral emissions illustrated in figure 59 above have identified that the deuterium lamp was indeed suitable for synthetic CVD diamond activation. The emission maxima of the deuterium lamp was identified to occur at approximately two hundred and twenty nanometers (220 nm) which was an ideal wavelength to be working at, since the band gap of diamond was 5.5 eV (225 nm).[96] Previous experimental procedures of photo-activating the synthetic CVD diamond were unsuccessful due to an inappropriate radiation source. Hence the oxidative system for benzyl alcohol oxidation needed to be repeated to investigate whether a photocurrent could be produced on the surface of the synthetic CVD diamond when irradiated with a suitable UVC photonic energy.

Initial investigations used the same oxygen-free environment and modified test tube (figure 56) while controlling the reaction times and the presence and/or absence on any synthetic CVD doped diamond powder (table 15).

Table 15: Deuterium lamp investigation of benzyl alcohol oxidation.[a]

Entry	BDD [54-80] (mg)	Time (hrs.)	Product 2 yield (%)	Product 3 yield (%)
67	0	6	2	<1
68	0	15	7	<1
69	15	6	1	<1
70	15	15	6	<1
71[†]	2% B-BDD (15)	6	2	<1
72[‡]	2% B-BDD (15)	15	5	<1
73[‡]	B(OH)$_3$ (1)	6	3	<1
74[†]	B(OH)$_3$ (1)	15	8	<1

[a] Benzyl alcohol (1 mmol) **(1)** was added to each reaction. Acetonitrile was used as the reactions' solvent for all of the reactions. In addition, each reaction was degassed with an argon environment after implementing the freeze-thaw method. †2% B(OH)$_3$ doped 54-80 micron BDD powder was the chosen oxidising agent. ‡Reactions were run with B(OH)$_3$ as the chosen oxidising agent. UVC radiation was utilised to irradiate the reactions for the respective periods. The yields of **(2)** and **(3)** were determined using peak areas on a PerkinElmer GC.

For each reaction performed in table 15, oxygen free environments were applied by the freeze-thaw method following argon purging. The reaction solvent was changed to

acetonitrile since the solvent study identified that it would not degrade and had the highest absorption window amongst the solvents tested.

Initially, to obtain a baseline standard, the oxidation of benzyl alcohol was performed without any synthetic CVD diamond powder in two concurrent reactions that were run for six (entry 67, table 15) and fifteen hours (entry 68, table 15) respectively. As expected, the detectable benzaldehyde and/or benzoic acid yields were minimal in both reactions.

After the baseline reaction was completed, another benzyl alcohol oxidation reaction was tested for six and fifteen hours (entries 69 and 70, table 15) respectively. The reactions used 15 mg of the 54-80 micron graded synthetic CVD diamond powder, oxygen free-argon purged environment and were exposed to the deuterium ultraviolet lamp source. Surprisingly, no significant productions of the oxidised products were detected upon quantitative gas chromatographic analysis.

It appeared improbable that the oxidation of benzyl alcohol was unachievable while using the synthetic CVD diamond powders under the irradiation of the deuterium lamp. However, one apparent reason for the lack of alcohol oxidation was the absence of boron doping in the synthetic CVD diamond powders (as disclosed by the distributors of the synthetic CVD diamond powders), which was vital for synthetic CVD diamond to be electrically conductive (see figure 36). As the synthetic CVD diamond powders were typically sold for grinding applications, boron doping was not considered during the manufacturing of the synthetic CVD diamond grains. The synthetic CVD diamond powders were manufactured without any boron in accordance with the commercial supplier's method. The presence of boron would weaken the inherent strength of the synthetic CVD diamonds and void their exceptional robustness in industrial tools and equipment.

Therefore as entries 71 and 72 of table 15 have illustrated, an attempt at doping the synthetic CVD diamond powders using boric acid was investigated. Entries 71 and 72 used 54-80 micron graded synthetic grains that were doped with two percent (2%) boric acid, meanwhile entries 73 and 74 were explored while only using one milligram

of boric acid as the catalyst for comparative purposes (the experimental procedure for developing the doped synthetic CVD diamond powder has been recorded in the supporting appendix). The results of the boron doping study were questionable, with only minor variations being detected amongst the yields that were almost consistent with entry 67 that used no catalyst. It was therefore concluded that if a benzyl alcohol oxidation reaction using a highly boron doped synthetic diamond was going to be tested, the synthetic diamond would have to be made in accordance with practiced literature methods which will be discussed later in the chapter.

However before searching for a literature method to synthesis highly boron doped synthetic diamonds, experimental data was required to confirm that the commercially obtained synthetic CVD diamond powders were undoped as disclosed. To confirm the inclusion or absence of boron, a solid-state nuclear magnetic resonance study was performed on each grading of synthetic CVD diamond powder to detect any boron present. Prior to studying the synthetic CVD diamond powders using solid-state nuclear magnetic resonance spectroscopy, inductively coupled plasma-optical emission spectroscopy (ICP-OES) was postulated to be an appropriate tool to measure the boron concentration. However, it was noted that due to the inherent chemical robustness of synthetic CVD diamond, it would be impossible to dissolve the synthetic CVD diamond powders in concentrated acid. In addition, non-destructive electron microprobe analysis was another possibility although due to the absence of available instrumentation at the University of KwaZulu-Natal, the need to utilise solid-state nuclear magnetic resonance spectroscopy was deemed necessary.

As organic chemists do not commonly use solid-state nuclear magnetic resonance spectroscopy, a brief explanation of the principles involved will be explained below (from the findings of Fyfe[146]). The literature presented by Fyfe will show that the data collected on the synthetic diamond powers indicated that boron was present in the powders.

Solid-state molecules that must possess intrinsic paramagnetism with other various nuclear interactions (electronic shielding, quadrupolar, Zeeman amongst a few) are important features for solid-state NMR studies. Subsequently, as the molecules are in a

fixed orientation within the solid sample, extremely fast decay times exist due to the absence of solvent effects. This results in the sample having fast nuclear decay times with very broad peaks that have severely poor resolution. As an example, Fyfe reported the dipole-dipole interactions of an ethanol solution phase being easily recorded in one percent of the 100 KHz field that was required to interpret a full solid-state spectrum of solid-phase ethanol.[146]

Although the peaks are extremely broad, they can be resolved by adjusting the spinning angle of the sample (known as the 'magic angle'). In a typical solid-state analysis, small ceramic rotors (approximately 100 mm x 3 mm x 3 mm) are packed with a reference standard and placed inside the NMR spectrometer for analysis, where the spinning angle is adjusted to 54.44°.[146] After the angular adjustments the standards are made, the standard is replaced with the sample of interest. Altering the magic angle significantly improves the resolution by apposing the inherent anisotropic effects of the sample. As this is only a brief overview of solid-state NMR, further advanced details of the subject are available in the text published by Fyfe.[146]

As illustrated by Fyfe in 'Solid state NMR for Chemists',[146] tetrahedral and trigonally coordinated ^{11}B species show broad signals in a solid-state NMR spectrum ranging from 0-100 ppm. After researching this data, analysis of the three diamond samples were investigated to identify if ^{11}B was present in the synthetic CVD diamond semiconductors.

Samples of each synthetic CVD diamond grain size were loaded into solid-state NMR rotors and analysed using a solid-state NMR probe on a Bruker 600 MHz spectrometer (operational parameters of the instrument have been recorded in the experimental data). Three spectra were recorded and an ^{11}B NMR spectrum of 0-1 micron graded BDD powder has been depicted below (figure 60, [The remaining two spectra are available in supporting appendix]).
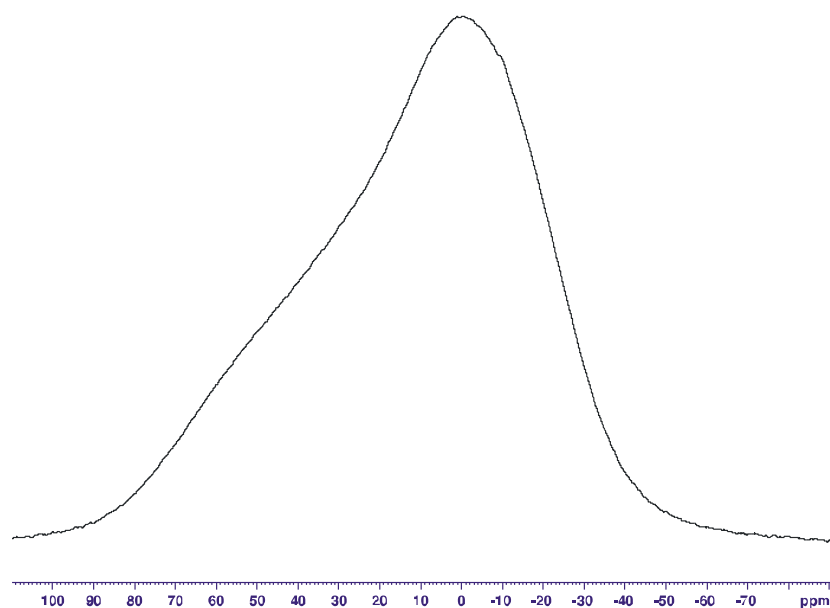
Figure 60: 0-1 micron synthetic CVD diamond grain size.

After contacting the suppliers of the synthetic CVD diamond powders, the company stated that the synthetic CVD powders did not contain boron, nor was boron used in any of the synthetic diamond manufacturing processes. This was however untrue since the results of the solid state NMR analysis did in-fact prove that all three synthetic CVD diamond powders were doped with boron. Unfortunately, the solid-state NMR analysis was unable to quantify the exact doping concentration, however it did confirm that boron was indeed present in the samples. The solid-state NMR data shown above illustrated that the only apparent difference between each synthetic CVD diamond sample (0-1, 20-40 and 54-80 micron graded) was the particle grading size.

From literature findings, diamond becomes a *p*-type doped conductive material when extrinsically loaded with boron. However, boron doped synthetic CVD diamond is only conductive at high boron doping concentrations. Reported by Latto,[107] Feng[147] and Halima;[148] 10^{20}, 10^{21} and 10^{23} boron atoms.cm^{-3} are typical doping levels for moderate, high and heavily boron doped electrically conductive synthetic CVD diamond samples respectively. Based on this information, the solid-state NMR analysis indicated that boron had been indeed incorporated into the synthetic CVD diamond powders, however the exact concentration was undeterminable. Based on the information received from

the supplier of the synthetic CVD diamond powders who explained that no boron was used during the manufacturing processes, it was considered acceptable to conclude that the boron was in concentrations that were too low to promote any degree of electrical conductivity in the diamond powders. Without the immediate availability of heavily boron doped synthetic CVD diamonds to test the oxidation of benzyl alcohol, another source of synthetic CVD diamonds became a necessity.

2.5) Hot filament chemical vapour deposition diamonds.

Through a very generous donation from Professor Paul May at the University of Bristol, United Kingdom; UVC irradiation of a two square centimeter silicon supported synthetic CVD diamond square was possible. Professor May grew a heavily boron doped (boron concentration = 10^{23} atoms cm^{-2}) synthetic CVD diamond sample on a *p*-type silicon wafer for seven hours using a hot filament chemical vapour deposition reactor (figure 61 and 62).
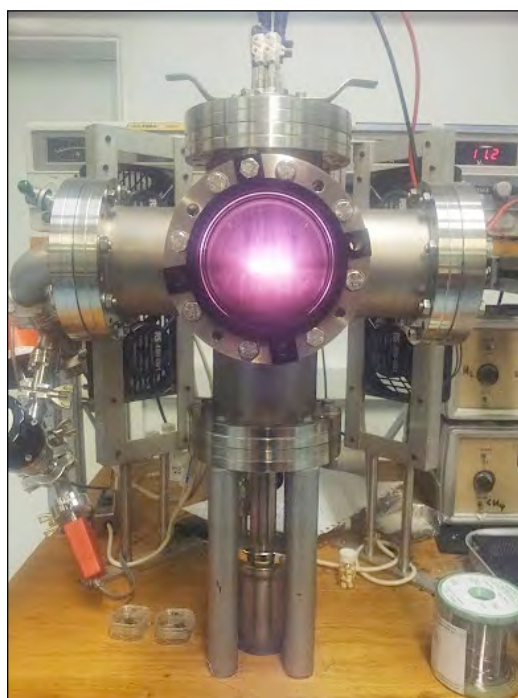
Figure 61: Hot filament chemical vapour deposition reactor at Bristol University.
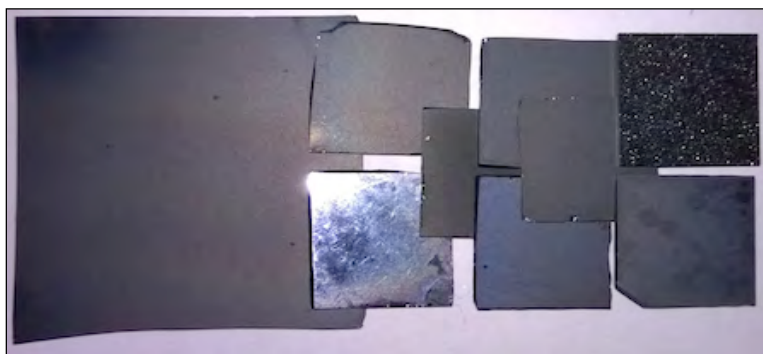
Figure 62: Heavily boron doped hot filament chemical vapour deposition diamond squares.

After identifying that the synthetic CVD diamond powders were unable to perform oxidation reactions, the newly received synthetic CVD diamond square had upon inspection all of the requirements to function as a highly suitable catalyst for benzyl alcohol oxidations. Unfortunately the synthetic CVD diamond square was too large to fit inside the modified test tube so an alternative setup was designed. It was more simplistic in construction but would serve the requirements of fulfilling 'proof of concept reactions' (figure 63).

$$h\mu \leq 225 \text{ nm}$$
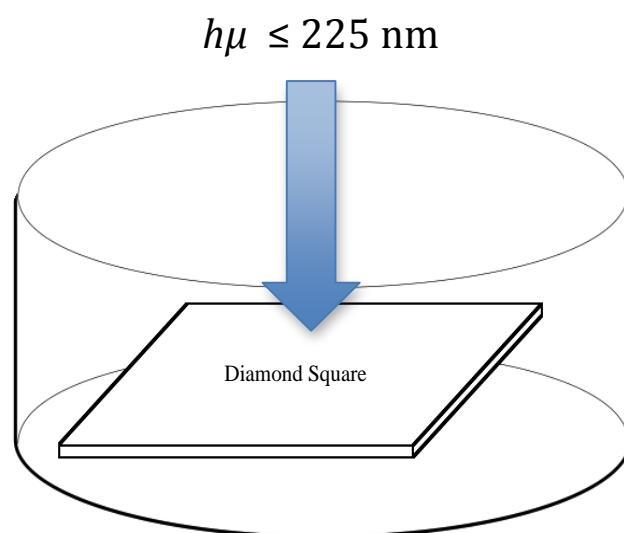
Diamond Square

Figure 63: 'Mini beaker' setup used to house the diamond square for alcohol oxidation.

The synthetic CVD diamond square's capabilities were investigated while attempting to oxidise benzyl alcohol in the mini beaker as part of the proof of concept study. An immediate concern with the mini beaker was that it was exposed to atmospheric oxygen, which had been identified to radicalise under ultraviolet irradiation. There was however an easy solution where an identical reaction would be run without the presence of the synthetic CVD diamond square. Any differences in product yields would be noted for further calculations. A second concern with the mini beaker was that there was no condensing unit above the solution to prevent solvent evaporation. However as this design was only required to prove if the synthetic CVD diamond square was able to oxidise an alcohol, it would be suitable for the current application.

An investigation while testing multiple reactions with the new synthetic CVD diamond square and UVC radiation was probed for the oxidation of benzyl alcohol. Every foreseen variable had been reviewed and hence the outcomes of the experiments were expected to yield good results (table 16).

Table 16: Benzyl alcohol oxidation using a heavy boron doped diamond square.[a]
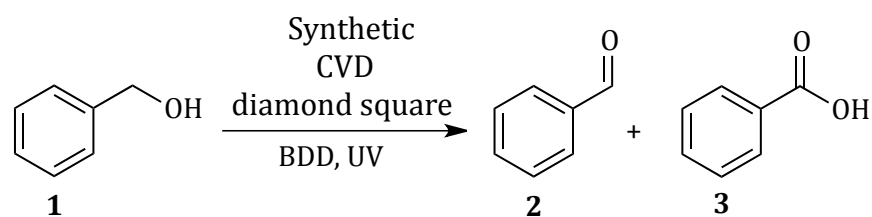
Entry	Time (hrs.)	Product **2** yield (%)	Product **3** yield (%)
75	3	0	0
76	3	0	0
77	7	0	0
78	7	0	0

[a] Benzyl alcohol (1 mmol) **(1)**, acetonitrile (7.5 ml) and the synthetic CVD diamond square were placed in the 'mini-beaker' setup for each reaction. The 'mini-beaker' was then irradiated with a UVC radiation source (UVC deuterium lamp) that was sourced from a Shimadzu spectrophotometric detector. The yields of **(2)** and **(3)** were determined using chromatographic peak areas on a Shimadzu GC-MS.

For reasons unknown at this point in the study, benzyl alcohol oxidation using the synthetic CVD diamond square did not occur (?) From all literature findings recorded and read, the oxidation of benzyl alcohol using the synthetic CVD diamond square in the current conditions was expected to yield excellent results. However, from the data shown in table 16, this was not true. While assessing the newly found results of the un-oxidised benzyl alcohol, a collaboration with Bristol University was being potentially explored in an attempt to identify why the synthetic CVD diamond was not capable of performing the oxidation reactions.

2.6) Extended synthetic CVD diamond studies.

Through a period of planning, a five-week visit to the University of Bristol in August 2014 was possible. The University of Bristol housed numerous instruments that were made available to grow, analyse and study synthetically grown diamonds. Not only was the equipment on-site, but also a wealth of knowledge was shared amongst all academia.

The research period entailed the identification of the optimal synthetic CVD diamond growing conditions using diborane (B_2H_6) as a dopant, with time allocated to synthesising various synthetic CVD diamond squares of different carbon: boron ratios on silicon wafers. The hydrogenation and oxygenation of the synthesised synthetic CVD diamond surfaces would also been investigated to explore surface conductivities. One commercially available synthetic CVD diamond square was also provided which was grown without the presence of a silicon substrate that made it exhibit extreme chemical robustness with a high electrical conductivity due to its heavy boron doping.

Seven synthetic CVD diamond samples were grown on *p*-type silicon substrates (due to it being an inexpensive and excellent seeding medium for growing synthetic CVD diamond grains) with various carbon: boron doping ratios. Before the synthetic CVD diamonds could be grown on *p*-type silicon, the surface of the silicon substrate required pre-treatment. The University of Bristol offered two pre-treatment techniques, both of which were evaluated to identify the optimal seeding method for synthetic CVD diamond growth. The first approach was performed by physically abrading the silicon surface using ultrafine micron-grade synthetic CVD diamond powder. This process was chosen for its seeding abilities where the silicon sub-surface was physically implanted with micron synthetic CVD diamond grains. The micron synthetic CVD diamond grains functioned as growth sites for diamond nanoparticles while the silicon substrate square was in the hot filament chemical deposition reactor. The second technique that was tested was an electron spray (figure 64), which passed a very high potential (1.5 kV) through a mist of aqueous suspended synthetic CVD diamond nanoparticles. The potential difference accelerated the diamond mist towards the rotating *p*-type silicon substrate for uniform seeding.
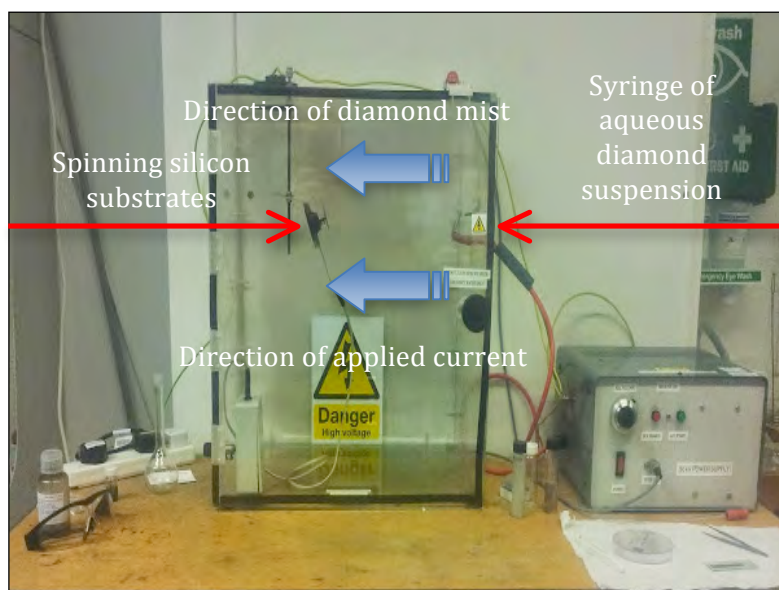
Figure 64: Electron spray technique used for the seeding of *p*-type silicon with synthetic nanodiamonds.

Once the seeding treatments were complete, either *via* physical abrasion or from electro-seeding, the silicon samples were place on a stage, which was housed in the hot filament reactor. As the technique describes, three hot filaments made from tantalum wire bridged the synthetic CVD diamond stage and after ignition with a twelve-amp (12 A) current, the wire would initiate diamond deposition of methane and diborane gas onto the *p*-silicon.

After the synthetic CVD diamond growth was complete (seven hours), the hot filament chemical vapour deposition chamber was switched off and left to cool for a half hour before collecting the samples. In accordance with recognised method of quantitative assessment at the University of Bristol, the newly grown synthetic CVD diamonds were analysed microscopically for uniform polycrystalline synthetic CVD diamond growth. The study of benzyl alcohol oxidation was then possible to investigate as prepared synthetic CVD diamond squares had been manufactured to user specifications. The subsequent step was to place the synthetic CVD diamond squares and benzyl alcohol in front of a high-powered 30 W deuterium lamp source that was recently bought for ultraviolet electrochemistry studies. The previous deuterium lamp that was sourced from a Shimadzu HPLC detector at The University of KwaZulu-Natal in South Africa

possessed a power rating of only 3 W and was suspected of having low UVC emissions. The 3 W emissions were assumed to be too low for the synthetic CVD diamond square to produce a constant photocurrent. Therefore the new 30 W deuterium lamp was a superior option.

To meet the requirements for the benzyl alcohol oxidation, the synthetic CVD diamond square was submerged in a solution of acetonitrile and benzyl alcohol while being irradiated through a quartz window of a purposed built test tube (figure 65 and 66).

Figure 65: Reaction setup of diamond irradiation.
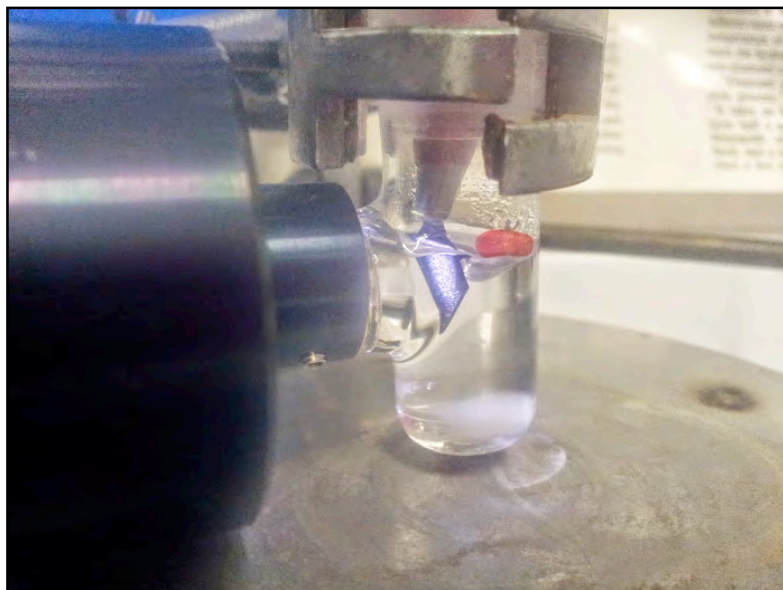
Figure 66: Close up representation of Figure 66.

After numerous attempts using both the commercial and synthesised CVD diamonds (figure 62), the oxidation of benzyl alcohol was spectroscopically determined using ^{1}H NMR and found to be unsuccessful without any benzaldehyde or benzoic acid being detected. Various solvents and typically aqueous solutions of sulfites and sulfates were suggested by the alumni, which were explained to have good hole scavenging properties. This was however unsuitable since the positive holes in the valence band were a requirement for benzyl alcohol oxidation to occur.

In other discussions, a platinum wire was postulated to be an effective counter electrode in the reaction setup to scavenge conduction band free electrons (the literature data explained that platinum had a high affinity for electrons).[149] Reasoning suggested that after the synthetic CVD diamond was photolytically excited, the valence band electrons would be promoted into the conduction band. Without an available exit route, the electrons would bank up in the conduction band of the synthetic CVD diamond until a point where the electrons would saturate the conduction band; hence inhibiting any further electron promotions and e^-/h^+ excitations from occurring. It was further postulated that without the platinum wire, the electrons would fall back into the valence band and recombine with positive holes and hence limit the rate of photocurrent generation. Therefore the concept of introducing a platinum counter electrode was

believed to be a plausible option to remove surface bound electrons while allowing the positive hole to oxidise benzyl alcohol.

To construct the synthetic CVD diamond-platinum wire setup, the synthetic CVD diamond was attached to a crocodile clip and connected to a platinum wire *via* a copper wire. Both the synthetic CVD diamond and platinum wire were submerged into the reaction solution where the ultraviolet light irradiated the synthetic CVD diamond surface. The commercial synthetic CVD diamond was used for the majority of the oxidation reactions as it had known conductivity measurements.[150] Evaluating the oxidation reactions with a recognised commercially available synthetic CVD square with known conductivity parameters was considered to be appropriate to obtain the 'proof of concept study'. After the oxidation of benzyl alcohol had been proven successful using the commercial synthetic CVD diamond, the reactions would be repeated while using user-designed synthetic CVD diamonds in an attempt to improve upon the proof of concept study.

Multiple benzyl alcohol oxidation reactions were completed with both the commercial and user grown synthetic CVD diamonds while using the platinum wire. To great disbelief there was still neither detectable benzaldehyde nor benzoic acid, even after attaching a platinum wire to the synthetic CVD diamond to maintain charge neutrality. Therefore, the literature needed evaluating once more.

After numerous hours reviewing doping levels, *n* and *p*-type dopants, dopant concentrations, reaction times, solvent volumes and test tube proximity to the irradiation source, the band gap structure of synthetic CVD diamond was inspected. After reading an article published by Zhu and co-workers[119] in Nature Materials, evidence (a band gap diagram) illuminated why the synthetic CVD diamonds were seemingly incapable of oxidising benzyl alcohol (figure 67).
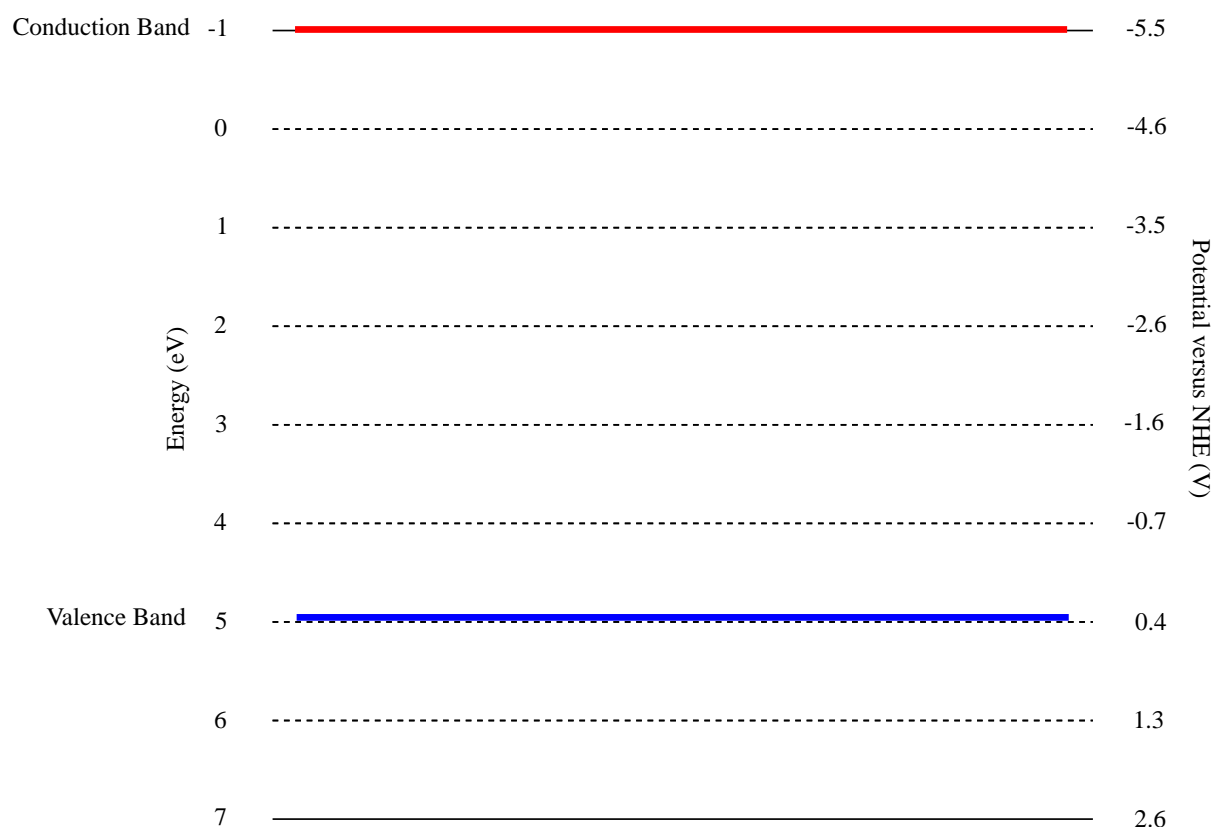
Figure 67: Band gap structure reproduced from Zhu, *et al.*[119]

Figure 67 clearly illustrated the band gap positioning of synthetic CVD diamond. The value of the valence band was reported by Zhu to lie at approximately 0.4 V (4.9 eV), while the conduction band was positioned at approximately -5.5 V (-1.0 eV). This data provided crucial evidence to support the findings that synthetic CVD diamond appeared to be incapable of oxidising alcohols. From redox chemistry, a species that has a high (more positive) potential (V) has a strong affinity for electrons, thus oxidising the reactant. Parallel to this explanation, species that have a lower (more negative) potential, are less likely to accept electrons and species that have strong negative potentials will actually prefer to loose electrons and cause reduction while being oxidised themselves. This statement was in agreement with Zhu, *et al.,* who described synthetic CVD diamond to possess a poor oxidising potential due to the shallow oxidation potential level of the synthetic CVD diamond's valence band.[119]

Finally, an answer was identified to support all of the findings during the course of the study. Unfortunately, the newly found evidence suggested that the oxidation of alcohols

to aldehydes and ketones was not possible since the oxidation potential of the valence band of synthetic CVD diamond was very poor (~0.4 V). However, figure 67 did depict a fascinating study, which would require detailed attention and focus with a strong possibility for success.

Figure 67 illustrated that while the valence band of synthetic CVD diamond was unsuitable for oxidation reactions, it seemed highly plausible to utilise strongly negative free-conduction band electrons for reductive purposes. Zhu has already published this theory in the works of nitrogen reduction (as reference to figure 67)[119] as well as in the reduction of carbon dioxide to carbon monoxide.[120]

2.7) Coextending studies

2.7.1) Methylene blue oxidation

Methylene blue has been reported to be a common organic water pollutant (figure 68) that has toxic effects on the natural fauna and flora in rivers and streams.[151] Various literature sources have reported numerous methods for methylene blue degradation through de-methylation.[151],[61] Mohabansi, *et al.,*[151] reported methylene blue degradation using titanium dioxide, zinc oxide and hydrogen peroxide (H_2O_2) while monitoring the oxidation efficiency of different catalyst loadings. Shen and co-workers also disclosed a study of zinc oxide and how preparatory measures alter the photocatalytic capabilities of zinc oxide. They investigated the topic using various techniques of preparing zinc oxide and measured its oxidative function with methylene blue oxidation.[61] Lastly, Chakrabarti, *et al.,* also announced methylene blue degradation while using zinc oxide. They explored an in-depth study monitoring methylene blue and Eosin Y dye concentration, catalyst loadings and controlling the rate of air exposure to the reaction mixture under controlled ultraviolet irradiations.[152]
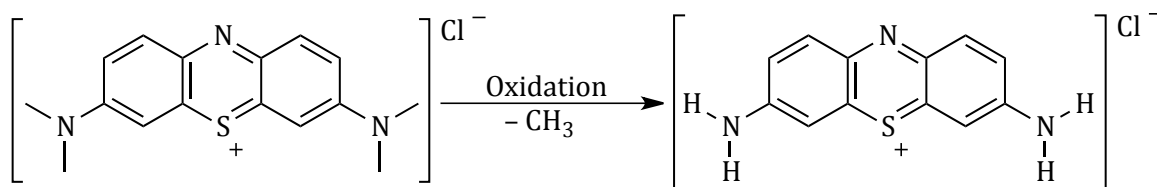
Figure 68: Semiconductor mediated de-methylation of methylene blue.

Therefore as part of a brief coextending study, methylene blue oxidation was investigated to explore its possible degradation while using the 0-1 micron graded synthetic CVD diamond powder under ultraviolet irradiation (OSRAM® 2000 W Ultramed lamp). In order to establish the effect of the synthetic CVD diamond on dye degradation, blank samples were run conjointly while being exposed to the ultraviolet irradiation.

The experimental procedure consisted of filling quartz test tubes with 15 ml of a prepared methylene blue solution (2 mg/ 100 ml) with pre-adsorption of the solution onto the synthetic CVD diamond powder (15 mg of 0-1 micron graded synthetic CVD powder) before ultraviolet exposure. The organic dye was then purged with oxygen above the reactants for two and a half minutes. Subsequently, the test tubes were placed horizontally (for maximum ultraviolet exposure) in front of the OSRAM® ultraviolet lamp and irradiated for five hours with aliquots extracted every hour for absorption measurements (figure 69).
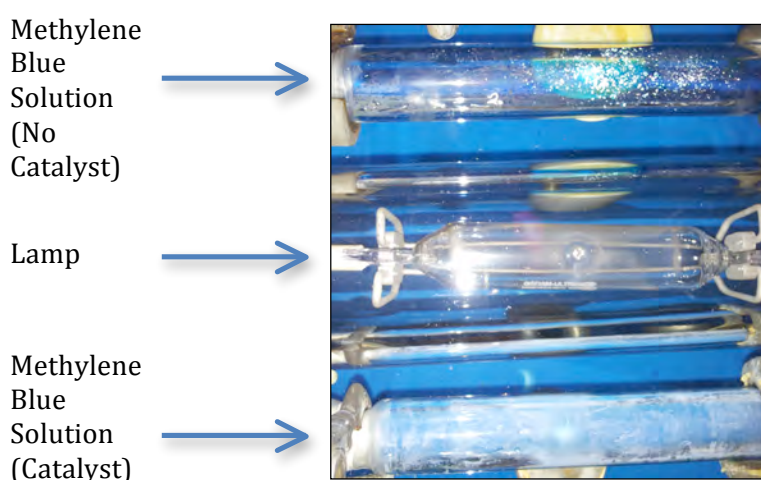
Figure 69: Horizontal test tube setup for methylene blue oxidation.

After the reaction had run for the designated period (five hours) and the five aliquots had been spectroscopically analysed using UV/Vis spectroscopy, the samples were linearly arranged. As presented in figure 70, the successful de-methylation of methylene blue was evident by the change in solution colour (from blue to colourless).
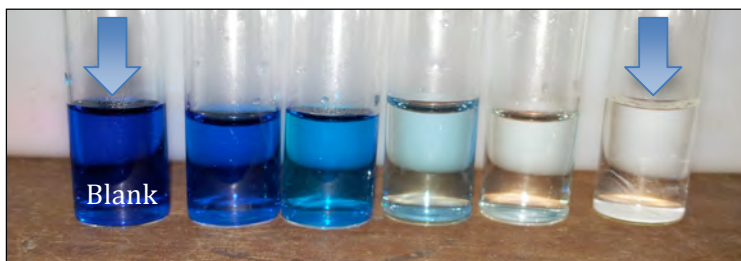
Figure 70: Methylene blue colour change over five hours (the immediate left vial was not irradiated-blank).

From each aliquot taken for spectrophotometric analysis using UV/Vis spectroscopy, the absorbance measurements were recorded against time and have been displayed in figure 71 below.

2.7.2) Methylene blue degradation over time.
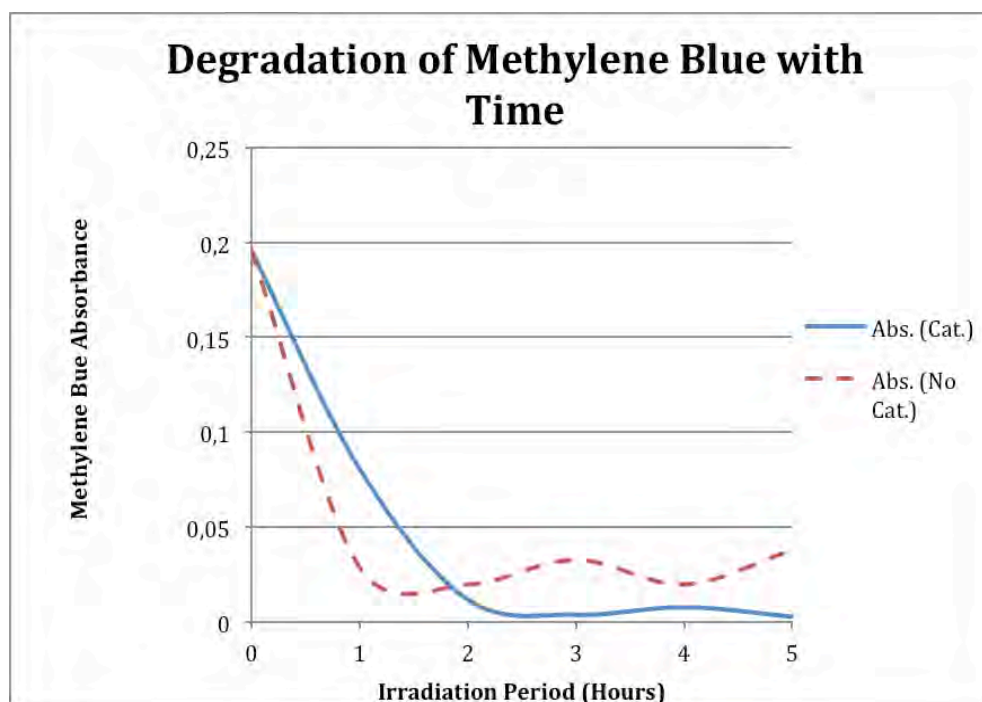
Figure 71: Methylene blue degradation with and without synthetic CVD diamond powder (cat.) added.

Figure 71 has illustrated that the synthetic CVD diamond semiconductor was effectively mediating an enhanced degradation of the methylene blue (blue line) when compared to the sample run without the synthetic CVD diamond powder (dashed red line) over the five-hour period. This was evident from figure 71 by reviewing the absorbance figures of methylene blue from two to five hours for the synthetic CVD diamond mediated reaction compared to the sample run without the synthetic CVD diamond powder. Pre-treating the synthetic CVD diamond powder *via* adsorption of the reactant dye molecules onto the catalyst surface prior to ultraviolet irradiation appeared to facilitate an enhanced photocatalytic activity. Linsebigler, *et al.,* had reported this in their *Chem. Rev.* publication.[56] The article detailed the pre-adsorption of the reactant species onto the photocatalyst surface and showed an improvement in the electron-transfer (reactant to catalyst) process and by virtue, the dye oxidation.

A point of significance was to note the involvement of the ultraviolet lamp in the degradation of the dye. The blue line in figure 71 has depicted that the synthetic CVD diamond powder hastened the dye degradation over the five-hour period, however it was evident that the ultraviolet lamp contributed significantly (dashed red line in figure 71). This was an interesting observation since it was unthought-of for the lamp to initiate an oxidative function into the reactant's environment. However, from the findings which revealed that the synthetic CVD diamond powder was incapable of oxidising organic molecules (benzyl alcohol), it was concluded that the dye degradation was primarily due to the OSRAM® Ultramed ultraviolet lamp.

2.7.3) Synthesis of *N*-benzylidenebenzylamines

Within this research group, previous semiconductor findings on a silver (AgNO$_3$)/ alizarin red (dye)/ zinc oxide (ZnO) (silver/dye/ZnO) system showed excellent alcohol oxidation results that have been published in *Chemical Communications.* and *Dalton Transactions*.[73],[74] Therefore, while aiming to compose a nucleophilic trapping study towards to the synthesis of *N*-benzylidenebenzylamines, an attempt for the submission of a short article to the Royal Society of Chemistry in honor of Professor Richard Taylor's 65th Birthday was further investigated. During the study, various nucleophiles and new

quantitative measures were implemented to extend the knowledge basis within the group on the silver/dye/ZnO catalytic system.

As previously reported by Jeena and Robinson,[73] the silver/dye/ZnO system showed an excellent proficiency for alcohol oxidations (as mentioned in section 1.6.1 of the introduction) with a mechanistic insight into the oxidative nature of the catalyst. Electron spin resonance (ESR) and UV/Visible spectroscopy data verified the postulated mechanism which has been acknowledged in the chemical literature.[73],[74] There was however a concern with the oxidative system. In order to facilitate the smooth transformation of alcohols into aldehydes, an excessive loading (eighteen equivalents) of silver nitrate was required to promote the reaction. Therefore the opportunity arose to approach the current oxidative system and optimise it for similar or more effective alcohol oxidations.

The oxidative process was investigated through an attempt to oxidise benzyl alcohol while using six equivalents and finally three equivalents of silver nitrate. This was achieved by monitoring the volume of water and silver nitrate loading used for each oxidation reaction. The outcome of this adjustment resulted in a sequential decrease in the quantity of silver nitrate used, however while still maintaining the molar concentration of aqueous silver nitrate in a lesser volume. Tabulated below are the results of the optimisation study with the respective volumes of water and masses of silver nitrate used (table 17).

Table 17: Optimisation of reaction conditions.

Entry	Alcohol	Water (ml)	AgNO$_3$ (eq.)	Yield (%)[c]
79[a]	Benzyl alcohol	1	6	99[c]
80[b]	Benzyl alcohol	0.5	3	99[c]

[a] Benzyl Alcohol (0.1 mmol), *d*-ZnO (20 mg), TEMPO (0.0013 mmol), 3 hrs.
[b] Benzyl Alcohol (0.2 mmol), *d*-ZnO (20 mg), TEMPO (0.0013 mmol), 3 hrs.
[c] GC-MS Yield.

From previous findings within the group,[73] eighteen equivalents of silver nitrate only produced a benzaldehyde yield of 82%. When lowering the silver loadings to six (entry

79, table 17) and three equivalents (entry 80, table 17), the yields were not only superior (99% for both cases) but reproducible as well (Table 17). Therefore based on the results of the newly found optimisation study, benzyl alcohol along with nine various alcohols were investigated to evaluate the efficiency and scope of the re-designed silver/dye/ZnO oxidation system (figure 72).
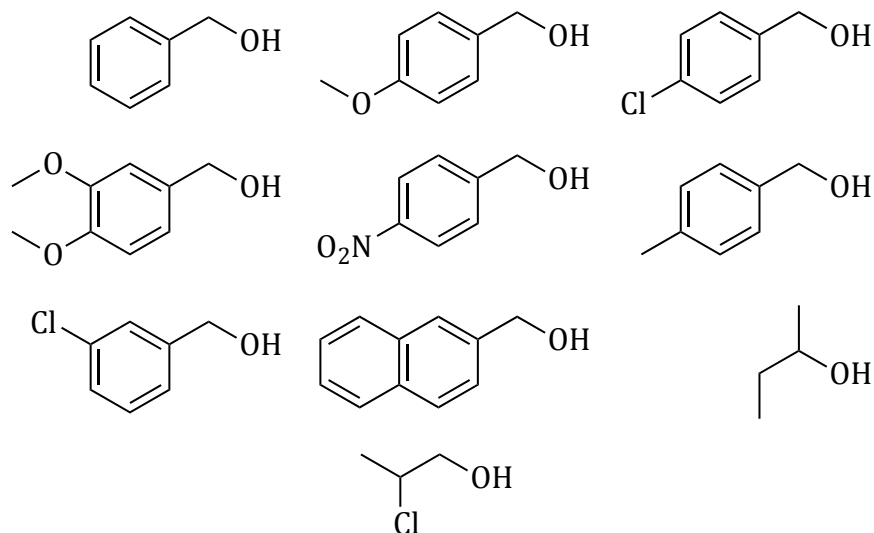
Figure 72: Various alcohols tested using the optimised dye-silver-zinc oxide system.

After each alcohol had been oxidised, it was extracted using a '*Pseudo-tandem oxidation approach'* where the aldehyde/ketone was extracted into dichloromethane and refluxed for two hours with benzyl amine to afford various *N*-benzylidenebenzylamines (figure 73).
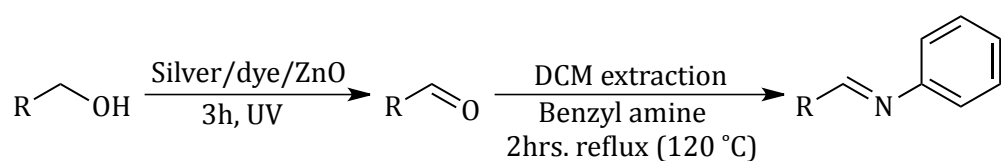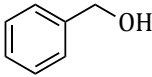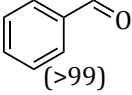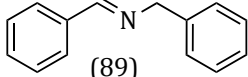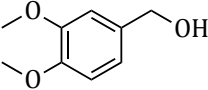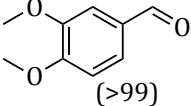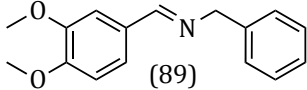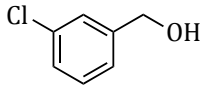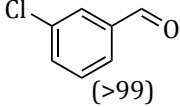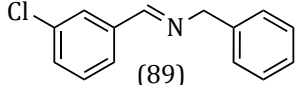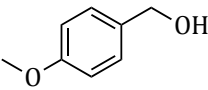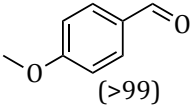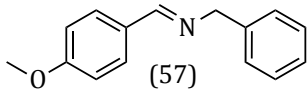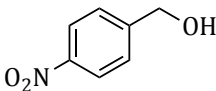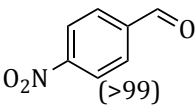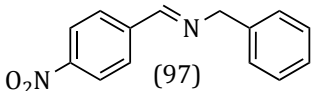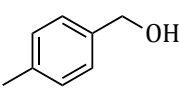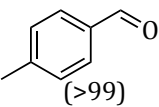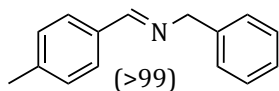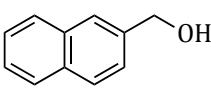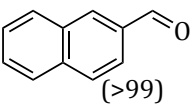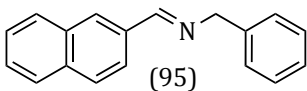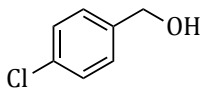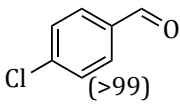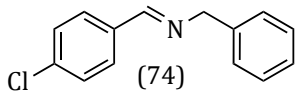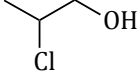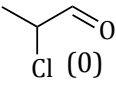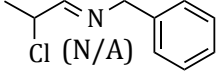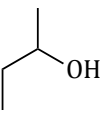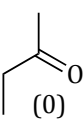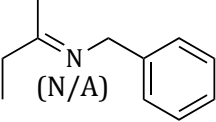
Figure 73: *Pseudo-tandem oxidation* of alcohols.

Through an intensive literature search, the phrase '*pseudo tandem oxidation'* could not be identified within the chemical community. Hence, an opportunity was identified to introduce this newly found photocatalytic chemistry through the production of various *N*-benzylidenebenzylamines. In summary, the pseudo tandem

oxidation process was a method developed to accommodate reagants that would be otherwise unsuitable to comply with the operational parameters of either a tandem oxiation or one-pot process. Such conditions would safeguard the reagents from various chemical and environmental impacts that might occur during the tandem oxiation or one-pot processes. Examples include light sensitive commpounds such as aniline being sensitised before nucleophilic coupling could occur or Wittig reagents complexing to silver in an aqueous silver nitrate solution.[153],[154]

The one-pot process and tandem oxidation routes are more suited towards reagents that are typically stable throughout the course of a reaction until the point where their reactivity within the medium exists. However in the present study, due to the benzyl amine being light sensitive, the requirement for a pesudo tandem oxidation process was merited. The process of implementing the newly found pseudo tandem oxidation technique was completed while studying the oxidation of ten various alcohols (figure 72). Alcohol oxidation conversions were all in excess of 99% with chromatographic imine yields ranging from 57-99% (table 18).

Table 18: Imine production using optimised dye-silver-zinc oxide system.[a]

Entry	Starting Material	H_2O (ml)	Catalyst	Product (Yield, %)[†]	Product (Yield, %)[‡]
81	(benzyl alcohol)	0.5	20	(>99)	(89)
82	(3,4-dimethoxybenzyl alcohol)	0.5	20	(>99)	(89)
83	(3-chlorobenzyl alcohol)	0.5	20	(>99)	(89)
84	(4-methoxybenzyl alcohol)	0.5	20	(>99)	(57)
85	(4-nitrobenzyl alcohol)	0.5	20	(>99)	(97)
86	(4-methylbenzyl alcohol)	0.5	20	(>99)	(>99)
87	(2-naphthylmethanol)	0.5	20	(>99)	(95)
88	(4-chlorobenzyl alcohol)	0.5	20	(>99)	(74)
89	(2-chloropropanol)	0.5	20	(0)	(N/A)
90	(2-butanol)	0.5	20	(0)	(N/A)

[a] Reaction conditions: 0.1 mmol alcohol, 0.12 mmol benzyl amine and 3 mol eq. AgNO$_3$ in 0.5 ml of 18 mΩ de-ionised water. [†]Reaction time of alcohol oxidation was 3 hours; [‡]nucleophilic coupling was a 2 hour reflux at 120 °C. Alcohol conversion and imine yields determined using GC-MS calibration curves.

Initial synthetic CVD diamond studies measured the benzyl alohol conversions using gas chromatographic peak areas. However, 'The Fundamentals of Analytical Chemistry'[155] identified that chromatographic peak areas would only yield relative concentrations. The text reported that external standard calibrations would produce highly accurate quantitative measures of analysis, which finalised the decision for the application of external standards in the pseudo tandem study. Furthermore, the ability to analyse complex reaction mixtures, minimalise *on-line* interferences and process data sets (molecular ion identification using mass spectrometry) supported the application of external standard calibration.

External standard calibrations were performed on a Shimadzu GCMS-QP 2010 SE for each alcohol investigated in the pesudo tandem oxidation study. Aliquots of the converted alcohol and imine products were analysed according to the systematic process recorded below.

1) Five analytical standards of each alcohol were prepared to construct a calibration curve with concentrations ranging from 20-120 parts per million (ppm).
2) Subsequently, the pseudo tandem oxidation was applied to oxidise each alcohol and the aldehyde extracted into dichloromethane after the irradiation period. To quantify the alcohol conversion, a 60-ppm volume was extracted and analysed using the Shimadzu GC-MS to determine the remaining alcohol and aldehyde produced. One mol of alcohol was converted into one mol of aldehyde. Therefore the amount of aldehyde detected would equal the amount of alcohol converted. Subsequently, the solution was refluxed for two hours with benzyl amine.
3) To achieve an accurate imine yield after the refluxing period, a further 60-ppm volume was extracted and analysed to determine the remaining aldehyde. The difference in the aldehyde concentration between steps 2) and 4) would equal the imine yield.

For example, the analysis of N-benzylidenebenzylamine was performed as described below.

1) The conversion of the alcohol to the imine product occurred via the following synthetic route:

$$[Alcohol] \xrightarrow{\text{Oxidation}} [Aldehyde] \xrightarrow[\text{Coupling}]{\text{Nucleophilic}} [Imine]$$
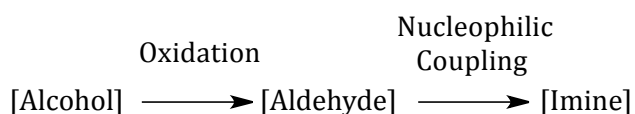
2) Allow the concentration of the alcohol (measured in parts per million [ppm]) before the oxidation to be 'W', 'X' after the oxidation and the peak area of the aldehyde before the nucleophilic coupling to be 'Y' and the final aldehyde peak area to be 'Z'.

$$[W] \longrightarrow [X] \longrightarrow Y \longrightarrow Z \qquad [\ ] \text{ in ppm}$$
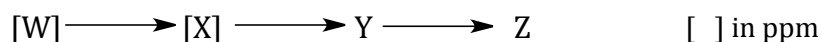
3) Example: Remaining alcohol post alcohol oxidation:

$$[W] = 3600$$
$$[X] = 19 \text{ x dilution factor } (57.5)$$

$$\text{Alcohol conversion to aldehyde} = 1 - \left(\frac{1092.5}{3600}\right)$$
$$= 70\%$$

Yield of N-benzylidenebenzylamine:

$$Y = 1907.5$$
$$Z = 152$$

$$\text{Imine yield} = \left(\frac{1097.5 - 152}{1097.5}\right) \text{x } 100$$
$$= 86\%$$

After completing an accurate procedure for quantification, the ten alcohols of figure 72 were tested using the pseudo tandem process with the results tabulated above (table 18).

Once the results from the pseudo-tandem process had been obtained, the imines needed purification. As reported earlier, imines are well known to degrade when purified using silica gel, even after silica gel neutralisation.[133] Therefore, basic alumina was a necessity for work-up stages.

2.7.4) Movement to methyl acrylates

Despite the good conversion of alcohols into aldehydes and on to N-benzylidenebenzylamines, it was identified that manually separating imines using an alumina gel column was timeous. Purification of each imine in table 18 would solely require a lengthy period and was deemed unsuitable to meet the submission date to commemorate Professor Richard's Taylor's achievement. Therefore to complete the article in time for the submission, new alcohol oxidation reactions were undertaken and coupled to methyl (triphenylphosphoranylidene)acetate to afford various methyl acrylates (figure 74).
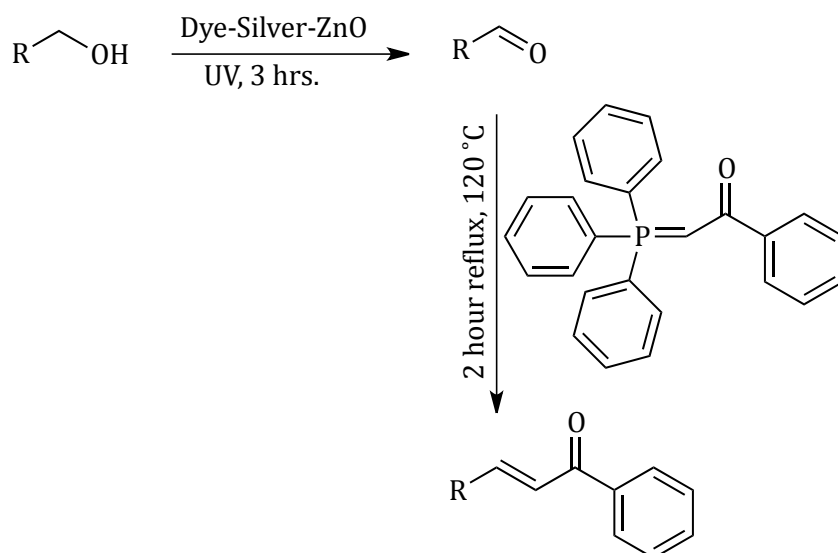
Figure 74: Dye-Silver-ZnO mediated synthesis of methyl acrylates.

The work up stages to purify the methyl acrylates proved significantly easier. After implementing the same synthetic procedure that was used for the *N*-benzylidenebenzylamine reactions, the crude methyl acrylates were simply eluted through a silica plug with hexane:ethyl acetate (10: 1) to separate the methyl acrylate product in the first fraction.

In the previous attempt where the pseudo tandem process was applied to the synthesis of various *N*-benzylidenebenzylamines, quantitative analysis was determined using an external standard calibration method on the Shimadzu GC-MS. After attempting to isolate and determine the yields of entries 89 and 90 of table 18, a limitation was identified with the current chromatographic method of quantification. During the post reaction work-up stages, great care was taken to ensure that the solvent (dichloromethane) and short chain volatile aldehydes were not spilt nor evaporate during the quantitative analysis (the sample preparation only required less than 30 microlitres for analysis; hence a loss of a minute aliquot would greatly impact the yields of the various *N*-benzylidenebenzylamines produced). However, inconclusive peak area data was collected for entries 89 and 90 of table 18 after numerous attempts and subsequently further coupling of benzyl amine was unachievable.

Therefore a new method of quantification was required to measure the conversions of all the alcohols and the methyl acrylate yields. As reported in the chemical literature, an excellent spectroscopic technique to monitor *in-vivo* concentrations was quantitative ^{1}H nuclear magnetic resonance spectroscopy (^{1}H *q*NMR) using the 'Electronic Reference To access In vivo Concentrations' (ERETIC) technique.[156] This was an ideal method of quantification for the pseudo tandem process, as the reactants could be measured *on-line* without interfering with the contents of the reaction. Akoka, *et al.,*[156] evaluated the ERETIC's accuracy against a known spectroscopic internal standard (trimethylamine) and produced higher precision for quantitative lactate detection; while other studies showed equally exceptional quantitative results for complex lipids and fatty acids of microalgae with the same method.[157],[158],[159]

Once the new ^{1}H *q*NMR quantification technique had been identified, fifteen various alcohols were oxidised in the second tandem oxidation study (table 19). After each

alcohol had been irradiated for three hours, it was extracted in accordance with the pseudo tandem process and quantified while using the ^{1}H *qNMR* method. Each aldehyde was then coupled to methyl (triphenylphosphoranylidene)acetate to afford various methyl acrylates (table 20).

The ^{1}H *q*NMR quantitative technique was used in addition to determine the structural identity of the aldehydes and methyl acrylates (supporting ^{13}C NMR and COSY spectra have been reported in the appendix to confirm the structural identity of the methyl acrylate products).

Table 19: Alcohol oxidation study using the refined dye/silver/ZnO system.[a]
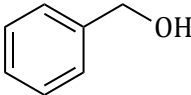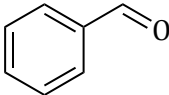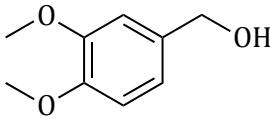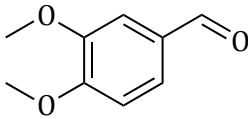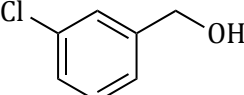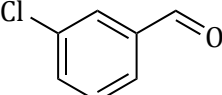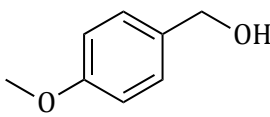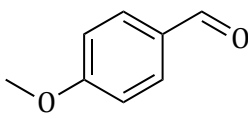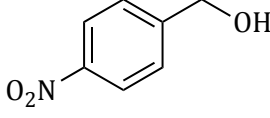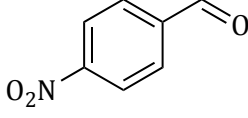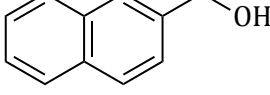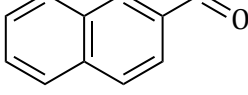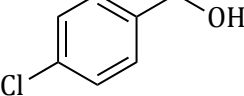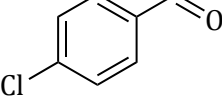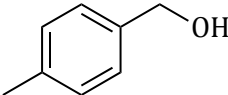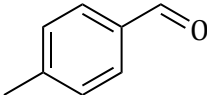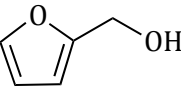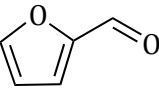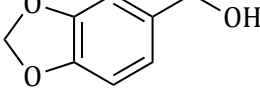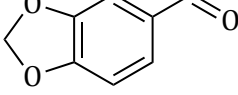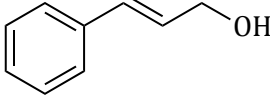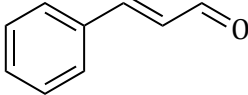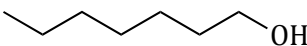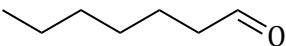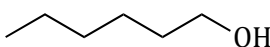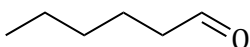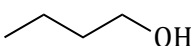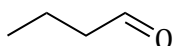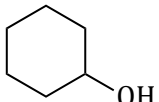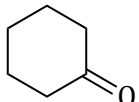
Entry	Alcohol	Carbonyl Intermediate	Alcohol Conversion[b]
91			99
92			99
93			99
94			99
95			99
96			93
97			99
98			99
99			99
100			99
101			95

Table 19 continued

Entry	Alcohol	Carbonyl Intermediate	Alcohol Conversion[b]
102	~~~~~OH	~~~~~O	12
103	~~~~OH	~~~~O	7
104	~~OH	~~O	12
105	cyclohexanol (OH)	cyclohexanone (O)	63

[a]Reaction conditions: 0.2 mmol alcohol, 20 mg d-ZnO, 1.3 mmol TEMPO, AgNO$_3$ (3 eq.), de-ionised water (0.5 ml), 3 hrs. incandescent irradiation. [b]Conversion determined by ^{1}H qNMR using a digital ERETIC method.

Table 20: Methyl acrylates produced after nucleophilic trapping of intermediate aldehydes.[a]
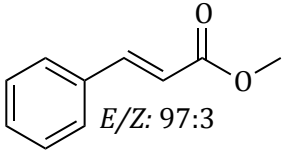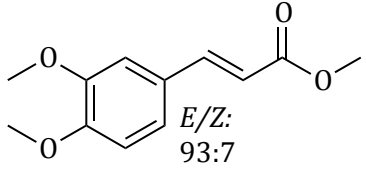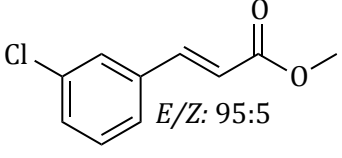
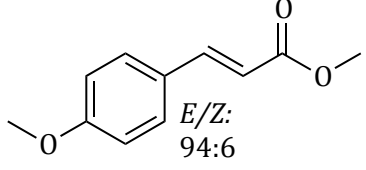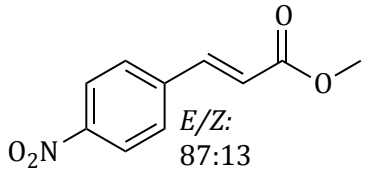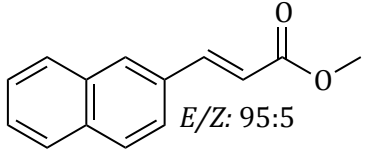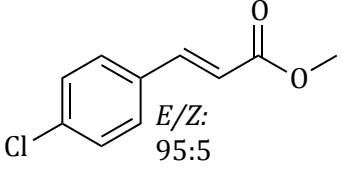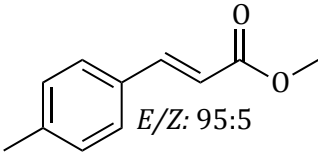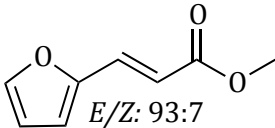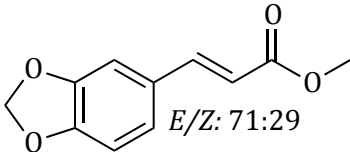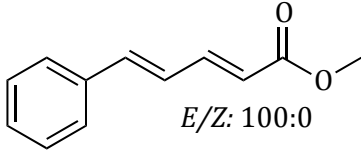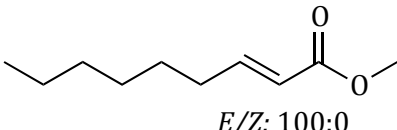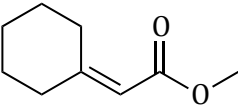| Entry	Acrylate[b]	Acrylate Yield (%)[c]
106	*E/Z:* 97:3	98
107	*E/Z:* 93:7	39
108	*E/Z:* 95:5	99
109	*E/Z:* 94:6	25
110	*E/Z:* 87:13	99
111	*E/Z:* 95:5	89
112	*E/Z:* 95:5	95

Table 20 continued

Entry	Acrylate[b]	Acrylate Yield (%)[c]
113	*E/Z:* 95:5	75
114	*E/Z:* 93:7	81
115	*E/Z:* 71:29	91
116	*E/Z:* 100:0	91
117	*E/Z:* 100:0	Trace
118		N/D

[a]Product from table 19, 3 ml dichloromethane and methyl (triphenylphosphoranylidene)acetate (0.2 mmol), 2 hrs. 120 ℃ reflux.

[b] E/Z selectivity determined using NMR integral values.

[c] 1H qNMR yield, N/D – not detected.

Each methyl acrylate yield presented in table 20 was determined from the tabulated 1H *q*NMR data of table 19 except for entries 103 and 104 of table 19. It was evident from table 19 that limitations existed with the dye/silver/ZnO system as aliphatic alcohols were poorly converted. The low aliphatic alcohol conversions were not unique to the dye/silver/ZnO system after identifying in the chemical literature that the active

N-oxoammonium salt of TEMPO was a poor oxidant of primary unactivated alcohols.[68],[160] An attempt to couple heptanal (entry 102, table 19) to methyl (triphenylphosphoranylidene)acetate only afforded trace quantities of methyl-2-noneoate (entry 117, table 20). Therefore after obtaining a trace quantity of methyl-2-noneoate (entry 117, table 20) while using the pseudo tandem oxidation process, further attempts at coupling the remaining aliphatic aldehydes (entry 103 and 104, table 19) in the Wittig Olefination process were deemed redundant. The findings on this research have been identified as acceptable for submission and are currently awaiting publication in an ISI rated journal (the full article is available in the supporting appendix, pages 61-65).

CHAPTER 3: Conclusion

From the initiation of this study, the project was intended to build upon the momentum gathered from previous findings reported within this group on a silver/dye/ZnO oxidative system.

Benzyl alcohol oxidation studies were the main focus of this project while using synthetic CVD diamonds and a diverse array of chemical and environmental conditions.

However, despite multiple benzyl alcohol reactions, the synthetic CVD diamonds were incapable of oxidising benzyl alcohol. Later findings in solid-state nuclear magnetic resonance identified low boron concentrations in the synthetic CVD diamonds that voided its electrical conductivity and applications in oxidation reactions. Identifying that the boron concentrations were low was highly significant to the study, as it identified that the boron doping in the synthetic CVD diamond was too low and provided insight as to why the synthetic CVD diamonds were unable to oxidise benzyl alcohol.

Later, molecular oxygen was identified to be the active oxidant in the oxidation investigations (after being radicalised by the ultraviolet radiation) affecting the high conversions of benzyl alcohol into benzaldehyde and benzoic acid. However, although the benzyl alcohol oxidations did not proceed *via* a semiconductor mediated-photocatalysed approach, numerous seminal findings were revealed during the course of the study.

The extensive research into the mechanical and physical properties of the synthetic CVD diamond's band gap illuminated a clear understanding that synthetic CVD diamond possessed a very large band gap (5.5 eV), which required harsh radiation (UVC) conditions for photocurrent activation. In addition, the research lead to conclude that band gap positioning of semiconductors drastically affects their redox potentials. The knowledge gathered from this research was highly prevalent to the field of semiconductors as it developed a clear understanding for the reason why synthetic CVD diamonds were incapable of oxidising benzyl alcohol.

In conclusion, initial research suggested that synthetic CVD diamonds had the potential to perform oxidative functions. However after scrutinising the synthetic CVD diamond's band gap, it had a poor oxidation and strong reduction potential.

These findings have stimulated future investigations where semiconductors could be specifically designed to perform a reductive function of converting aldehydes into alcohols and carbon dioxide into methanol.

Lastly, with the knowledge gathered from the synthetic CVD diamond studies, an understanding of semiconductor chemistry provided the necessary input to improve upon a silver/dye/ZnO semiconductor system to effectuate a concise collection of oxidised products. Various alcohols were converted into aldehydes and ketones with aromatic alcohols obtaining a pleasing 93-99% conversion while aliphatic alcohols were modestly converted which ranged from 7-63%. The results of the silver/dye/ZnO study have been identified as worthy of publication and are waiting review.

CHAPTER 4: Future Outcomes

While the oxidation of alcohols using synthetic CVD diamonds has appeared to be impossible from the results collected throughout this thesis, future studies are focused towards the reduction of organic compounds *via* synthetic CVD diamond excitron (e⁻/h⁺) production (from the illumination of synthetic CVD diamonds using high powered UVC radiation sources).

The concept will aim to harness synthetic CVD diamond conduction band electrons in aqueous, organic and biphasic solvents (Figure 75).
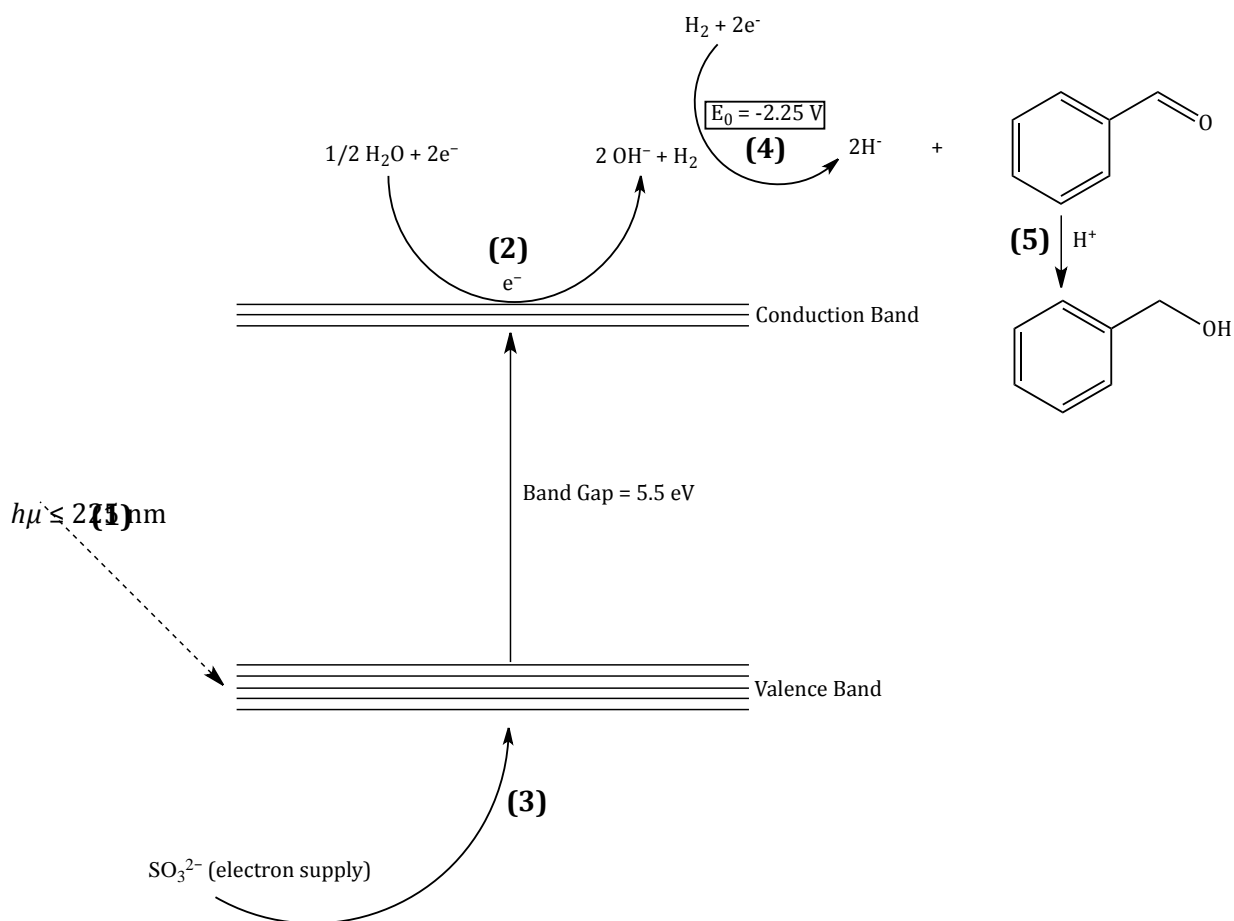

Figure 75: Acid promoted reduction of carbonyl compounds to alcohols using synthetic CVD diamonds.

The scheme has been proposed to follow accordingly:

(1) Synthetic boron doped CVD diamond activation will occur via irradiation with a UV source ≤ 225 nm.

(2) An electron from the valence band will be promoted into the conduction band, which shall cause the reduction of water to hydroxyl radicals and hydrogen gas.

(3) A continuous supply of electrons from sulfite ions (that are hole scavengers providing electrons to trap the holes) will promote the catalytic cycle to continue.

(4) Since the conduction band electrons of synthetic CVD diamond have a potential difference of ~5 V, they will be capable of reducing water as well as activating hydrogen gas that only requires an E_0 of −2.25 V to be reduced to hydride ions.

(5) Since synthetic CVD diamond has been identified as a poor oxidising agent, an external supply of protons (from an acid) would be required to complete the reduction of the aldehyde to alcohol.

A second study will be to replicate similar findings to those published by Rios-Bernÿ, et al.,[66] Rios-Bernÿ reported aniline production after nitrobenzene was reduced on the surface of titanium dioxide. Once the titanium dioxide had been irradiated, the conduction band free electrons were harnessed to reduce nitrobenzene to aniline meanwhile the valence band positive holes oxidised aliphatic alcohols to aldehydes and ketones. The products of oxidation and reduction were then capable of nucleophilic attack and produced various imines (figure 76).
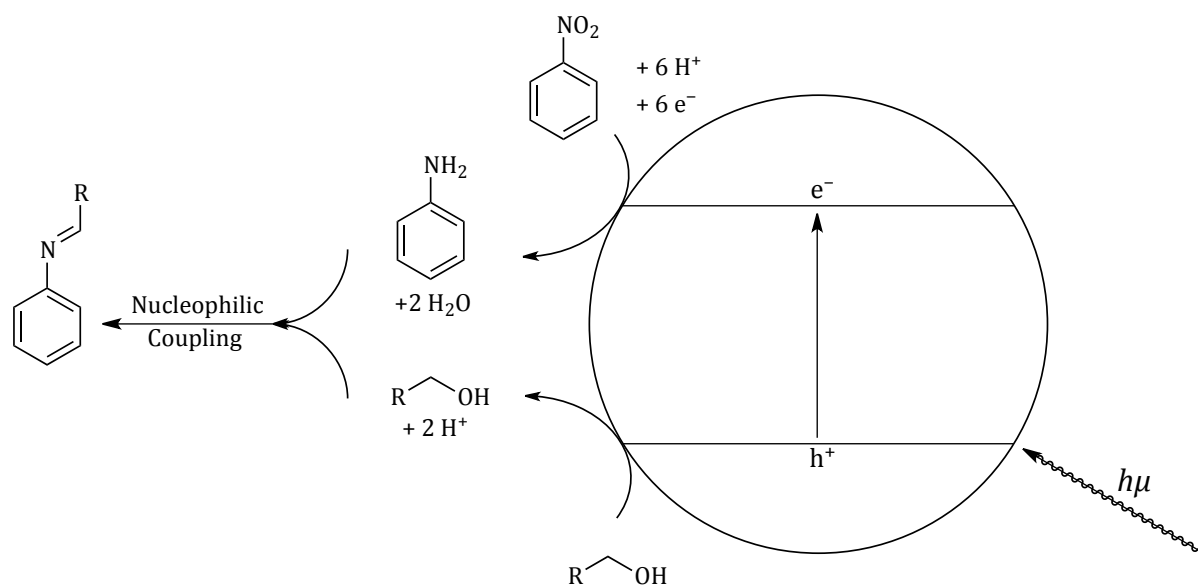
Figure 76: Imine synthesis proposed by Rios-Bernÿ, et al.[66]

To attempt similar reductions using the synthetic CVD diamond square, a suitable irradiation source ($\lambda \leq 225$ nm) will be required to irradiate the synthetic CVD diamond square in alcoholic solutions of nitro benzenes and aldehydes. It was noted by Rios-Bernÿ, *et al.,*[66] that various alcohols were tested during their optimisation study and that there was no need for a proton source (i.e. acid) to complete the reductive cycle as the oxidation of alcohols to aldehydes promoted a supply of readily available hydrogen ions from the positive holes. The positive holes would mediate the oxidation of the alcoholic solvent which functioned not only as a solvent medium but also as a source of electrons from being an intrinsic sacrificial electron donor.[66] However, since synthetic CVD diamond has a valence band with a poor oxidation potential,[119] investigations into the addition of an acid support catalyst will need to be explored.

CHAPTER 5: Experimental

5.1) Instrumentation

5.1.1) Nuclear magnetic resonance

Nuclear magnetic resonance spectroscopic data was collected while using a Bruker Avance III 400 MHz spectrometer that was fitted with a 5 mm BBO-Z probe at 30 ℃. ^{1}H NMR spectra were referenced against deuterated chloroform (δ_H = 7.28 ppm) while ^{13}C NMR spectra were also referenced against deuterated chloroform at δ_C = 77.00 ppm. Quantitative ^{1}H NMR spectra were collected on a Bruker Avance III 400 MHz spectrometer that was fitted with a 5 mm BBO-Z probe at 30 ℃ while using the Electronic **Re**ference **T**o access **I**n vivo **C**oncentrations (ERETIC) method. Solid-state ^{11}B NMR studies were analysed on a Bruker Avance III 600 MHz spectrometer equipped with a 4 mm MAS BB/1H. The ^{11}B spectra were referenced against boric acid with a basic transmitter frequency for ^{11}B of 192.535 MHz with a spin cycle of 12 KHz, relay delay of one second and a magic spinning angle of 54.7 degrees.

Use of abbreviations in NMR spectrometric data; s-singlet, d-doublet, q-quartet, t-triplet, m-multiplet and ppm-parts per million.

5.1.2) Gas chromatography

Analysis of benzyl alcohol samples while using gas chromatographic peak areas were recorded on a PerkinElmer Clarus 500 GC. The instrument was equipped with an Elite-5MS, 30 m, ID:0.25 μm, DF: 0.25 μm column (catalogue number: N9316282).

The GC oven temperature programme was set accordingly:

> ➢ 40 ℃ for 1 minute.
> ➢ 10 ℃/min to 250 ℃-hold for 0.00 minutes.

5.1.3) Gas chromatography-mass spectrometry

Analysis of benzyl alcohol and *N*-benzylidenebenzylamine samples while using gas chromatograph-mass spectrometer (GC-MS) were recorded on a two GC-MS instruments that both used instrument grade helium (Helium Grade 5.0).

The first GC-MS instrument that was used was a Thermo Finnigan Trace gas chromatograph equipped with a PolarisQ mass spectrometer. The column used in the Thermo Finnigan GC was a SGE, BP5, 30 m, ID:0.25 μm, diameter: 0.32 mm.

The GC oven temperature programme was set accordingly:

- ➢ 40 °C for 1 minute.
- ➢ 10 °C/min to 250 °C – hold for 0.00 minutes.

The second GC-MS instrument that was used was a Shimadzu GCMS-QP2010 SE GC-MS. The column used in the gas chromatograph was a Intercap 5MS/Sil, 30 m, ID:0.25 μm, diameter: 0.25 mm.

The GC oven temperature programme was set according to the choice of alcohol oxidised in table 19. Each method file for the Shimadzu GCMS-QP2010 SE has been reported in the appendix section accordingly.

5.1.4) UV/Vis spectroscopy

The methylene blue absorption studies were performed on a PG Instruments Limited T80 UV/VIS spectrophotometer equipped with UVWin5 analytical software (V5.1.1.1).

5.2) Radiation setups

5.2.1) Incandescent radiation setup

The synthesis of various *N*-benzylidenebenzylamines and methyl acrylates while using the silver/dye/ZnO system utilised a purpose build incandescent radiation setup that housed quartz test tubes around an OSRAM® VIALOX 70W incandescent lamp.

5.2.2) UVA/UVB radiation setup

The study of activating the synthetic CVD diamond powders (0-1, 20-40 and 54-80 micron graded) for benzyl alcohol oxidation and *N*-benzylidenebenzylamine synthesis was performed in a purpose built water chilled bath that housed a 2000W OSRAM® Ultramed ultraviolet UVA/UVB lamp. The lamp was mounted inside a cylindrical quartz tube that passed through the vertical sidewalls of a basin to promote uniform radiation emissions while allowing the lamp to remain cool. A fan was also placed within close proximity of the lamp to pass cool air through the quartz cylinder to ensure that the lamp would not over-heat.

5.2.3) UVC radiation setup

The UVC radiation setup for benzyl alcohol oxidation while using the synthetic CVD diamond square was build with a deuterium lamp from a Shimadzu SPD-6A UV spectrophotometric detector (No. 279706LP). The deuterium lamp was removed from the spectrophotometric detector and secured inside a metal box with a machined hole to allow the UVC emissions to exit the lamp's enclosure. The metal box containing the deuterium lamp was placed on top of a borosilicate "mini-beaker" glassware apparatus, which allowed for the irradiation of the synthetic CVD diamond square that was submerged in the reaction solution.

5.3) Chemicals

All the chemical reagents used during the undertaken study were obtained from the supplier as is without further purification except for hexane (Merck UniLAB® hexane fraction, grade: SAAR2868020LC) which was distilled before being used for chromatographic purification of the *N*-benzylidenebenzylamine and methyl acrylate products.

5.4) Synthetic procedures

The undertaken project was aimed to further the foundations of the TiO_2 and ZnO studies that have been conducted within this group. Therefore the oxidation of benzyl alcohol oxidation while using the synthetic CVD diamonds was explored. The main aim of the project was to identify the optimal reaction conditions to oxidise benzyl alcohol with the synthetic CVD diamonds that could be expanded to a wide alcohol substrate analysis and nucleophilic coupling reactions.

However since the synthetic CVD diamonds were unable to impart an oxidative function, benzyl alcohol was the sole alcohol used during the course of the study.

Therefore to present a succinct experimental overview for the oxidation of benzyl alcohol oxidation reactions listed in this thesis without reiterating near-identical reaction conditions, a sample reaction while using the variables investigated during the study have been recorded below (table 21) with a tabulation of the benzaldehyde, benzoic acid and *N*-Benzylidenebenzylamine yields obtained from each reaction attempt respectively.

Table 21: Synthetic CVD diamond benzyl alcohol oxidation conductions.

Table	Entry	BDD [mg]	Solvent [ml]	O_2 Env.	UV (A/B/C)	Time (hrs.)	Base (mol%)	CHO (%)	COOH (%)	Other (%)	Imine (%)
2	3	(0-1) [15]	CH_3CN [2.0]	O_2 purge	A+B	8	0	12	0	N/D	N/A
4	11	(0-1) [2]	CH_3CN [0.5]	O_2 purge	A+B	8	0	13	25	19	N/A
5	13	(0-1) [0.4]	CH_3CN [0.5]	O_2 purge	None	8	0	4	86	3	N/A
5	14	(0-1) [0.3]	CH_3CN [0.5]	O_2 purge	A+B	8	0	11	55	7	N/A
5	16	(0-1) [0.1]	CH_3CN [0.5]	O_2 purge	A+B	8	0	7	56	13	N/A
10	35	(54-80) [45]	TCE [3]	O_2 bubbling	A+B	8	0	9	75	8	N/A
12	38	(54-80) [15]	TCE [3]	O_2 purge	Sunlight	7	0	4	<1	0	N/A
12	39	(54-80) [15]	TCE [3]	O_2 purge	Incandescent	7	0	<1	<1	0	N/A
13	41	(54-80) [15]	CH_3CN [0.5]	O_2 bubbling	A+B	7	0	2	86	9	N/A
13	42	0	CH_3CN [0.5]	O_2 bubbling	A+B	7	0	3	96	0	N/A
13	43	(54-80) [15]	CH_3CN [0.5]	O_2 bubbling	A+B	7	0	0	97	3	N/A
13	45	0	CH_3CN [0.5]	Argon purge	A+B	7	0	6	1	0	N/A
15	46	(54-80) [15]	CH_3CN [0.5]	Atm.	C	7	0	2	<1	0	N/A

Table 21 continued

Table	Entry	BDD [mg]	Solvent [ml]	O_2 Env.	UV (A/B/C)	Time (hrs.)	Base (mol%)	CHO (%)	COOH (%)	Other (%)	Imine (%)
15	51	0	CH_3CN [0.5]	Atm.	C	7	0	6	<1	0	N/A
15	52	(2% B-BDD) (54-80) CH_3CN [15]	CH_3CN [0.5]	Atm.	C	7	0	2	<1	0	N/A
15	54	B(OH)$_3$ [1]	CH_3CN [0.5]	Atm.	C	7	0	3	<1	0	N/A
16	56	BDD Square	CH_3CN [0.5]	Atm.	C	7	0	0	0	0	N/A
Optimisation studies towards the synthesis of *N*-benzylidenebenzylamine											
6	19	(0-1) [10]	CH_3CN [0.5]	O_2 purge	A+B	8	0	N/A	N/A	N/A	99
6	20	(0-1) [10]	CH_3CN [0.5]	O_2 purge	A+B	8	0	N/A	N/A	N/A	38
7	24	(0-1) [10]	CH_3CN [0.5]	O_2 purge	A+B	8	10% KOH	N/A	N/A	N/A	35
7	28	(0-1) [10]	CH_3CN [0.5]	O_2 purge	A+B	8	130% NaOH	N/A	N/A	N/A	65

5.4.1) Freeze/thaw method to remove gaseous and dissolved oxygen
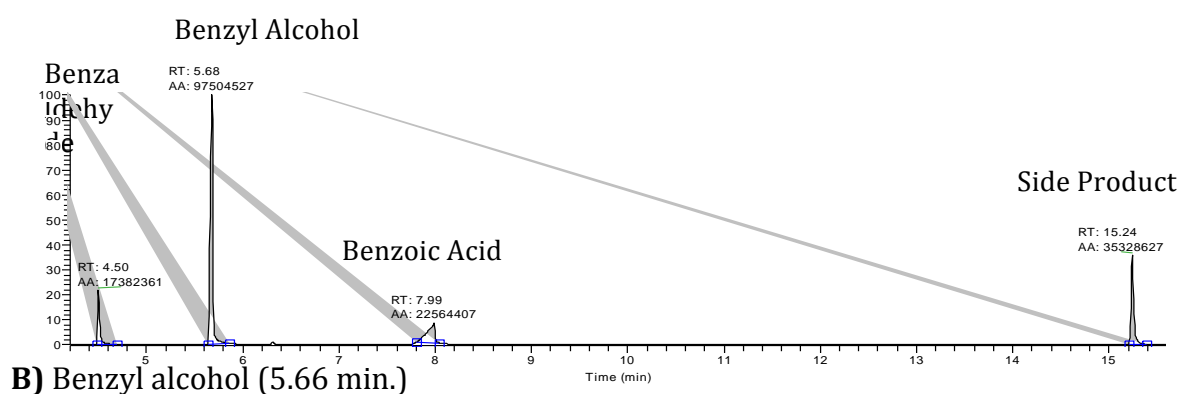
To remove any traces of dissolved or gaseous oxygen from the reaction's environment and solvent, the test tube and the reaction contents were frozen in liquid nitrogen. Once the reaction contents were completely frozen, they well left to warm up to room temperature and then placed under reduced pressure for a period of five minutes to remove any dissolved or gaseous oxygen in the test tube. Once degassed, the test tube was backfilled with argon.
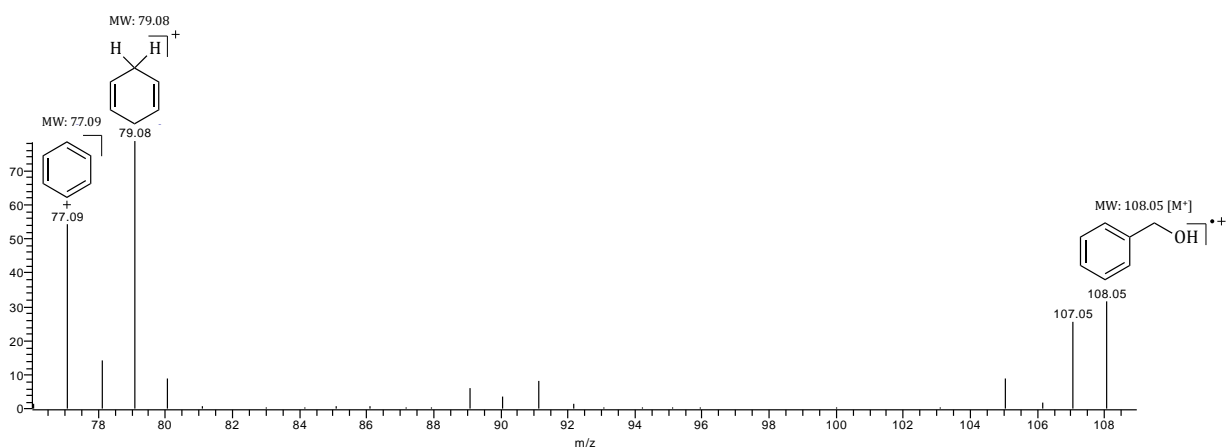
5.5) Analytical data

The major analytical technique used throughout the undertaken study for quantitative measures were recorded while using gas chromatographic data while either using a PerkinElmer Clarus 500 gas chromatograph, Thermo Finnigan Trace GC-MS or a Shimadzu GP2010 SE GC-MS. Therefore a sample data set has been presented below to illustrate the yield calculations of benzaldehyde and benzoic acid. The remaining data sets have been tabulated in the supporting appendix.

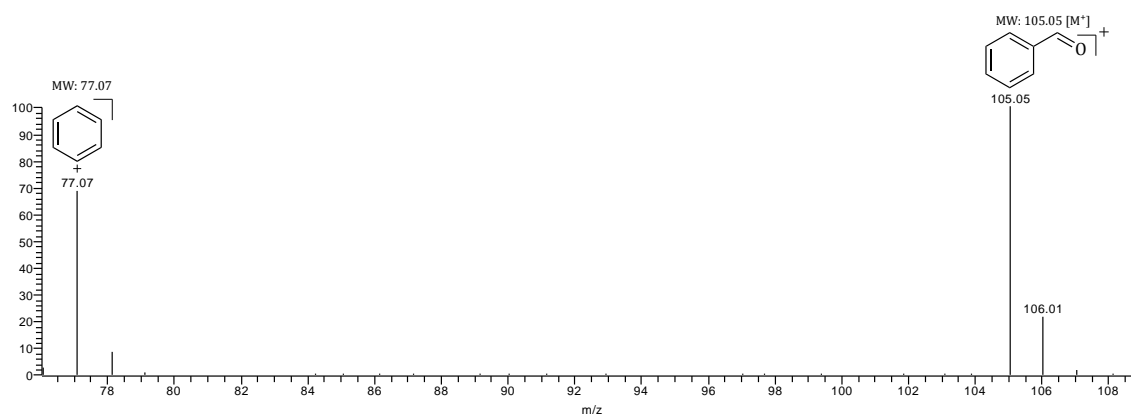**Benzyl alcohol oxidation to benzaldehyde and benzoic acid**

a) Complex reaction mixture.

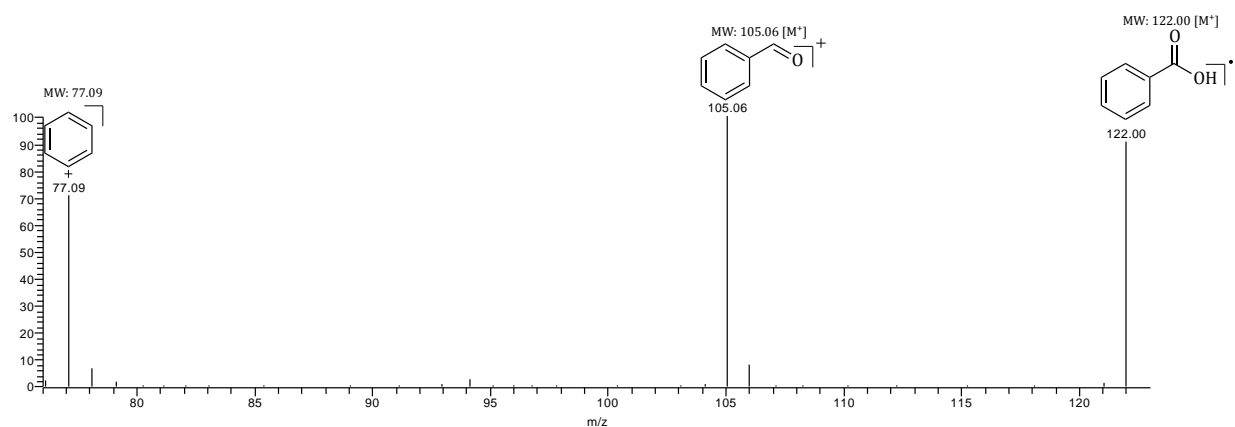**B)** Benzyl alcohol (5.66 min)

C) Benzaldehyde (4.56 min.)

MW: 105.05 [M⁺]

105.05

MW: 77.07

77.07

106.01

m/z

D) Benzoic acid (7.83 min.)

MW: 105.06 [M⁺]

105.06

MW: 122.00 [M⁺]

122.00

MW: 77.09

77.09

m/z

Figure 31: Gas chromatograph-mass spectrometry data of entry five, table three.

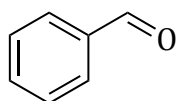**Sample Calculation:**

OH PA:	Benzyl alcohol peak area
CHO PA:	Benzaldehyde peak area
COOH PA:	Benzoic acid peak area
SP PA:	Side product peak area

$$\text{Benzaldehyde yield} = \left(\frac{\text{[CHO] PA}}{\text{[OH+CHO+COOH+SP] PA}} \right) \text{X } 100$$

$$\text{Benzaldehyde yield} = \left(\frac{17711827}{17711827+97704631+22728630+35510025} \right) \text{x } 100$$

$$= 10\%$$

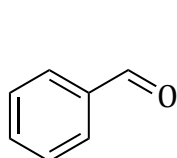### 5.5.1) Attempts to optimise the benzyl alcohol oxidation studies.
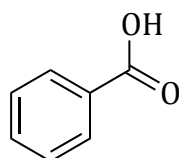
Table 2, entry 2

Benzaldehyde

To a volume of acetonitrile (0.5 ml), benzyl alcohol (1 mmol) and 0-1 micron graded synthetic CVD powder (15 mg) were added to a quartz test tube. The test tube was then purged with oxygen gas (industrial grade, product code: K091C, product of Air Products) for two and a half minutes and then sealed with a rubber septum and Parafilm tape to ensure a tight seal. The test tube was then placed in front of the OSRAM® 2000W Ultramed ultraviolet lamp for eight hours. After the irradiation period, the crude mixture was filtered through a cotton wool filter plug and the solvent reduced under vacuum. The crude product were dissolved in deuterated chloroform and analysed using ^{1}H NMR. Benzaldehyde (18%) was identified as the sole product from the ^{1}H NMR data with a yield based on peak area ratios.

Table 3, entry 5

Benzaldehyde   Benzoic acid

To a volume of acetonitrile (0.5 ml), benzyl alcohol (1 mmol) and 0-1 micron graded synthetic CVD powder (2 mg) were added to a quartz test tube. The test tube was then purged with oxygen gas for two and a half minutes and then sealed with a rubber septum and Parafilm tape to ensure a tight seal. The test tube was then placed in front of the OSRAM® 2000W Ultramed ultraviolet lamp for eight hours. After the irradiation period, the crude mixture was filtered through a cotton wool filter plug and the taken for quantitative analysis using a Thermo Finnigan GC coupled to a PolarisQ mass spectrometer. Based of the peak areas collected from the Thermo Finnigan GC, the

reaction afforded benzaldehyde (15%), benzoic acid (46%) and unidentified side products (10%).
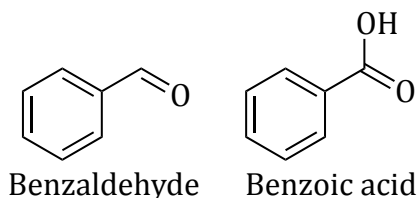
Table 5, entry 14

Benzaldehyde   Benzoic acid

To a volume of acetonitrile (0.5 ml), benzyl alcohol (1 mmol) and 0-1 micron graded synthetic CVD powder (0.3 mg) were added to a quartz test tube. The test tube was then purged with oxygen gas for two and a half minutes and then sealed with a rubber septum and Parafilm tape to ensure a tight seal. The test tube was then placed in front of the OSRAM® 2000W Ultramed ultraviolet lamp for eight hours. After the irradiation period, the crude mixture was filtered through a cotton wool filter plug and 10 microlitres were taken for quantitative analysis using a Thermo Finnigan GC coupled to a Polaris$Q$ mass spectrometer. Based of the peak areas co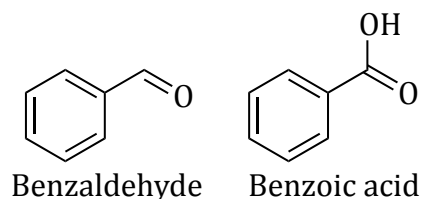llected from the Thermo Finnigan GC, the reaction afforded benzaldehyde (11%), benzoic acid (55%) and unidentified side products (28%).

Table 12, entry 38

Benzaldehyde   Benzoic acid

To a volume of distilled 1,1,2-trichloroethane (3 ml), benzyl alcohol (1 mmol) and 54-80 micron graded synthetic CVD powder (15 mg) were added to a quartz test tube. The test tube was then purged with oxygen gas for two and a half minutes and then sealed with a rubber septum and Parafilm tape to ensure a tight seal. The test tube was then placed in direct sunlight for seven hours. After the irradiation period, the crude mixture was

filtered through a cotton wool filter plug and 10 microlitres were taken for quantitative analysis using a PerkinElmer Clarus 500 gas chromatograph (GC). Based of the peak areas collected from the PerkinElmer Clarus 500 GC, the reaction afforded benzaldehyde (4%) and benzoic acid (<1%).

Table 12, entry 38

Benzaldehyde   Benzoic acid

To a volume of acetonitrile (0.5 ml), benzyl alcohol (1 mmol) and 54-80 micron graded synthetic CVD powder (15 mg) were added to a quartz test tube. The test tube was then purged with oxygen gas for two and a half minutes and then sealed with a rubber septum and Parafilm tape to ensure a tight seal. The test tube was then placed in front of an OSRAM® VIALOX 70W incandescent lamp for seven hours. After the irradiation period, the crude mixture was filtered through a cotton wool filter plug and 10 microlitres were taken for quantitative analysis using a PerkinElmer Clarus 500 gas chromatograph (GC). Based of the peak areas collected from the PerkinElmer Clarus 500 GC, the reaction afforded benzaldehyde (<1%) and benzoic acid (<1%).

Table 13, entry 42

Benzaldehyde   Benzoic acid

To a volume of acetonitrile (3 ml), benzyl alcohol (1 mmol) was added to a quartz test tube.. The test tube was then placed in front of the OSRAM® 2000W Ultramed ultraviolet lamp for seven hours with continuous oxygen saturation. After the irradiation period, the crude mixture was filtered through a cotton wool filter plug and 10 microlitres were

taken for quantitative analysis using a PerkinElmer Clarus 500 gas chromatograph (GC). Based of the peak areas collected from the PerkinElmer Clarus 500 GC, the reaction afforded benzaldehyde (3%) and benzoic acid (96%).
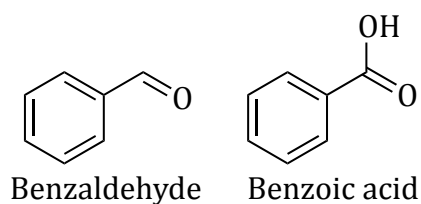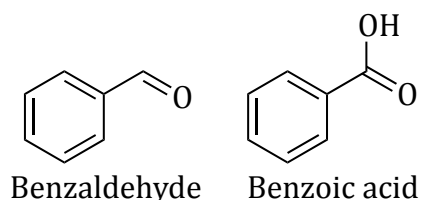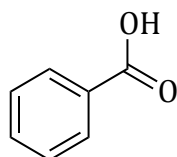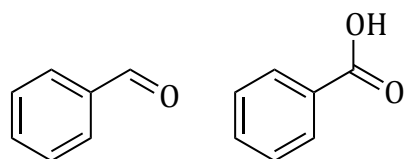
Table 13, entry 43

Benzoic acid

To a volume of distilled 1,1,2-trichloroethane (3 ml), benzyl alcohol (1 mmol) and 54-80 micron graded synthetic CVD powder (15 mg) were added to a quartz test tube. The test tube was then placed in front of the OSRAM® 2000W Ultramed ultraviolet lamp for seven hours with continuous oxygen saturation. After the irradiation period, the crude mixture was filtered through a cotton wool filter plug and 10 microlitres were taken for quantitative analysis using a PerkinElmer Clarus 500 gas chromatograph (GC). Based of the peak areas collected from the PerkinElmer Clarus 500 GC, the reaction afforded benzoic acid (99%).

Table 15, entry 50

Benzaldehyde   Benzoic acid

To a volume of acetonitrile (3 ml), benzyl alcohol (1 mmol) was added to a quartz test tube. The test tube was degassed of any gaseous or dissolved oxygen gas by using a freeze/thaw method. The freeze/thaw process was repeated three times and then the test tube was placed in front of the deuterium (UVC) lamp source taken from a Shimadzu SPD-6A UV spectrophotometric detector for seven hours. After the irradiation period, the crude mixture was filtered through a cotton wool filter plug and 10 microlitres were

taken for quantitative analysis using a PerkinElmer Clarus 500 gas chromatograph (GC). Based of the peak areas collected from the PerkinElmer Clarus 500 GC, the reaction afforded benzaldehyde (2%) and benzoic acid (1%).
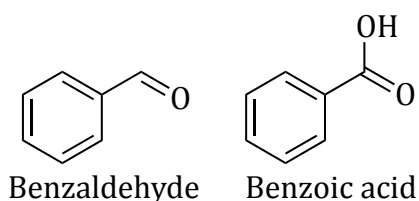
Table 15, entry 51

Benzaldehyde   Benzoic acid

To a volume of acetonitrile (3 ml), benzyl alcohol (1 mmol) and 54-80 micron graded synthetic CVD diamond powder (15 mg) were added to a quartz test tube. The test tube was degassed of any gaseous or dissolved oxygen gas by using a freeze/thaw method. The test tube and the reaction contents were frozen in liquid nitrogen. Once the reaction contents had frozen, they well left to warm up to room temperature, after such time they were placed under reduced pressure for a period of five minutes to remove any dissolved or gaseous oxygen present in the test tube. The freeze/thaw process was repeated three times and then the test tube was placed in front of the deuterium (UVC) lamp source taken from a Shimadzu SPD-6A UV spectrophotometric detector for seven hours. After the irradiation period, the crude mixture was filtered through a cotton wool filter plug and 10 microlitres were taken for quantitative analysis using a PerkinElmer Clarus 500 gas chromatograph (GC). Based of the peak areas collected from the PerkinElmer Clarus 500 GC, the reaction afforded benzaldehyde (1%) and benzoic acid (<1%).
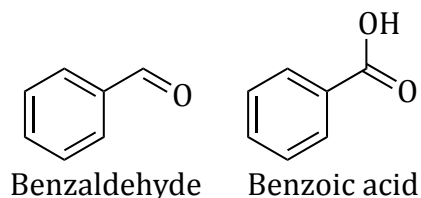
Table 15, entry 53

Benzaldehyde   Benzoic acid
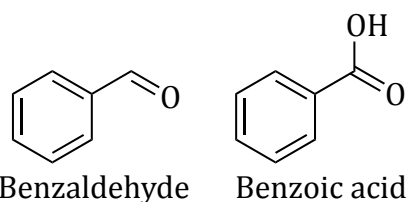
To a volume of acetonitrile (3 ml), benzyl alcohol (1 mmol) and 2% boric acid (B[OH]$_3$) doped 54-80 micron graded synthetic CVD diamond powder (15 mg) were added to a quartz test tube. The test tube was degassed of any gaseous or dissolved oxygen gas by using a freeze/thaw method. The freeze/thaw process was repeated three times and then the test tube was placed in front of the deuterium (UVC) lamp source taken from a Shimadzu SPD-6A UV spectrophotometric detector for seven hours. After the irradiation period, the crude mixture was filtered through a cotton wool filter plug and 10 microlitres were taken for quantitative analysis using a PerkinElmer Clarus 500 gas chromatograph (GC). Based of the peak areas collected from the PerkinElmer Clarus 500 GC, the reaction afforded benzaldehyde (2%) and benzoic acid (<1%).

Table 15, entry 54

Benzaldehyde   Benzoic acid

To a volume of acetonitrile (3 ml), benzyl alcohol (1 mmol) and boric acid (B[OH]$_3$, 1 mg) doped 54-80 micron graded synthetic CVD diamond powder (15 mg) were added to a quartz test tube. The test tube was degassed of any gaseous or dissolved oxygen gas by using a freeze/thaw method. The freeze/thaw process was repeated three times and then the test tube was placed in front of the deuterium (UVC) lamp source taken from a Shimadzu SPD-6A UV spectrophotometric detector for seven hours. After the irradiation period, the crude mixture was filtered through a cotton wool filter plug and 10 microlitres were taken for quantitative analysis using a PerkinElmer Clarus 500 gas

chromatograph (GC). Based of the peak areas collected from the PerkinElmer Clarus 500 GC, the reaction afforded benzaldehyde (3%) and benzoic acid (<1%).
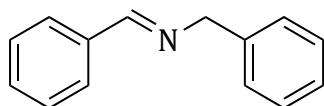
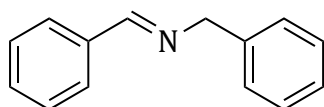### 5.5.2) Attempts to optimise the *N*-benzylidenebenzylamine synthesis.

Table 6, entry 19

N-benzylidenebenzylamine

0-1 micron graded synthetic CVD powder (10 mg) was added to a neat solution of benzyl alcohol (1 mmol) and benzyl amine (2 mmol) in a quartz test tube. The mixture was purged with oxygen gas for two and a half minutes and then sealed with a rubber septum and Parafilm tape to ensure a tight seal. The test tube was then placed in front of the OSRAM® 2000 W Ultramed ultraviolet lamp for eight hours. After the irradiation period, the crude mixture was filtered through a cotton wool filter plug and 10 microlitres were taken for quantitative analysis using a Thermo Finnigan GC coupled to a Polaris*Q* mass spectrometer. Based of the peak areas collected from the Thermo Finnigan GC, the reaction afforded *N*-benzylidenebenzylamine (99%).

Table 7, entry 24

N-benzylidenebenzylamine

0-1 micron graded synthetic CVD powder (10 mg) and 10 mol% potassium hydroxide (KOH) were added to a neat solution of benzyl alcohol (1 mmol) and benzyl amine (2 mmol) in a quartz test tube. The mixture was purged with oxygen gas for two and a half minutes and then sealed with a rubber septum and Parafilm tape to ensure a tight seal. The test tube was then placed in front of the OSRAM® 2000W Ultramed ultraviolet lamp for eight hours. After the irradiation period, the crude mixture was filtered through a

cotton wool filter plug and 10 microlitres were taken for quantitative analysis using a Thermo Finnigan GC coupled to a Polaris*Q* mass spectrometer. Based of the peak areas collected from the Thermo Finnigan GC, the reaction afforded *N*-benzylidenebenzylamine (35%).
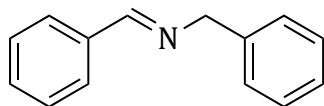
Table 7, entry 26

N-benzylidenebenzylamine

0-1 micron graded synthetic CVD powder (10 mg) and 130 mol% sodium hydroxide (NaOH) were added to a neat solution of benzyl alcohol (1 mmol) and benzyl amine (2 mmol) in a quartz test tube. The mixture was purged with oxygen gas for two and a half minutes and then sealed with a rubber septum and Parafilm tape to ensure a tight seal. The test tube was then placed in front of the OSRAM® 2000 W Ultramed ultraviolet lamp for eight hours. After the irradiation period, the crude mixture was filtered through a cotton wool filter plug and 10 microlitres were taken for quantitative analysis using a Thermo Finnigan GC coupled to a Polaris*Q* mass spectrometer. Based of the peak areas collected from the Thermo Finnigan GC, the reaction afforded *N*-benzylidenebenzylamine (52%).

5.6) Silver/dye/ZnO alcohol oxidation study

¹H Proton Nuclear Magnetic Resonance and Mass Spectrometry data.

5.6.1) Table 20, entry 88

(E)- Methyl-cinnamate
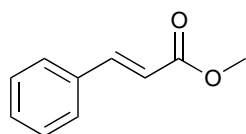
¹H *q*NMR (400 MHz, Neat DCM, 25 ˚C): δ: 7.72 (d, J=15.9 Hz, 1H), 7.53-7.56 (m, 2H), 7.39-7.41 (t, 3H), 6.97 (d, J=12.73 Hz, 1H-*Z* enantiomer), 6.46 (d, J=16.1 Hz, 1H), 5.97 (d, J=12.78 Hz, 1H-*Z* enantiomer), 3.83 (s, 3H).[161] ¹³C NMR (400 MHz, CDCl₃, 25 ˚C): δ: 167.41, 144.87, 134.42, 130.32, 128.89, 128.07, 117.82, 51.64.[162]

GC-MS spectrometric data: EI-MS: *m/z* 162 (M⁺, 50%), 131 (100), 117 (5), 103 (71), 77 (34), 51 (22).

5.6.2) Table 20, entry 89

(*E*)-Methyl 3,4-dimethoxycinnamate
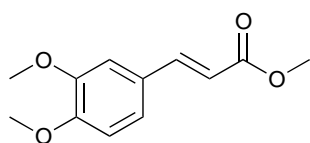
¹H *q*NMR (400 MHz, Neat DCM, 25 ˚C): δ: 7.64 (d, J=15.9 Hz, 2H), 7.07 (s, 1H), 6.89 (d, 1H), 6.85 (d, J=13.00 Hz-*Z* enantiomer), 6.31 (d, J=15.9 Hz, 1H), 5.86 (d, J=12.81 Hz, 1H-*Z* enantiomer), 3.93 (s, 6H), 3.82 (s, 3H). ¹³C NMR (400 MHz, CDCl₃, 25 ˚C): δ: 167.69, 151.08, 149.26, 144.70, 122.63, 127.41, 115.57, 111.02, 109.65, 55.94, 51.62.[163]

GC-MS spectrometric data: EI-MS: *m/z* 222 (M⁺, 100%), 191 (52), 164 (9), 147 (14), 119 (11), 91 (11), 77 (10), 51 (8).

5.6.3) Table 20, entry 90

(*E*)-Methyl 3-chlorocinnamate
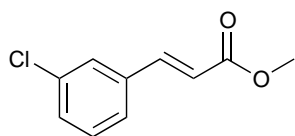
¹H *q*NMR (400 MHz, Neat DCM, 25 °C): δ: 7.68 (d, J=16.11 Hz, 1H), 7.55 (s, 1H), 7.34-7.46, 6.94 (d, J=12.72, 1H-*Z* enantiomer), (m, 3H), 6.46 (d, J=16.03 Hz, 1H), 6.05 (d, J=12.71 Hz, 1H-*Z* enantiomer), 3.87 (s, 1H). ¹³C NMR (400 MHz, CDCl₃, 25 °C): δ: 166.47, 142.78, 135.72, 134.47, 129.69, 127.41, 125.74, 118.81, 51.36.[164]

GC-MS spectrometric data: EI-MS: *m/z* 196 (M⁺, 47%), 165 (100), 137 (42), 102 (52), 111 (4), 75 (28), 51 (24).

5.6.4) Table 20, entry 91

(*E*)-Methyl 4-methoxychlorocinnamate
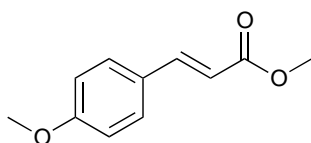
¹H *q*NMR (400 MHz, Neat DCM, 25 °C): δ: 7.67 (d, J=16.1 Hz, 1H), 7.49 (d, J=8.8 Hz, 2H), 6.92 (d, J=8.80 Hz, 2H), 6.84 (d, J=12.84 Hz, 1H-*Z* enantiomer), 6.33 (d, J=11 Hz, 1H), 5.82 (d, J=12.80 Hz, 1H-*Z* enantiomer), 3.85 (s, 3H), 3.81 (s, 3H).[163] ¹³C NMR (400 MHz, CDCl₃, 25 °C): δ: 167.82, 161.38, 144.55, 129.80, 127.10, 115.26, 114.43, 55.42, 51.47.[165]

GC-MS spectrometric data: EI-MS: *m/z* 192 (M⁺, 92%), 161 (100), 133 (45), 118 (15), 89 (15), 77 (12), 51 (5).

5.6.5) Table 20, entry 92

(*E*)-Methyl 4-nitrocinnamate
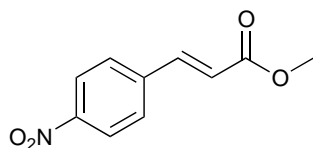
^{1}H *q*NMR (400 MHz, Neat DCM, 25 ˚C): δ: 8.27 (d, J=8.77 Hz, 2H), 7.74 (d, J=16.12 Hz, 1H), 7.70 (d, J=8.77 Hz, 2H), 7.02 (d, J=12.45 Hz, 1H-*Z* enantiomer) 6.58 (d, J=16.11 Hz, 1H), 6.13 (d, J=12.73 Hz, 1H-*Z* enantiomer), 3.87 (s, 3H). ^{13}C NMR (400 MHz, CDCl$_3$, 25 ˚C): δ: 166.38,141.86, 140.40, 128.56, 124.40, 122.12, 52.10.[166]

GC-MS spectrometric data: EI-MS: EI-MS: *m/z* 207 (M$^+$, 41%), 176 (100), 130 (47), 118 (17), 102 (35), 76 (20), 51 (13).

5.6.6) Table 20, entry 93

Methyl (E)-3-(2-naphthyl)-2-propenoate
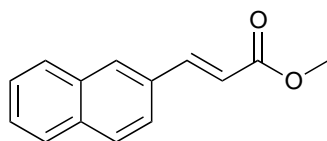
^{1}H *q*NMR (400 MHz, Neat DCM, 25 ˚C): δ: 7.97 (s, 1H), 7.83-7.92 (m,4 H), 7.62-7.65 (dd, J=8.52, 1.6 Hz), 7.51-7.57 (m,2H), 7.10 (d, J=12.60 Hz, 1H-*Z* enantiomer), 6.58 (d, J=15.98 Hz, 1H), 6.04 (d, J=12.51, 1H-*Z* enantiomer), 3.86 (s, 3H). ^{13}C NMR (400 MHz, CDCl$_3$, 25 ˚C): δ: 167.41, 144.97, 134.24, 133.30, 131.90, 129.88, 128.69, 128.55, 127.76, 127.22, 126.70, 123.50, 117.99, 51.69.[167]

GC-MS spectrometric data: EI-MS: *m/z* 212 (M$^+$, 100%), 181 (89), 154 (12), 152 (69), 127 (12), 90 (11), 76 (49), 51 (4).

5.6.7) Table 20, entry 94

(*E*)-Methyl 4-chlorocinnamate
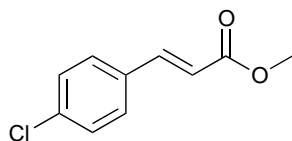
^{1}H *q*NMR (400 MHz, Neat DCM, 25 °C): δ: 7.47 (d, J=8.60 Hz, 2H), 7.66 (d, J=15.95 Hz, 1H), 7.38 (d, J=8.42 Hz, 2H), 6.89 (d, J=12.80 Hz, 1H-*Z* enantiomer), 6.43 (d, J=16.14 Hz, 1H), 5.97 (d, J=12.58 Hz, 1H-*Z* enantiomer) 3.83 (s, 1H). ^{13}C NMR (400 MHz, CDCl$_3$, 25 °C): δ: 167.24, 143.35, 136.29, 132.88, 129.22, 129.20, 118.54, 51.85.[167]

GC-MS spectrometric data: EI-MS: *m/z* 196 (M$^+$, 53%), 165 (100), 137 (46), 111 (4), 102 (48), 75 (24), 51 (27).

5.6.8) Table 20, entry 95

(*E*)-Methyl 4-methylcinnamate
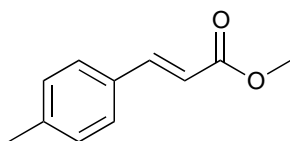
^{1}H *q*NMR (400 MHz, Neat DCM, 25 °C): δ: 7.88 (d, J=7.88 Hz, 2H), 7.69 (d, J=15.95, 1H), 7.44 (d, J=8.19, 2H), 6.89 (d, J=12.58 Hz, 1H-*Z* enantiomer), 6.42 (d, J=15.97 Hz, 1H), 5.88 (d, J=12.70 Hz, 1H-*Z* enantiomer), 3.82 (s, 3H), 2.39 (s, 1H).[161] ^{13}C NMR (400 MHz, CDCl$_3$ Neat DCM, 25 °C): δ: 167.69, 144.93, 140.61, 132.19, 129.68, 128.09, 116.71, 51.62, 21.35.[168]

GC-MS spectrometric data: EI-MS: *m/z* 176 (M$^+$, 64%), 145 (100), 117 (40), 115 (49), 91 (16), 65 (10), 57 (9), 39 (7).

5.6.9) Table 20, entry 96

(*E*)- Methyl 3-(furan-2-yl)acrylate
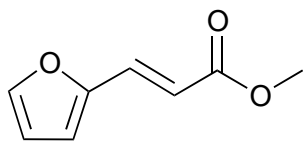
^{1}H *q*NMR (400 MHz, Neat DCM, 25 ˚C): δ: 7.50 (d, J=1.70 Hz, 1H), 7.40 (d, J=15.90 Hz, 1H), 6.79 (d, J=12.87, 1H-*Z* enantiomer), 6.63 (d, J=3.28 Hz, 1H), 6.49 (dd, J=1.98, 1.98 Hz, 1H), 6.34 (d, J=15.82 Hz, 1H), 5.74 (d, J=12.87, 1H-*Z* enantiomer), 3.78 (s, 3H). ^{13}C NMR (400 MHz, CDCl₃, 25 ˚C): δ: 167.38, 150.96, 144.73, 131.22, 115.43, 114.60, 112.11, 51.64.[167]

GC-MS spectrometric data: EI-MS: *m/z* 152 (M⁺, 46%), 121 (100), 93 (11), 65 (43), 39 (25).

5.7.0) Table 20, entry 97

Methyl (2E)-3-(1,3-benzodioxol-5-yl)acrylate
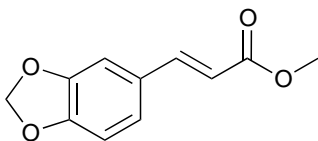
^{1}H *q*NMR (400 MHz, Neat DCM, 25 ˚C): δ: 7.62 (d, J=15.86 Hz, 1H), 7.41 (d, J=7.90 Hz, 1H-*Z* enantiomer), 7.05 (s, 1H), 7.03 (d, J=7.92 Hz, 1H), 6.95 (d, J=7.92 Hz, 1H-*Z* enantiomer), 6.83 (d, J=7.96 Hz, 1H), 6.29 (d, J=15.95 Hz, 1H), 6.02 (s, 2H), 3.81 (s, 1H).[169] ^{13}C NMR (400 MHz, CDCl₃, 25 ˚C): δ: 190.22, 167.58, 153.03, 149.50, 132.05, 128.52, 115.63, 108.57, 106.49, 102.13, 51.63, 30.85.

GC-MS spectrometric data: EI-MS: *m/z* 206 (M⁺, 100%), 190 (1), 175 (69), 145 (61), 117 (25), 89 (37), 63 (21), 43 (1), 39 (8).

5.7.1) Table 20, entry 98

(*2E, 4E*)- Methyl 5-phenylpenta-2,4-dienoate
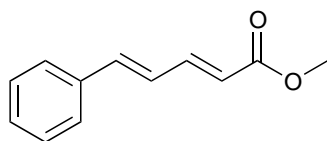
^{1}H qNMR (400 MHz, Neat DCM, 25 °C): δ: 7.30-7.51 (m, 6H), 6.90 (dd, J=15.39 and 15.39 Hz, 2H), 6.02 (d, J=15.40 Hz, 1H), 3.79 (s, 3H).[170] ^{13}C NMR (400 MHz, CDCl$_3$, 25 °C): δ: 167.40, 144.86, 140.56, 136.05, 132.16, 128.88, 127.24, 126.22, 121.09, 51.63.[171]

GC-MS spectrometric data: EI-MS: *m/z* 188 (M$^+$, 18%), 157 (13), 129 (100), 130 (10), 102 (6), 64 (9), 51 (9).

5.7.2) Table 20, entry 99

(E)- Methyl 2-nonenoate
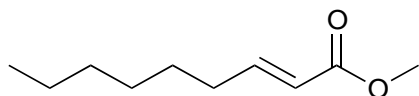
^{1}H qNMR (400 MHz, Neat DCM, 25 °C): δ: 6.99 (m, J=15.66 Hz, 1H), 5.84 (d, J=15.65 Hz, 1H), 2.20 (q, 2H), 1.26-1.52 (m, 11H), 0.91 (t, 3H). ^{13}C NMR (400 MHz, CDCl$_3$, 25 °C): δ: 167.16, 149.70, 120.82, 51.22, 32.16, 31.78, 28.73, 27.93, 22.53, 13.99.[172]

5.7.3) Table 20, entry 100

Cyclohexanone
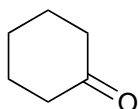
^{1}H qNMR (400 MHz, Neat DCM, 25 °C): δ: 2.28 (t, 4H), 1.84 (m, 4H), 1.70 (m, 2H).[173]

CHAPTER 6: References

[1]   S. Higashimoto, N. Kitao, N. Yoshida, T. Sakura, M. Azuma, H. Ohue, Y. Sakata, *Journal of Catalysis* **2009**, *266*, 279-285.

[2]   M. Zhang, C. Chen, W. Ma, J. Zhao, *Angewandte Chemie* **2008**, *120*, 9876-9879.

[3]   K. R. Phillips, S. C. Jensen, M. Baron, S.-C. Li, C. M. Friend, *Journal of the American Chemical Society* **2013**, *135*, 574-577.

[4]   K. A. D. Swift, *Advances in Flavours and Fragrances, From the Sensation to the Sythesis, Vol. 277*, The Royal Society of Chemistry, Thomas Graham House, Science Park, Milton Road, Cambridge, CB4 0WF, **2002**.

[5]   J. E. Bäckvall, *Modern oxidation methods, Vol. 1*, Wiley-VCH, Mörlenbach, **2004**.

[6]   I. Fleming, *Selected organic syntheses*, Wiley-Interscience, The Pitman Press, Bath, Great Britain, **1972**.

[7]   V. Satam, A. Harad, R. Rajule, H. Pati, *Tetrahedron* **2010**, *66*, 7659-7706.

[8]   M. Hudlicky, *Oxidations in organic chemistry*, American Chemical Society, Washington, DC, **1990**.

[9]   C. M. Hartmann, V., *Berichte der deutschen chemischen Gesellschaft* **1893**, *26*, 1727-1732.

[10]   D. B. M. Dess, J. C., *The Journal of Organic Chemistry* **1983**, *48*, 4155-4156.

[11]   M. Frigerio, M. Santagostino, *Tetrahedron Letters* **1994**, *35*, 8019-8022.

[12]   M. Traoré, S. Ahmed-Ali, M. Peuchmaur, Y. Wong, *Tetrahedron* **2010**, *66*, 5863-5872.

[13]   J. Jeong, C. Guo, P. Fuchs, *Journal of the American Chemical Society* **1999**, *121*, 2071-2084.

[14]   Y. Kita, K. Higuchi, Y. Yoshida, K. Iio, S. Kitagaki, K. Ueda, S. Akai, H. Fujioka, *Journal of the American Chemical Society* **2001**, *123*, 3214-3222.

[15]   Nicolaou, Zhong, Baran, *Angewandte Chemie (International ed. in English)* **2000**, *39*, 625-628.

[16]   J. D. Lou, Z. N. Xu, *Tetrahedron letters* **2002**, 43, 6095-6097.

[17]   K. B. Wilberg, *Oxidation in organic chemistry, Vol. 5 A*, ACADEMIC PRESS, New York, United States of America, **1965**.

[18]   A. Riahi, F. Henin, J. Muzart, *Tetrahedron Letters* **1999**, *40*, 2303-2306.

[19]   J. Muzart, *Tetrahedron Letters* **1987**, *28*, 2133-2134.

[20]   E. J. Corey, G. W. J. Fleet, *Tetrahedron Letters* **1973**, *14*, 4499-4501.

[21]   J. M. Aizpurua, M. Juaristi, B. Lecea, C. Palomo, *Tetrahedron* **1985**, *41*, 2903-2911.

[22]   J. M. Aizpurua, C. Paloma, *Tetrahedron Letters* **1983**, *24*, 4367-4370.

[23]   J. M. Lalancette, G. Rollin, P. Dumas, *Canadian Journal of Chemistry* **1972**, *50*, 3058-3062.

[24]   J. D. Lou, Z. N. Xu, *Tetrahedron letters* **2002**, *43*, 6095-6097.

[25]   H. Zhao, W. Sun, C. Miao, Q. Zhao, *Journal of Molecular Catalysis A: Chemical* **2014**, *393*, 62-67.

[26]   K. C. Weerasiri, A. E. V. Gorden, *Tetrahedron* **2014**, *70*, 7962-7968.

[27]   V. A. Golubev, Rozantsev, E.G., Neiman, M.B., *Akademiia nauk SSSR. Izvestiia. Seriia khimicheskaia.* **1965**, *11*, 1927.

[28]   J. Cella, J. Kelley, E. Kenehan, *The Journal of Organic Chemistry* **1975**, *40*, 1860-1862.

[29]   R. Curci, A. Giovine, G. Modena, *Tetrahedron* **1966**, *22*, 1235-1239.

[30]   C. Robinson, L. Milewich, P. Hofer, *The Journal of Organic Chemistry* **1966**, *31*, 524-528.

[31]   D. Swern, *Chemical Reviews* **1949**, *45*, 1-68.

[32]   H. Richter, O. García Mancheño, *Organic letters* **2011**, *13*, 6066-6069.

[33]   G. F. Smith, V. R. Sullivan, G. Frank, *Industrial & Engineering Chemistry Analytical Edition* **1936**, *8*, 449-451.

[34]   T. Beineke, J. Delgaudio, *Inorganic Chemistry* **1968**, *7*, 715-721.

[35]   P. Shanmugam, P. Perumal, *Tetrahedron* **2006**, *62*, 9726-9734.

[36]   S. Madabhushi, V. S. Vangipuram, K. Kumar Reddy Mallu, R. Jillella, S. Kurva, S. R. Pamulaparthi, *Tetrahedron Letters* **2013**, *54*, 6737-6739.

[37]   A. Giraud, O. Provot, J.-F. Peyrat, M. Alami, J. D. Brion, *Tetrahedron* **2006**, *62*, 7667-7673.

[38]   M. J. Schultz, M. S. Sigman, *Tetrahedron* **2006**, *62*, 8227-8241.

[39]   N. Mase, T. Mizumori, Y. Tatemoto, *Chemical Communications* **2011**, *47*, 2086-2088.

[40]   Y. Kasai, N. Michihata, H. Nishimura, T. Hirokane, H. Yamada, *Angewandte Chemie International Edition* **2012**, *51*, 8026-8029.

[41]   P. T. Anastas, Warner, J. C., Oxford University Press: New York, **1998**, p. 30.

[42]   D. Fogg, E. dos Santos, *Coordination chemistry reviews* **2004**, *248*, 2365-2379.

[43]   S. Elmorsy, *Tetrahedron Letters* **1995**, *36*, 1341-1342.

[44]   R. Taylor, M. Reid, J. Foot, S. Raw, *Accounts of Chemical Research* **2005**, *38*, 851-869.

[45]   D. Phillips, K. Pillinger, W. Li, A. Taylor, A. Graham, *Tetrahedron* **2007**, *63*, 10528-10533.

[46]   S. Denmark, C. Senanayake, *The Journal of Organic Chemistry* **1993**, *58*, 1853-1858.

[47]   H. Outram, S. Raw, R. Taylor, *Tetrahedron Letters* **2002**, *43*, 6185–6187.

[48]   A. H. Michael, *Surface Science Reports* **2011**, *66*, 185-297.

[49]   L. Łukasiak, A. Jakubowski, *Journal of Telecommunications and information technology* **2010**, 3-9.

[50]   A. W. Bott, *Current Separations* **1998**, *17*, 87-91.

[51]   D. Vanmaekelbergh, *Electrochimica acta* **1997**, *42*, 1121-1134.

[52]   M. R. Hoffmann, S. T. Martin, W. Choi, B. D.W., *Chemical Reviews* **1995**, *95*, 69-96.

[53]   O. S. Mohamed, A. E. M. Gaber, A. A. Abdel-Wahab, *Journal of Photochemistry and Photobiology A: Chemistry* **2002**, *148*, 205-210.

[54]   A. N. Trukhin, K. Smits, G. Chikvaidze, T. I. Dyuzheva, L. M. Litywgina, *Central European Journal of Physics* **2011**, *9*, 1106-1113.

[55]   R. M. Chrenko, *Solid State Communications* **1974**, *14*, 511-515.

[56]   A. L. Linsebigler, G. Lu, J. T. Yates Jr., *Chemical Reviews* **1995**, *95*, 735-758.

[57]   A. O. Ibhadon, P. Fitzpatrick, *Catalysts* **2013**, *3*, 189-218.

[58]   K. Hashimoto, H. Irie, A. Fujishima, *Japanese Journal of Applied Physics.* **2005**, *44*, 8269-8285.

[59]   G. Liu, X. Li, J. Zhao, S. Horikoshi, H. Hidaka, *Journal of Molecular Catalysis A: Chemical* **2000**, *153*, 221-229.

[60]   A. Tanaka, K. Hashimoto, H. Kominami, *Journal of the American Chemical Society* **2012**, *134*, 14526-14533.

[61]   W. Shen, Z. Li, H. Wang, Y. Liu, Q. Guo, Y. Zhang, *Journal of Hazardous Materials* **2008**, *152*, 172-175.

[62]   R. T. Hitchcock, *Radio-Frequency and Mircowave Radiation*, 3rd ed., American Industrial Hygiene Association, Fairfax, Virginia, USA, **2004**.

[63]   J. Lambert, A. Edwards, *Electromagnetic Spectrum* **2014**.

[64]   H. Kirsh, *Angewandte Chemie International Edition* **2013**, *52*, 812-847.

[65]   V. Augugliaro, M. Bellardita, V. Loddo, G. Palmisano, L. Palmisano, S. Yurdakal, *Journal of Photochemistry and Photobiology C: Photochemistry Reviews* **2012**, *13*, 224-245.

[66]   O. Rios-Bernÿ, S. Flores, I. Córdova, M. Valenzuela, *Tetrahedron Letters* **2010**, *51*, 2730-2733.

[67]   V. Jeena, Chemistry thesis, University of KwaZulu-Natal (Pietermaritzburg), **2012**.

[68]   E. Skupien, R. J. Berger, V. P. Santos, J. Gascon, M. Makkee, *Catalysts* **2014**, *4*, 89-115.

[69]   J. A. Moulijn, A. E. van Diepen, J. Kapteijn, *Applied Catalysis A: General* **2001**, *212*, 3-16.

[70]   A. Fujishima, K. Honda, *Nature* **1972**, *238*, 37-38.

[71]   Y. Shiraishi, T. Hirai, *Journal of Photochemistry and Photobiology C: Photochemistry Reviews* **2008**, *9*, 157-170.

[72]   L. S. Yoong, F. K. Chong, D. B.K., *Energy* **2009**, *34*, 1652-1661.

[73]   V. Jeena, R. S. Robinson, *Chemical Communications* **2012**, *48*, 299-301.

[74]   V. Jeena, R. S. Robinson, *Dalton transactions* **2012**, *41*, 3134-3137.

[75]   S. Kegnæs, J. Mielby, U. V. Mentzel, T. Jensen, P. Fristrupa, A. Riisager, *Chemical Communications* **2012**, *48*, 2427-2429.

[76]   L. Martın, M. L. Timón, M. J. Petrón, J. Ventanas, *Meat science* **2000**, *54*, 333-337.

[77] M. J. Thomas, T. W. Robison, M. Samuel, *Free Radical Biology and Medicine* **1995**, *18*, 553-557.

[78] E. E. Stashenko, J. W. Wong, J. R. Martínez, A. Mateus, T. Shibamoto, *Journal of Chromatography A* **1996**, *752*, 209-216.

[79] K. V. Subba Rao, B. Srinivas, A. R. Prasadb, M. Subrahmanyam, *Chemical Communications* **2000**, 1533-1534.

[80] O. Beaune, A. Finiels, P. Geneste, P. Graffin, A. Guida, J. L. Olivé, A. Saeedan, *Studies in Surface Science and Catalysis* **1993**, *78*, 401-408.

[81] Q. Wang, *Angewandte Chemie International Edition* **2010**, *49*, 7976-7979.

[82] Y. Li, J. Du, S. Peng, D. Xie, G. Lu, S. Li, *International Journal of Hydrogen Energy* **2008**, *33*, 2007-2013.

[83] M. A. Nasalevich, E. A. Kozlova, T. P. Lyubina, *Journal of …* **2012**.

[84] Z. Teukam, J. Chevallier, C. Saguy, R. Kalish, D. Ballutaud, M. Barbé, F. Jomard, A. Tromson-Carli, C. Cytermann, J. E. Butler, M. Bernard, C. Baron, A. Deneuville, *Nature Materials* **2003**, *2*, 482-486.

[85] R. Trouillon, D. O'Hare, Y. Einaga, *Physical Chemistry Chemical Physics* **2011**, *13*, 5422-5429.

[86] R. Kalish, *Applied Physics Letters* **1997**, *70*, 999-1001.

[87] H. Yu, S. Chen, X. Quan, H. Zhao, Y. Zhang, *Environmental Science & Technology* **2008**, *42*, 3791-3796.

[88] R. S. Balmer, J. R. Brandon, S. L. Clewes, *Journal of Physics: Condensed Matter* **2009**, *21*, 1-51.

[89] Y. L. Zhong, K. P. Loh, *Chemistry – An Asian Journal* **2010**, *5*, 1532-1540.

[90] W. Dunnill, A. Kafizas, I. P. Parkin, *Chemical Vapor Deposition* **2012**, *18*, 89-101.

[91] K. Tang, *Journal of Physics: Conference Series* **2009**, *152*, 1-5.

[92] K. E. Bennet, K. H. Lee, J. N. Kruchowski, S. Y. Chang, M. M. P., A. A. Van Orsow, A. Paez, F. S. Manciu, *Materials* **2013**, *6*, 5726-5741.

[93] J. Shalini, K. J. Sankaran, C. L. Dong, C. Y. Lee, N. H. Tai, I. N. Lin, *Nanoscale* **2013**, *5*, 1159-1167.

[94] X. Zhao, J. Qu, H. Liu, Z. Qiang, R. Liu, C. Hu, *Applied Catalysis B: Environmental* **2009**, *91*, 539-545.

[95] K. Bobrov, A. J. Mayne, G. Dujardin, *Nature* **2001**, *413*, 616-619.

[96] A. Moore, V. Celorrio, M. Oca, D. Plana, W. Hongthani, M. J. Lázaro, D. J. Fermín, *Chemical Communications* **2011**, *47*, 7656-7658.

[97] F. Maier, M. Riedel, B. Mantel, J. Ristein, L. Ley, *Physical Review Letters* **2000**, *85*, 3472-3475.

[98]   C. He, L. Sun, C. Zhang, J. Zhong, *Physical Chemistry Chemical Physics* **2013**, *15*, 680-684.

[99]   J. J. Wei, C. M. Li, X. H. Gao, L. F. Hei, F. X. Lvun, *Applied Surface Science* **2012**, *258*, 6909-6913.

[100] E. Fritsch, K. Scarratt, *Gems & Gemology* **1992**, *28*, 35-42.

[101] P. Atkins, T. Overton, J. Rourke, M. Weller, F. Armstrong, *Shriver and Atkin's Inorganic Chemistry, Vol. 5*, Oxford University Press, The United States and Canada, **2010**.

[102] W. Hongthani, N. A. Fox, D. J. Fermín, *Langmuir* **2011**, *27*, 5112-5118.

[103] A. Yarnell, in *Chemical & Engineering News, Vol. 82*, Chemical & Engineering News, Washington, **2004**, pp. 26-31.

[104] O. A. Williams, *Diamond & Related Materials* **2011**, *20*, 621-640.

[105] V. N. Mochalin, O. Shenderova, D. Ho, Y. Gogotsi, *Nature Nanotechnology* **2012**, *7*, 11-23.

[106] J. Stotter, *Handbook of Electrochemistry, Vol. 17*, **2005**.

[107] M. N. Latto, D. J. Riley, P. W. May, *Diamond and Related Materials* **2000**, *9*, 1181-1183.

[108] P. G. Moreno, D. J. Riley, *Electrochemica Acta* **2002**, *47*, 2589-2595.

[109] Q. Zhuo, S. Deng, B. Yang, J. Huang, B. Wang, T. Zhang, G. Yu, *Electrochemica Acta* **2012**, *77*, 17-22.

[110] Z. Q. Ma, B. X. Liu, *Solar Energy Materials & Solar Cells* **2001**, *69*, 339-344.

[111] S. Bhattacharyya, O. Auciello, J. Birrell, J. A. Carlisle, L. A. Curtiss, A. N. Goyette, D. M. Gruen, A. R. Krauss, J. Schlueter, A. Sumant, P. Zapol, *Applied Physics Letters* **2001**, *79*, 1441-1443.

[112] Y. K. Liu, P. L. Tso, D. Pradhan, I. N. Lin, M. Clark, Y. Tzeng, *Diamond and Related Materials* **2005**, *14*, 2059-2063.

[113] T.-F. Younga, T.-S. Liub, D.-J. Jungb, T.-S. Hsid, *Surface & Coatings Technology* **2006**, *2000*, 3145-3150.

[114] Vandevelde, M. Nesladek, C. Quaeyhaegens, L. Stals, *Thin Solid Films* **1996**, *290-291*, 143-147.

[115] K. Hoshino, F. Shimojo, Y. Zempo, *Journal of Physics: Condensed Matter* **2000**, *12*, A189-A194.

[116] H. Kato, T. Makino, S. Yamasaki, H. Okushi, *Journal of Physics D: Applied Physics* **2007**, *40*, 6189-6200.

[117] J. Suna, H. Lua, H. Lina, W. Huanga, H. Lib, J. Lub, T. Cuib, *Materials Letters* **2012**, *83*, 112-114.

[118] J. H. T. Luong, K. B. Male, J. D. Glennon, *Analyst* **2009**, *134*, 1965-1979.

[119] D. Zhu, L. Zhang, R. E. Ruther, R. J. Hamers, *Nature Materials* **2013**, *12*, 836-841.

[120] L. Zhang, D. Zhu, G. M. Nathanson, R. J. Hamers, *Angewandte Chemie International Edition* **2014**, *53*, 1-5.

[121] S. Kegnæs, J. Mielby, U. V. Mentzel, C. H. Christensenc, A. Riisager, *Green Chemistry* **2010**, *12*, 1437-1441.

[122] Y.-J. Huang, K. L. Ng, H. Y. Huang, *International Journal of Hydrogen Energy* **2011**, *36*, 15203-15211.

[123] P. M. Wood, *Biochemical Journal* **1988**, *253*, 287-289.

[124] F. A.-Z. Gassim, A. N. Alkhateeb, F. H. Hussein, *Desalination* **2007**, *209*, 342-349.

[125] M. Vezzoli, Scientific thesis, Queensland University of Technology (Queensland, Australia), **2012**.

[126] M. L. Di Gioia, A. Leggio, A. Le Pera, A. Liguori, A. Napoli, C. Siciliano, G. Sindona, *Tetrahedron Letters* **2001**, *42*, 7413-7415.

[127] N. T. Burdzhiev, E. R. Stanoeva, *Tetrahedron* **2006**, *62*, 8318-8326.

[128] I. E. Markó, P. R. Giles, M. Tsukazaki, S. M. Brown, C. J. Urch, *Science* **1996**, *274*, 2044-2046.

[129] J. U. Ahmad, M. T. Räisänen, M. Kemell, M. J. Heikkilä, M. Leskelä, T. Repo, *Applied Catalysis A: General* **2012**, *449*, 153-162.

[130] L. Jiang, L. Jin, H. Tian, X. Yuan, X. Yu, Q. Xu, *Chemical Communications* **2011**, *47*, 10833-10835.

[131] R. Cano, D. J. Ramón, M. Yus, *The Journal of organic chemistry* **2011**, *76*, 5547-5557.

[132] S. Aldrich, in *1,1,2-Trichloroethane* (Ed.: S. Aldrich), The SIGMA-ALDRICH Group.

[133] B. Huang, H. Tian, S. Lin, M. Xie, X. Yu, Q. Xu, *Tetrahedron Letters* **2013**, *54*, 2861-2864.

[134] S. Suna, J. Dinga, J. Baoa, C. Gaoa, Z. Qia, X. Yanga, B. Hea, C. Lia, *Applied Surface Science* **2012**, *258*, 5031-5037.

[135] M. Addamo, V. Augugliaro, S. Coluccia, A. Di Paola, E. García-López, V. Loddo, G. Marcì, G. Martra, L. Palmisano, *International Journal of Photoenergy* **2006**, *2006*, 1-12.

[136] X. Yanga, X. Wanga, C. Lianga, W. Sub, C. Wanga, Z. Fengb, C. Lib, J. Qiu, *Catalysis Communications* **2008**, *9*, 2278-2281.

[137] P. Klán, J. Wirz, *Photochemistry of organic compounds: From concepts to practice*, John Wiley & Sons, **2009**.

[138] M. Reagents, *Uvasol® Solvents and auxillaries for spectroscopy*, Merck, E. Merck, Darmstadt, Federal Republic of Germany.

[139] S. Aldrich, in *Dichloromethane* (Ed.: S. Aldrich), The SIGMA-ALDRICH Group.

[140] S. Aldrich, in *2-Propanol* (Ed.: S. Aldrich), The SIGMA-ALDRICH Group.

[141] P. Y. Bruice, *Organic Chemistry, Vol. 6*, Prentice Hall, United States, **2011**.

[142] M. Giorgio, M. Trinei, E. Migliaccio, P. G. Pelicci, *Nature Reviews Molecular Cell Biology* **2007**, *8*, 722-728.

[143]   S. Kataria, A. Jajoo, K. N. Guruprasad, *Journal of Photochemistry and Photobiology B: Biology* **2014**, *137*, 55-66.

[144]   É. P. F. d. Lausanne, University*, Vol. 2014*, École Polytechnique Fédérale de Lausanne University, Switzerland, **2014**.

[145]   H. N. GmbH, January 2007 ed., Heraeus, Germany, **2007**, p. 12.

[146]   C. A. Fyfe, *Solid State NMR For Chemists, Vol. 1*, C.F.C. Press, P.O. Box 1720, Guelph, Ontario, Canada, N1H 6Z9, **1983**.

[147]   Y. Feng, J. Lv, J. Liu, N. Gao, H. Peng, Y. Chen, *Applied Surface Science* **2011**, *257*, 3433-3439.

[148]   A. F. Halima, U. A. Rana, D. R. MacFarlane, *Electrochemica Acta* **2014**, *115*, 639-643.

[149]   M. Jansen, *Solid State Sciences* **2005**, *7*, 1464-1474.

[150]   R. S. Balmer, *e. al.*, *Journal of Physics: Condensed Matter* **2009**, *21*, 1-51.

[151]   N. P. Mohabansi, V. B. Patil, N. Yenkiw, *Rasayan Journal of Chemistry* **2011**, *4*, 814-819.

[152]   S. Chakrabarti, B. K. Dutta, *Journal of Hazardous Materials* **2004**, *B112*, 269-278.

[153]   S. J. Sabounchei, M. Sarlakifar, S. Salehzadeh, M. Bayat, *Polyhedron* **2012**, *38*, 131-136.

[154]   J. Vicente, M. T. Chicote, J. Fernandez-Baeza, J. Martin, I. Saura-Llamas, J. Turpin, *Journal of Organimetallic Chemistry* **1987**, *331*, 409-421.

[155]   Skoog, West, Holler, Crouch, *Fundamentals of Analytical Chemistry*, Eighth ed., David Harris, **2004**.

[156]   S. Akoka, L. Barantin, M. Trierweiler, *Analytical Chemistry* **1999**, *71*, 2554-2557.

[157]   V. Molinier, B. Fenet, J. Fitremann, A. Bouchu, *Carbohydrate Research* **2006**, *341*, 1890-1895.

[158]   V. Silvestre, S. Goupry, M. Trierweiler, R. Robins, *Analytical Chemistry* **2001**, *73*, 1862.

[159]   G. Nuzzo, C. Gallo, G. d'Ippolito, A. Cutignano, A. Sardo, A. Fontana, *Marine drugs* **2013**, *11*, 3742-3753.

[160]   M. F. Semmelhack, C. R. Schmid, D. A. Cortes, C. S. Chou, *Journal of the American Chemical Society* **1984**, *106*, 3374-3376.

[161]   A. Kamal, V. Srinivasulu, B. N. Seshadri, N. Markandeya, A. Alarifi, N. Shankaraiah, *Green Chemistry* **2012**, *14*, 2513-2522.

[162]   D. Könning, T. Olbrisch, F. D. Sypaseuth, *Chemical …* **2014**.

[163]   A. Sharma, N. Sharma, A. Shard, R. Kumar, D. Mohanakrishnan, Saima, A. K. Sinha, D. Sahal, *Organic & Biomolecular Chemistry* **2011**, *9*, 5211-5219.

[164]   J. Ruan, X. Li, O. Saidi, J. Xiao, *Journal of the American Chemical Society* **2008**, *130*, 2424-2425.

[165]   X. R. Wang, F. Chen, *Journal of Chemical Research* **2010**.

[166]   J. Li, L. Liu, Y.-Y. Zhou, S.-N. Xu, *RSC Adv.* **2012**, *2*, 3207-3209.

[167]   V. R. Chintareddy, A. Ellern, J. G. Verkade, *The Journal of Organic Chemistry* **2010**, *75*, 7166-7174.

[168]   X. Wang, R. Liu, Y. Jin, X. Liang, *Chemistry-A European Journal* **2008**.

[169]   V. Polshettiwar, R. S. Varma, *Organic & Biomolecular Chemistry* **2009**, *7*, 37-40.

[170]   N. M. Neisius, B. Plietker, *Angewandte Chemie International Edition* **2009**, *48*, 5752-5755.

[171]   N. M. Neisius, B. Plietker, *Angewandte Chemie International Edition* **2009**, *48*, 5752-5755.

[172]   K. C. Y. Lau, P. Chiu, *Tetrahedron* **2011**, *67*, 8769-8774.

[173]   H. Hooshyar, H. Rahemi, K. A. Dilmagani, S. F. Tayyari, *Journal of Theoretical and Computational Chemistry* **2007**, *6*, 459-476.